ERA report series

27 Operational global reanalysis: progress, future directions and synergies with NWP

H Hersbach, P de Rosnay, B Bell, D Schepers, A Simmons, C Soci, S Abdalla, M Alonso Balmaseda, G Balsamo, P Bechtold, P Berrisford, J Bidlot, Eric de Boisséson, M Bonavita, P Browne, R Buizza, P Dahlgren, D Dee, R Dragani, M Diamantakis, J Flemming, R Forbes, A Geer, T Haiden, E Hólm, L Haimberger, R Hogan, A Horányi, M Janisková, P Laloyaux, P Lopez, J Muñoz-Sabater, C Peubey, R Radu, D Richardson, J-N Thépaut, F Vitart, X Yang, E Zsótér, Hao Zuo

Presented to the Scientific Advisory Committee, 8 October 2018, including updates on the ERA5 production status.

Series: ERA Report Series

A full list of ECMWF Publications can be found on our web site under:

http://old.ecmwf.int/publications/

Contact: library@ecmwf.int

European Centre for Medium Range Weather Forecasts
Shinfield Park, Reading, Berkshire RG2 9AX, England

Abstract

Within the Copernicus Climate Change Service (C3S), ECMWF is currently producing the ERA5 reanalysis which embodies a detailed record of the global atmosphere, land surface and ocean waves from 1950 onwards. This new reanalysis will replace the highly successful ERA-Interim reanalysis that was started in 2006 (spanning 1979 onwards), and will also encompass the period covered by ERA-40. ERA5 is based on the Integrated Forecasting System (IFS) Cycle 41r2 which was operational in 2016. Therefore, ERA5 benefits from a decade of developments in model physics, numerics and data assimilation. In addition to a significantly enhanced horizontal resolution of 31 km, compared to 80 km for ERA-Interim, ERA5 has a number of innovative features. These include hourly output throughout, and an uncertainty estimate (3-hourly at half the horizontal resolution). The step forward regarding quality and level of detail is evident. Forecasts from ERA5 analyses show a gain of up to one day in skill with respect to ERA-Interim.

One important novelty of ERA5 is the availability within 5 days of real time which will serve users that need recent meteorological information in combination with a long and consistent climate record. Such guaranteed timeliness requires that the ERA5 reanalysis is generated as an operational product.

The operational services in the Copernicus Programme build upon the massive European investments in mature science and technology. For climate reanalysis, this is a two-way interaction for ECMWF. On the one hand, ERA5 benefits greatly from the leverage of the developments in the IFS. On the other hand, the operational model development at ECMWF benefits from reanalysis. One excellent example of this is the Research and Development work performed within the European-Commission funded research projects ERA-CLIM and ERA-CLIM2.

This paper provides an overview of ECMWF's atmospheric, ocean and land reanalysis activities. In particular, it presents the ERA5 reanalysis system and its performance. It also describes challenges that were encountered and their practical solutions. The outcomes of the ERA-CLIM and ERA-CLIM2 projects will be summarized. Subsequent developments in, and plans for, the IFS in support of future reanalyses, aligned with the ECMWF strategy, are described.

1 Introduction

This paper provides a detailed overview of the configuration, innovation, status and performance of ERA5, the latest ECMWF reanalysis for the atmosphere, ocean waves and land. It also summarizes recent and current research work towards a future coupled reanalysis system, and the synergies and opportunities that exist with the research and development plans for the medium-range, monthly and seasonal forecasting systems.

The role of reanalyses in climate monitoring applications is now widely recognized. ECMWF's current flagship reanalysis (ERA-interim, (Dee et al., 2011)) is periodically used, together with other datasets, as input to the World Meteorological Organization (WMO) annual assessment of the State of the Climate, routinely presented at the Conference of the Parties of the United Nations Framework Convention on Climate Change (UNFCCC). ERA-interim is also a resource for the production of Essential Climate Variables (ECVs) and Climate Indicators recommended by the Global Climate Observing System (GCOS). By optimally combining observations and models, reanalyses indeed provide consistent "maps without gaps" of ECVs and strive to ensure integrity and coherence in the representation of the main Earth system cycles (e.g. water, energy).

ERA5 will soon replace the very successful ERA-Interim reanalysis, which is progressively becoming outdated. ERA5 is based on a recent IFS cycle (41r2). One of the innovative aspects is a timely, preliminary product, ERA5T, available within 5 days of real time. To guarantee such timeliness, ERA5 is produced in an operational environment. ERA5 is a highly visible activity within the Copernicus Cli-

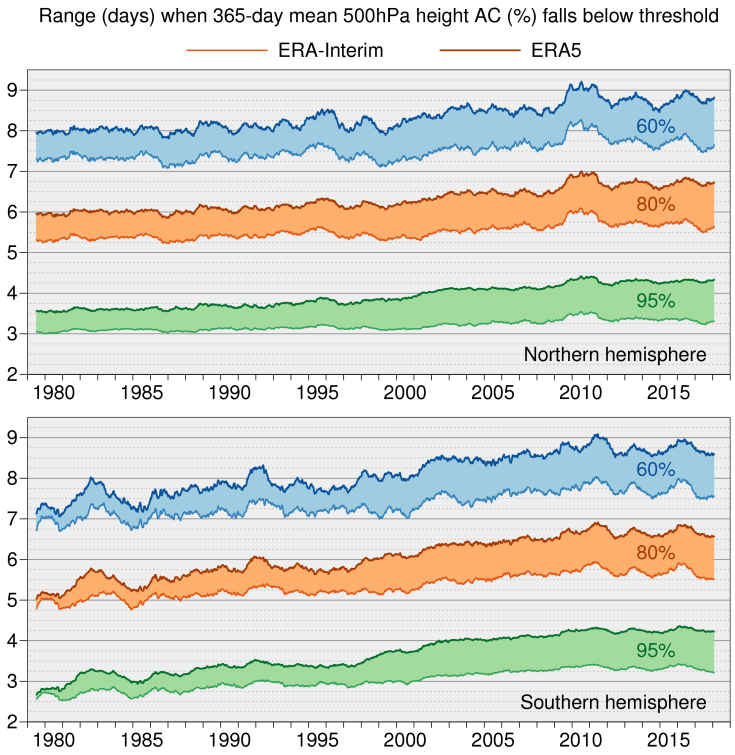

*Figure 1: Range (days) at which running 365-day mean anomaly correlations of 500*hPa*height forecasts from 00 and 12 UTC reach 95% (green), 80% (orange) and 60% (blue), for the extra-tropical northern (upper) and southern (lower) hemispheres, from 1979 onwards. The heaviest lines denote ERA5, the thin lines denote ERA-Interim. Shading denotes the difference between ERA5 and ERA-Interim. Results for dates from 2000 are based on the officially released product, while earlier results are from yet to be released data.*

mate Change Service (C3S), where it provides an improved and consistent record for a large number of ECVs for the C3S Climate Data Store (CDS, Raoult et al. (2017)). Besides a considerable increase in resolution (both in the horizontal and vertical) and the benefit of 10-years of model and data assimilation developments, ERA5 provides an enhanced number of output parameters (such as the 100m wind product), hourly output throughout and uncertainty information (3-hourly). This uncertainty information is obtained from the underlying 10-member ensemble 4D-Var data assimilation system.

The step forward with ERA5 is illustrated by Figure 1 which shows a gain of up to one day in skill of 10-day forecasts started from ERA5 (thick lines) analyses, compared to ERA-Interim (thin lines).

ECMWF has a long history with reanalysis. An overview is presented in Figure 2. Activities on atmospheric reanalysis started back in 1979 with the First Global Experiment of the Global Atmospheric Research Programme (FGGE) project, followed by the production of ERA-15 (Gibson et al., 1999) in the mid 90s, ERA-40 (Uppala et al., 2005) from 2001-2003 and ERA-Interim from 2006 onwards. In this series, ERA5 is the fifth full-observing-system atmospheric reanalysis at ECMWF. They all include a land component, and from ERA-40 an ocean surface wave component as well. In addition, ECMWF has produced a number of dedicated ocean reanalyses, starting with ORAS3 (2006, Balmaseda et al. (2008)), ORAS4 (2010, Balmaseda et al. (2013a)), and recently ORAS5 (2016, Zuo et al. (2018)). These reanalysis systems provide initial conditions for re-forecasts that are used to spin-up a model climatology for the medium-range ensemble, extended and seasonal forecasts. As such, they require a near-real-time component and for this reason these ocean reanalyses were the first operational reanalysis systems at ECMWF.

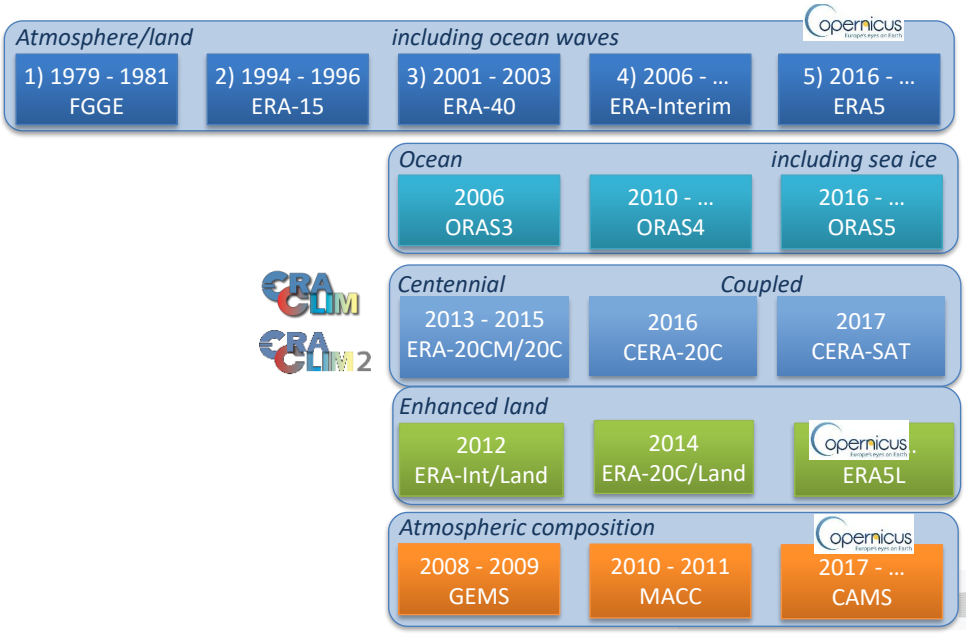

Figure 2: Overview of reanalysis activities at ECMWF. Years indicate the period of production.

Within the European-Commission funded GEMS (Global and regional Earth-system Monitoring using Satellite and in-situ data) and MACC (Monitoring Atmospheric Composition and Climate) projects, and now the Copernicus Atmospheric Monitoring Service (CAMS), ECMWF has also delivered reanalyses for atmospheric composition (2008, 2010 (Inness et al., 2013) and 2018, respectively).

Preceding and in parallel with the development of ERA5, ECMWF has recently produced centennial reanalyses within the EC-funded ERA-CLIM and ERA-CLIM2 research projects. Coordinated by ECMWF, these projects were undertaken by a wide international consortium. One aspect was the provision of boundary datasets over the oceans (SST and sea-ice provided by the Met Office Hadley Centre) and forcing terms in radiation (CMIP5) to provide a good representation of their evolution over the 20th century. This was successfully implemented and used in a century-long 10-member ensemble model-only integration (ERA-20CM, Hersbach et al. (2015)). The next step was the production of a century-long reanalysis using surface pressure and marine wind observations only (ERA-20C, Poli et al. (2016)). In ERA-CLIM2, research towards coupling with the ocean culminated in a century-long 10-member reanalysis (CERA-20C, Laloyaux et al. (2018)) that is based on outer-loop coupling between the ocean and atmosphere, and an 8-year reanalysis (CERA-SAT, Schepers et al. (2018)) for the current-day full observing system with the same resolution as the ensemble component of ERA5. In this respect developments in reanalysis have advanced the development of the ECMWF operational numerical weather prediction (NWP) model. The CERA system provides an important step towards an Earth system approach, which is a key part of the ECMWF road map for 2016-2025.

Recent developments have shown that coupled ocean-atmosphere assimilation is highly relevant for NWP. A weakly-coupled sea-ice atmosphere assimilation was implemented in IFS cycle 45r1 and weakly-coupled SST is expected in 46r1. In parallel, results using the CERA-type ocean-atmosphere outer-loop coupling approach exposed some challenging issues in the NWP system. Ongoing research aims to address these and to explore new methods combining weak and outer-loop coupling. Taking into account the data-centre move to Bologna, such a coupled system will not be part of the ECMWF operational NWP system before 2021.

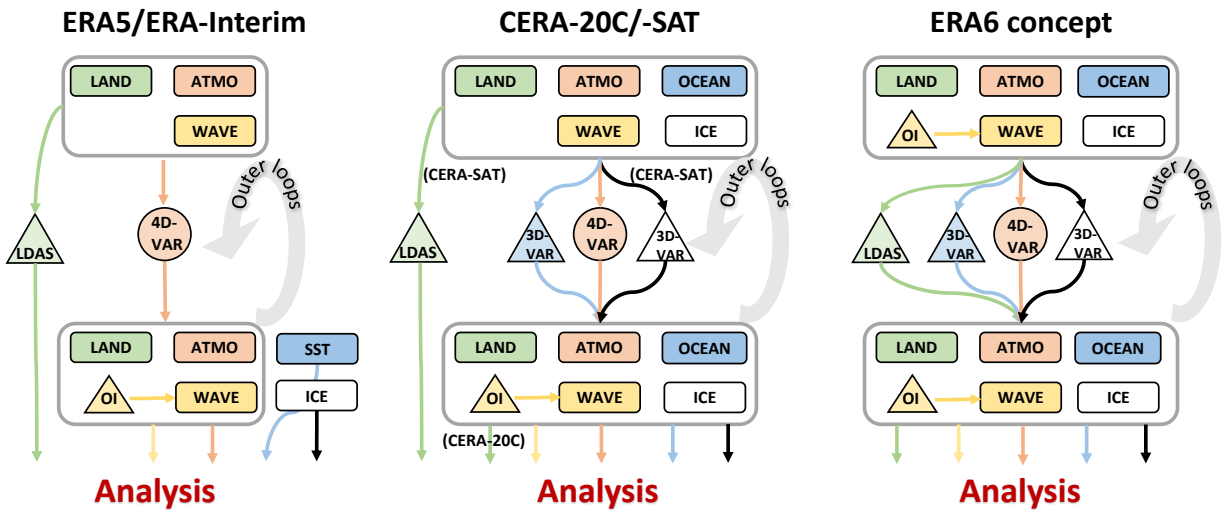

Figure 3: Assimilation diagrams for ERA5 and ERA-Interim (left), CERA-20C and CERA-SAT (middle) and the preferred configuration for the future ERA6 reanalysis (right panel) regarding the atmosphere (atmo), land surface (land), ocean waves (waves), sea ice (ice) and ocean. Atmospheric composition is not yet included. Large boxes represent outer-loop integrations (trajectories) where the indicated domains are coupled. Triangles are either 3D-Var, land-data assimilation (LDAS) or optimal interpolation (OI), while circles correspond to 4D-Var inner loops. The ocean-wave OI assimilation is performed only inside the final trajectory. However, for ERA6 this may extend to other outer loops. CERA-20C has no LDAS or ice assimilation. For ERA5 the LDAS assimilation is an example of weak coupling where the influence from land-surface and other observations is only mixed in the next analysis window via the coupled short forecast from the current analysis. It represents outer-loop coupling (a form of Quasi-Strong coupling) in the ERA6 configuration where the influence from all observations is mixed inside the assimilation window in question.

The assimilation system for future reanalyses will also rely on a coupled approach between atmosphere, ocean, sea ice and land, ideally based on outer-loop coupling. This will embrace a new full-observing-system reanalysis, ERA6, as well a new extended centennial reanalysis going back to 1900 or earlier. Close links between reanalysis and NWP are essential. An overview of the data-assimilation configuration for the various reanalysis systems is provided in Figure 3, which also illustrates the difference between weak and outer-loop coupling.

Land reanalysis is becoming increasingly important for climate monitoring, coupling developments between land surface and atmosphere, and for carbon cycle monitoring. ERA5 incorporates a weakly-coupled land assimilation system, combining in situ and satellite observations (including scatterometer soil moisture data records). In addition, ECMWF has produced dedicated enhanced land model products, that are constrained by down-scaled atmospheric reanalysis forcing fields. These are ERA-Interim land (2012, Balsamo et al. (2015)) and ERA-20C land (2014). The cost of such model-based products is considerably lower than that of a data-assimilation system. ERA5-Land will provide such a land product at enhanced resolution that matches that of the current ECMWF high resolution system (9 km).

The organisation of this Special Topic Paper is as follows. Section 2 gives an overview of the reanalysis user landscape. Reanalysis forms a source of climate information to more than 30,000 users worldwide. In particular, ERA-Interim, and now ERA5, provides important information for ECMWF forecast products and for ECMWF member states. The ERA5 reanalysis is the topic of Section 3. This is by far the largest Section, since (in contrast to the other reanalysis work discussed in this document) this has not been documented in the literature so far. A peer-reviewed paper is in preparation. The configuration, characteristics and novelties are listed. Here also the challenges that were encountered during the production and how these were subsequently handled are detailed. The section provides an evaluation

of performance and the improved data usage of ERA5 with respect to ERA-Interim. In Section 4 the ERA5 land product is described. Ocean reanalysis is the topic of Section 5. The work on an ocean-atmosphere coupled data-assimilation system as developed in the ERA-CLIM2 project is the subject of Section 6. The main achievements of the CERA-20C and CERA-SAT reanalyses are summarized. Development towards a coupled ERA6 system is described in Section 7. These developments are planned to be streamlined with those of the ECMWF 2025 strategy to move to an Earth-system NWP model, and will form an active and essential part of synergies between reanalysis and NWP. The paper ends with concluding remarks.

2 User landscape and synergies with NWP

2.1 Global usage of ERA Interim

As the precursor of ERA5, ERA-Interim has attracted over 30,000 users worldwide during the period between 1 January 2015 and 30 April 2018, and has been recognized as a well established reanalysis dataset in the research community. China, USA and UK are the top three countries regarding number of users. Figure 4 illustrates geographical user distribution in Europe by country.

ERA-Interim is popular with a wide range of users, from academic to the private sector. The ERA-Interim peer reviewed paper (Dee et al., 2011) has been cited over 10,000 times, and the total volume of downloads from ECMWF totaled 1.4 Petabyte in 2017 alone. A breakdown for 2017 is provided in Table 1. However, ERA-Interim is getting progressively outdated (see, e.g., Table 2), and the number of observations that it can ingest is declining (as evident from Figure 17). For this reason it is planned to retire ERA-Interim after the ERA5 segment from 1979 has been available for about half a year.

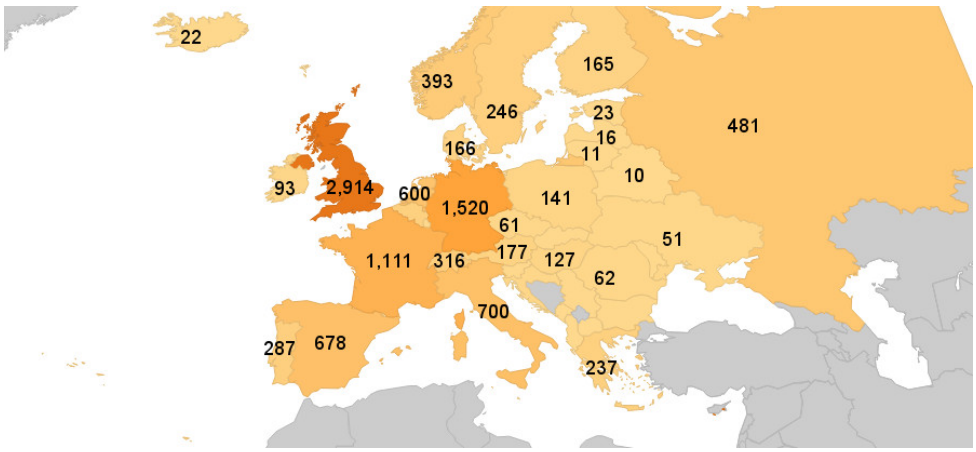

Figure 4: ERA-Interim user distribution in Europe, 1 January 2015 - 30 April 2018.

According to a user satisfaction survey carried out by C3S in June/July 2017, as a mature dataset, ERA-Interim generated a lot of positive feedback. Many researchers appreciated the dataset: *"This Interim data is a very valuable source for researchers", "I was only aware of ERA-Interim products, not any others. However, I am very satisfied with ERA-Interim"*. In addition, the survey identified that nearly 90% of users are either extremely or very satisfied with the support they received. See Hennermann et al. (2017) for a summary of the survey.

Sector	Total	Active	New
Academic / Research	13,605	10,037	6,917
Public / Governmental	1,692	1,205	745
Non-governmental (NGO)	136	88	61
Individual user	676	438	294
Other	1,316	905	662
Unknown	12,857	4,797	465

Table 1: ERA-Interim users by sector for 2017.

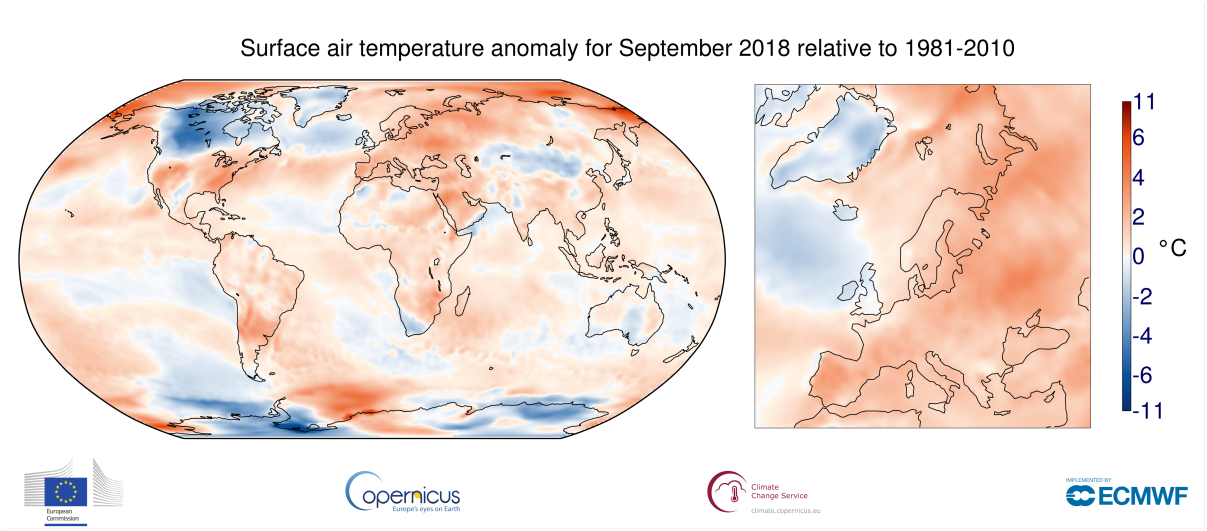

Figure 5: Surface air temperature anomaly for September 2018 relative to the September average for the period 1981-2010, based on ERA-Interim, from https://climate.copernicus.eu/.

2.2 Importance of reanalysis at ECMWF

ECMWF in particular is one of the many users of its own reanalysis products. Most of these applications are currently based on ERA-Interim, however, the move towards ERA5 is in progress, and for some applications already in place (Haiden et al., 2017).

Since August 2015 C3S provides a monthly-updated climate bulletin (https://climate.copernicus.eu/monthly-maps-and-charts), incorporating a global and European monitoring report covering, initially, surface air temperature and, subsequently (from March/April 2017), sea-ice and hydrological climate variables as well. An example for air-temperature anomalies is provided in Figure 5. Currently based on ERA-Interim, these summaries are published within one week of the end of the month, which well pre-dates releases from other climate centres, such as the National Oceanic and Atmospheric Administration (NOAA). Achieving such timeliness is facilitated by the fact that, since October 2015, ERA-Interim is produced within an operational environment. The move to ERA5 is currently in preparation, and the transition will occur after the full climate record from 1979 is available.

Reanalysis products (ERA-Interim and ORAS5) are also required in order to run, twice-weekly, an ensemble of re-forecasts for the past 20 years which are used to calibrate ensemble, extended-range and seasonal forecasts. Initial results suggest that re-forecasts initialized from ERA5 are significantly more skilful up to a lead time of 4 weeks, instead from ERA Interim (even when verified against ERA Interim analyses).

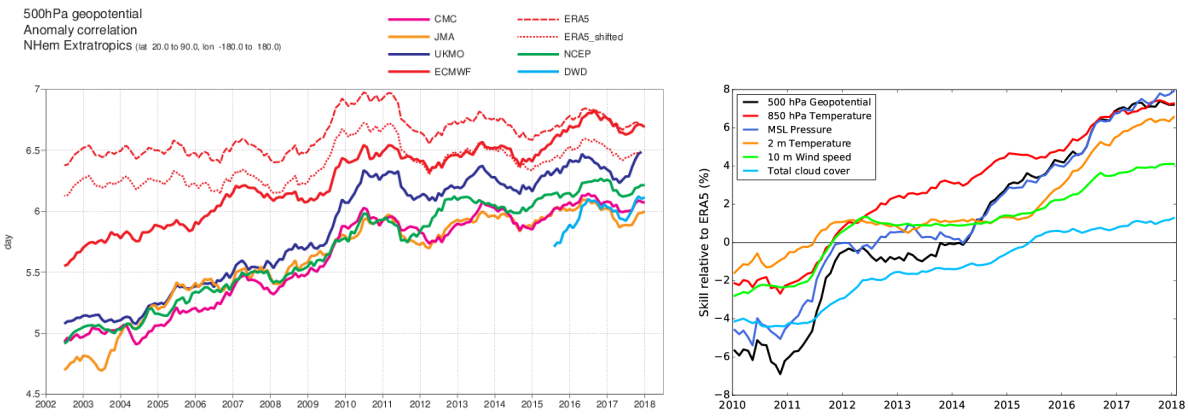

Figure 6: Evolution over the northern hemisphere for (left) the range at which the anomaly correlation coefficient (ACC) for Z500 drops to 80%, and (right) the standard deviation of ECMWF HRES forecast error relative to ERA5 for a number of different parameters, for day 5 (T+120). Verification is against analysis for Z500, T850, MSLP and against observations for the surface fields. For ERA5, some curves (red dotted curve in left panel, and reference in right panel) are penalised by six hours as they use six hours of data more into the future, and highlight that its forecast are produced later.

ERA5 is used for the evaluation of trends in forecast skills, since the natural variability of predictability can mask changes in the performance of the ECMWF operational HRES. By comparing the long-term evolution of skill with those from ERA5 (left panel of Figure 6) a more balanced assessment of the true gain in skill over time can be obtained (right panel of Figure 6). Although inter-annual variability in predictability affects all models, other models change regularly and, in contrast to reanalysis, cannot be used as such as a reference. Until now exchange of WMO scores for surface parameters has not been organised so far and the only reference at this point is reanalysis.

Reanalysis also provides a climatology for the Extreme Forecast Index, and is used to evaluate the reliability and skill of ECMWF ensemble forecasts. Such climatologies are also used to determine anomalies on which many forecast scores rely (such as the anomaly correlation coefficient). ERA-Interim is used for that purpose at ECMWF and now also in the WMO exchange of forecast scores. One other example is the definition of probabilistic events, such as temperature anomalies in the upper tercile.

In addition, reanalysis is widely used as a benchmark or reference. An example is the provision of a model climate against which R&D developments in the model are assessed.

Many other examples can be provided. For instance, ERA5 plays already an essential part for the at ECMWF-based Copernicus Emergency Management Service (CEMS) Flood group. It has been used to analyse the different (GloFAS) model configuration options, and to evaluate the impact of land data assimilation on river discharge. ERA5 has been applied in the initialisation of the GloFAS-seasonal system since its implementation in November 2017.

2.3 Benefit of ECMWF research to reanalysis

Being the world leader in global numerical weather prediction, ECMWF is the ideal location to conduct global reanalysis. The latest operational IFS cycle is an excellent starting point, since it incorporates the latest state-of-the-art and thoroughly-tested R&D. The available in-depth expertise at ECMWF in many areas allows for the choice of an optimal configuration for reanalysis, such as on details of the assimilation system, or the optimal usage of particular types of observations. The operational infrastructure allows for conducting the reanalysis on the ECMWF high-performance computing (HPC) facility,

archiving into the Meteorological Archival and Retrieval System (MARS), and provides a guarantee for the timely availability of ERA5T. This timely update also benefits from the detailed monitoring of the operational NWP system and any resolved data-related issues (such as temporal blacklisting of data that show signs of degradation) can be incorporated accordingly.

3 The ERA5 reanalysis

3.1 Overview and innovative features

This chapter provides an overview of the configuration of ERA5 and a preliminary assessment of its characteristics and performance. The focus will be on innovative features and how ERA5 differs from ERA-Interim. A concise overview is displayed in Table 2.

ERA5 will cover the period from 1950 onwards. Production is split into two phases. The first phase, which covers the same period as ERA-Interim from 1979 was completed in October 2018. Currently, data from the year 2000 has been released, while the remainder from 1979 should be publicly available by the end of 2018. Like ERA-Interim, timely updates for ERA5 are released in one-monthly chunks, with a time lag of 2-3 months. New in ERA5 will be the provision of a pre-released version, ERA5T, with a delay of only 2-5 days. Usually the final product will be equivalent to this, but occasionally re-runs may be required to resolve identified issues which will benefit the quality of the final product but not ERA5T. Details on the production and the monitoring of progress and quality are provided in Section 3.3. For practical reasons, ERA5 is produced in a number of parallel streams. Seams between these will be discussed in Section 3.4.3.

After an overlap period of about 6 months where both ERA5 and ERA-Interim are available, it is planned to retire ERA-Interim, i.e. as it stands now, by mid 2019.

The production of the second phase from 1950 to 1978 has just started, with an anticipated completion date of autumn 2019. For this reason most of the results presented in this document apply to the first phase.

The starting point for ERA5 is IFS cycle 41r2, which was used in the operational medium-range forecasting system in 2016. With respect to ERA-Interim, it incorporates 10 years of R&D for all its components (atmosphere, land, ocean waves, observation operators, see Sections 3.5 and 3.7.1) and improvements in the data assimilation methodology, which is now based on Ensemble Data Assimilation (Section 3.2). The 10-member ensemble not only delivers more suitable estimates for flow-dependent background errors, it also allows for the estimation of uncertainties in the reanalysis. A concise assessment is provided in Section 3.8.

The advance of computer power over time has enabled a significant increase in resolution which, compared to ERA-Interim, has more than doubled in both the horizontal and vertical.

The IFS relies on a number of prescribed forcing fields in the radiation and ocean-surface conditions. ERA5 makes use of the R&D performed in the ERA-CLIM project on the selection of datasets that represent the low-frequency evolution of such quantities over time (Section 3.6.1).

One other novelty of ERA5 is hourly output throughout and three-hourly output for its uncertainty estimate. Although the length of the atmospheric analysis window remains 12 hours (though compared to ERA-Interim shifted by 6 hours), the analyses within these windows are stored hourly (rather than 6-hourly for ERA-Interim). In the absence of systematic analysis increments this will produce a seam-

	ERA-Interim	**ERA5**
Publicly available now, by end 2018, by autumn 2019	1979 - onwards until mid 2019 (final)	2000 - onwards 1979 - 1999 1950 - 1978
Availability behind real time	2-3 months	2-3 months (final product) 2-5 days (ERA5T)
Model cycle	31r2 (2006)	41r2 (2016)
Atmospheric DA window for 0, 12 (UTC)	12h 4D-Var ($15_{\text{day}-1}$, 03], (03,15]	12h 4D-Var ensemble ($21_{\text{day}-1}$, 09], (09, 21]
Model input *(radiation and surface)*	as in operations, inconsistent SST and sea ice	appropriate for climate, e.g., evolution greenhouse gases, aerosols, SST and sea ice
Spatial resolution Ocean waves Inner-loop resolution	79 km (TL255) 60 levels to 10 Pa 1 degree TL95, TL159	31 km (TL639) 137 levels to 1 Pa 0.36 degree TL95, TL159, TL255
Land-surface model Soil moisture DA Snow DA	TESSEL 1D-OI Cressman	HTESSEL SEKF 2D-OI
Uncertainty estimate	none	from the 4D-Var ensemble, 10 members at 62 km (TL319) TL127, TL159 inner loops ocean waves 1 degree
Output frequency	6-hourly for analyses, 3-hourly for forecasts	hourly throughout (uncertainty 3-hourly)
Output parameters		extended list (e.g., 100-metre wind)
Extra observations Reprocessed FCDRs	following ERA-40, GTS some	latest instruments many more
Radiative transfer model	RTTOV v7 clear-sky assimilation	RTTOV v11 partly all-sky assimilation
Var BC **Corrections radiosondes**	radiances only RAOBCORE	extended to ozone, surface pressure RISE
Dedicated land product	79 km, HTESSEL	9 km, HTESSEL

Table 2: Overview of characteristics and innovative features of ERA5. DA stands for Data Assimilation, and FCDR for Fundamental Climate Data Record. The ERA5 assimilation windows are based on the delayed cut-off of the early-delivery system, while ERA-Interim pre-dates that development, which explains the relative shift in assimilation windows.

less hourly product. However, some quantities (wind in the boundary layer) have been shown to display small, though systematic jumps between windows. The short forecasts that transport information between analyses are stored hourly as well.

For the ocean-surface analysis, the sea-surface temperature (SST) and sea-ice cover (see Section 3.6.2) are only available daily. The ingested SST represents a layer that is free from diurnal variations (the foundation temperature). However, hourly variations are represented in the ERA5 skin temperature at the ocean surface.

Over land, the analysis of screen-level parameters (2m-temperature and humidity) and snow are based on optimal interpolation. These are now performed hourly. Such analyses use data closest in time within $\pm$3-hourly windows, without making corrections for misfits in timing. For this reason, the non-synoptic analysis times may suffer from systematic biases where only synoptic observations are available, which is progressively the case when going further back in time. On the other hand, observations available at non-synoptic times, such as dominant over Australia can introduce systematic biases at synoptic times. This non-ideal situation should be better addressed in the future. Assimilation of soil moisture variables is based on a simplified extended Kalman filter, where time evolution is accounted for. Here analysis products are simply stored hourly within the 6-hourly windows.

Based on user requirements the number of output parameters was increased, such as 100-metre wind and additional quantities related to radiation. A full list may be found at https://confluence.ecmwf.int/display/CKB/ERA5+data+documentation. The total volume of the ERA5 dataset will be around 9 Petabyte and is accessible from the C3S Climate Data Store, partly online via a cloud server and the remainder via the MARS archive.

For ERA5 a great effort was made to improve on the ingested observations themselves. A large number of newly-available reprocessed datasets was acquired and assessed (Section 3.7.2). Compared to ERA-Interim, the more recent IFS version allows for the usage of data from many more instruments (mainly since the mid 2000s).

Several aspects on the performance and characteristics of ERA5 are described in Section 3.9.

3.2 The Ensemble Data Assimilation system

The ERA5 atmospheric analysis is based on a hybrid incremental 4-dimensional variational data assimilation (4D-Var) system (Isaksen et al., 2010; Bonavita et al., 2016). The ensemble component is an Ensemble of Data Assimilations (EDA) of 10 independent members which provides background error estimates for the deterministic high-resolution (HRES) 4D-Var data assimilation system. The EDA system provides estimates of analysis and short-range forecast uncertainty which are considered to represent the evolution of the errors in the HRES system.

Each EDA member, except the control, is run with different random perturbations added to the observations and the sea-surface temperature fields. The perturbations of observations are sampled from a zero-mean Gaussian distribution with variance equal to the expected variances of the observation errors. Likewise, the model physical tendencies are perturbed when the non-linear forecast model is run to cycle the analysis fields. The sea-surface temperature (SST) and the sea ice cover errors are taken from the spread within the range of available products (Hirahara et al., 2016). The perturbations applied to the observations, the SST and the model imply that the resulting background (i.e. short-range forecast) of each member is implicitly perturbed, thus avoiding the need for explicitly perturbing the background fields.

The incremental EDA 4D-Var analysis is run with an outer-loop at a horizontal grid spacing of about 62 km (spectral triangular truncation T319 on a linear grid) and 137 levels in the vertical, and two inner-loops minimizations, respectively at 157 km (TL127) and 125 km (TL159). The non-linear forecast model used to cycle the analysis is run at the same horizontal and vertical resolution as the outer-loop. Both the EDA and the HRES 4D-Var make use of a hybrid **B** formulation. This means that, like for the operational medium-range system a static, climatological background-error covariance matrix ($\mathbf{B}_{\text{cli}}$) is combined with a dynamic one computed using short-range forecasts from the EDA which brings in flow-dependent correlation structures to the resulting background-error covariance matrix. The weight given to the latter, is however half that of the operational NWP system (0.15, rather than 0.3), this to limit sampling errors from the smaller ensemble size (10 versus 25). In ERA5, **B** is modeled using the wavelet formulation described by Fisher (2003), with background-error correlations localized in both the spectral and the spatial domains.

The flow-dependent variances resulting from the spread of the EDA are used in the HRES 4D-Var analysis. The HRES 4D-Var outer-loop (and the forecast model) is run at a horizontal grid spacing of 31 km (TL639) and with 137 levels in the vertical, with three inner-loop minimizations respectively at 210 km (TL95), 125 km (TL159), and 78 km (TL255).

Both the HRES and the EDA benefit from using the variational bias correction method (Dee, 2005). In the EDA, the variational bias correction scheme is used to cycle the biases only in the control assimilation (Isaksen et al., 2010). In each ensemble member the variational bias correction coefficients are fixed to the control assimilation values for each cycle. The solution of using the variational bias correction method as part of the minimization algorithm only in the control is chosen in order to avoid artificially long correlations in the background error statistics derived for the short-range ensemble forecasts.

3.3 Production schedule and status

Although the development, testing and large part of quality assessment of ERA5 is performed in the C3S Reanalysis Team, the actual production is conducted in the Copernicus Production Section. In this way maximum synergy with the existing operational infrastructure can be achieved. First experience in running atmospheric reanalysis in an operational environment had been gained from October 2015 with ERA-Interim. Production of ERA5 started in January 2016 (Hersbach and Dee, 2016).

Given the constraints of the available time frame, production is split into a number of parallel streams, each of them completing around 7 reanalysis days per day.

Phase 1 of the production (1979 onwards) was envisaged to take place in 4 parallel streams of one per decade with overlaps of one year to allow for spin up. The actual production line is displayed in Figure 7 which, due to a number of issues as sketched below, became much more complex. Test runs for several periods at reduced resolution prior to production (called *scouts*), had shown that the performance in the 1980s was quite poor throughout the southern hemispheric troposphere, and less poor, but still not excellent in the 1990s. For this reason, initially only the streams for the 2000s and 2010s were started, and, given the time pressure, later a stream for the 1990s as well before the non-optimal performance had been completely understood. After thorough investigations, the poor performance in the early decades was traced down to problems with the background covariance matrix, where the correlation lengths which are based on the current high-density observing system appeared too short for the more data-sparse past. Details are described in Section 3.4.1. The remedy was a new static background covariance matrix that is more representative for the early decades (called 1979-$\mathbf{B}_{\text{cli}}$ hereafter). Only after this 1979-$\mathbf{B}_{\text{cli}}$ had been built up from a sufficient number of EDA samples could the production of the 1980s commence.

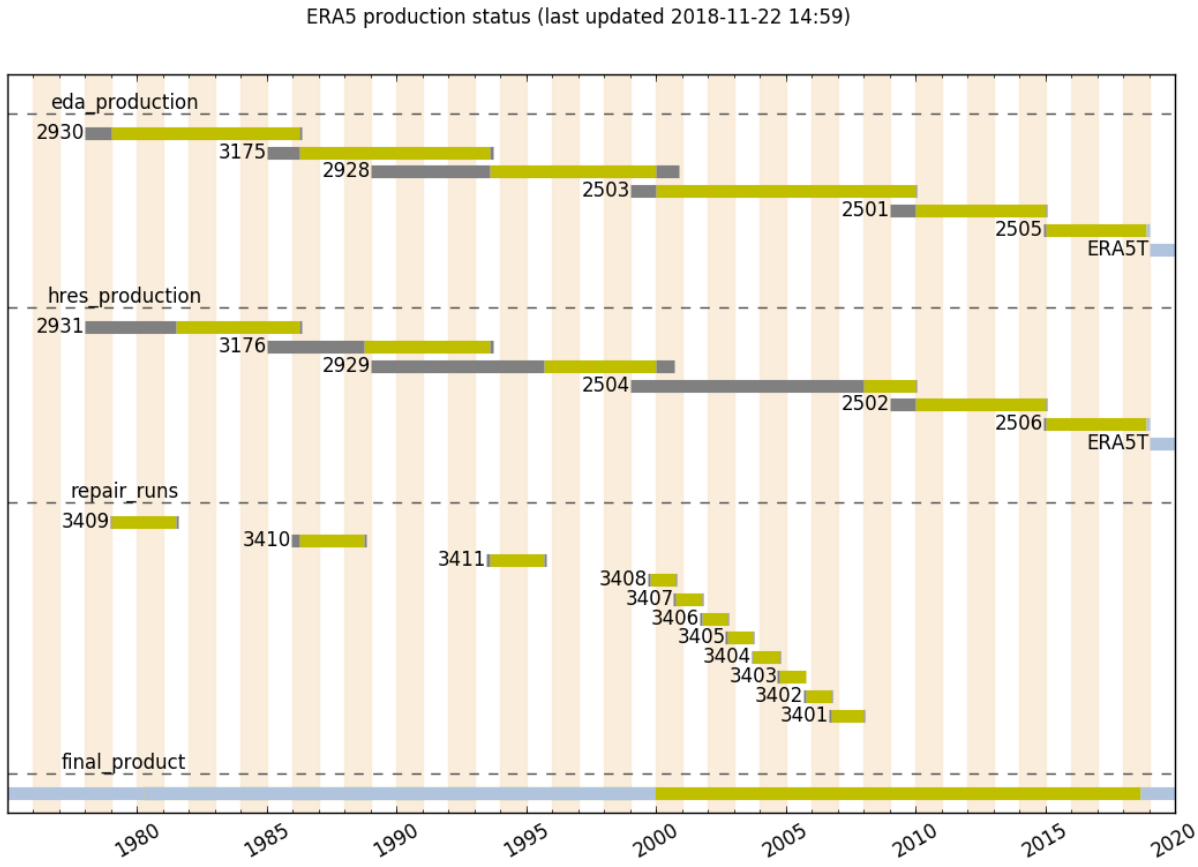

Figure 7: Overview of ERA5 production streams: completed and consolidated or to be consolidated (yellow), produced but will not be used (grey) and still to be produced and to be consolidated (light blue). Production streams were cold-started from ERA-Interim (with the exception of 2931 that was cold started from ERA-40) with a minimum of one year spin up, while repair runs were warm-started from underlying production runs, with a spin-up of two weeks and imposing the original VarBC coefficients to ensure that they evolve closely along the original stream, where required.

However, as described in Section 3.4.2, the progress of this stream was initially very slow due to issues with quality control of poor surface pressure data over the southern hemisphere. To accommodate the substantial time delay it was decided to conduct one extra stream from the mid 1980s. In the meantime undesired stratospheric temperature biases had been spotted in the 1990 and 2000 streams. In particular, in spite of imposing CMIP5 forcing for stratospheric sulphate (Section 3.6.1), the response to Pinatubo in 1991 emerged poorer than for ERA-Interim. It appeared that this was related to too-short background correlation lengths as well, and the usage of the 1979-$\mathbf{B}_{\mathrm{cli}}$, instead was found to perform much better. The 1990 stream had now also exposed excessively high values of ozone in the polar night, which was later resolved by blacklisting SBUV data above 5 hPa (Section 3.4.4). It was decided to continue the stream from the mid 1980s well into the 1990s, to resolve both the ozone and poor response to Pinatubo.

Quite late in the production (December 2017) a major issue was detected with erroneous sea ice in the Baltic during each summer before 2008 (Section 3.6.2). A solution was found, and it was decided to re-run those parts of the HRES production streams that had been affected. This was conducted in a large number of parallel repair runs to ensure that this would not delay completion times significantly. For these runs, special care was taken to ensure that the seams between these streams are small (Section 3.4.3).

Phase 1 was completed in October 2018. At the time of writing data from 2000 was publicly available. This final step takes place by consolidating (copying) the various production streams to the official release (version=0001, see lowest bar of Figure 7). For the remainder of the period (1979-1999) this consolidation is in progress. The production stream of the 2010s has caught up and is conducted a few days behind real time. Currently a mechanism is finalized to consolidate this stream directly (to version ERA5T) so that it becomes available 2-5 days behind real time.

Phase 2 (1950-1978) has just commenced, and will be conducted in 4 parallel streams of about 8 years each. It includes satellite data from VTPR (Section 3.7.2) that were assimilated in ERA-40 before, BUV ozone data, the inclusion of historical in-situ and upper-air data (Dahlgren, 2018a) as used in the ERA-CLIM ERA-PreSAT pilot reanalysis (Hersbach et al., 2017), an extended version of prescribed RISE radiosonde temperature bias corrections (Haimberger et al., 2012), a recently acquired surface dataset from NOAA before September 1957, and a dedicated static background covariance matrix for the pre-satellite era (1958-$\mathbf{B}_{\mathrm{cli}}$).

As illustrated above, a major effort is devoted to ensure the quality of ERA5. The progress and performance of the production streams are continuously monitored and analyzed using an extensive system of diagnostic tools. Results are scrutinized in weekly meetings and solutions to encountered issues are, where possible, resolved, tested and handed over to the Production Section for implementation. This intensive infra-structure of monitoring and quality control allowed for the early detection and mitigation of the problems as discussed above. Changes to the production suite are made with great care. Careful testing is required to verify that there is no impact on unrelated periods (all streams share the same code and scripts), but also, an additional constraint is that the model itself cannot be changed, since that would violate the principle of consistency in the reanalysis system. For this reason, only data-related changes are made, such as updating blacklists, quality control or the background covariance matrix (which is partly dictated by the underlying observing system).

3.4 Some challenges during production

This section provides more details on the challenges that were addressed during production as briefly described in Section 3.3.

3.4.1 Long-term evolution of the background covariance matrix

A key element of the ERA5 data assimilation system is the formulation of the background error covariance matrix **B**, as it, for example, determines how the background departures are spread in model space and between variables.

Prior to the production of ERA5, a number of scouts had been performed to test the correct ingestion of available observations and performance. These scouts were conducted at the EDA control resolution (TL319), however, without an associated ensemble. Therefore, these experiments did not benefit from the hybrid **B** formulation (Section 3.2) but were, like ERA-Interim, based on just the static part $\mathbf{B}_{\mathrm{cli}}$, instead. As a minimum the scouts should be able to outperform ERA-Interim, given higher resolution, newer IFS cycle and better observations. For experiments in the 2000s and beyond, this was, indeed evident. For the 1990s, however, scouts struggled to beat ERA-Interim over the southern hemisphere, and performance for scouts in the early 1980s was found to be significantly poorer for that hemisphere. This is illustrated by the left panels of Figure 8.

Investigations were conducted to identify the cause for these poor results. It was found that, in spite of

ingestion of exactly the same HIRS and MSU data, ERA5 assimilated about 30% fewer HIRS and 15% fewer MSU observations than ERA-Interim. For HIRS, this could be partly explained by an updated version of cloud detection (Krzeminski et al., 2009), that is more selective. However, experiments using the ERA-Interim configuration (TL255, 60 levels) with this cloud-detection scheme did not show a degradation. These experiments used a static background term which is more in line with that of ERA-Interim, that is representative for the model first-guess error in the early 2000s, where the observing system was not as rich as it is today. As a consequence, correlation lengths of this background are found longer than for the background in the poor-performing scouts, which is representative for 2016 (called 41r2-$\mathbf{B}_{\mathrm{cli}}$, hereafter). This is shown in Figure 9. It allows for a better, wider distribution of increments from the sparser observations, while the 41r2-$\mathbf{B}_{\mathrm{cli}}$ analysis increments are too local. The larger rejection rates for HIRS and MSU are more related to a lower quality of model first-guess, which, when compared to the observations, leads to larger number of rejections based on larger departures. This is particularly the case for the HIRS cloud screening.

With this concept in mind, a new $\mathbf{B}_{\mathrm{cli}}$ was constructed that is more representative for the observing system of 1979. Guided by expertise in NWP, where such construction is periodically performed for the latest model cycle, this was achieved by combining a large number of short-range forecasts from a dedicated hybrid EDA experiment. In total 63 days were used spanning both winter and summer cases.

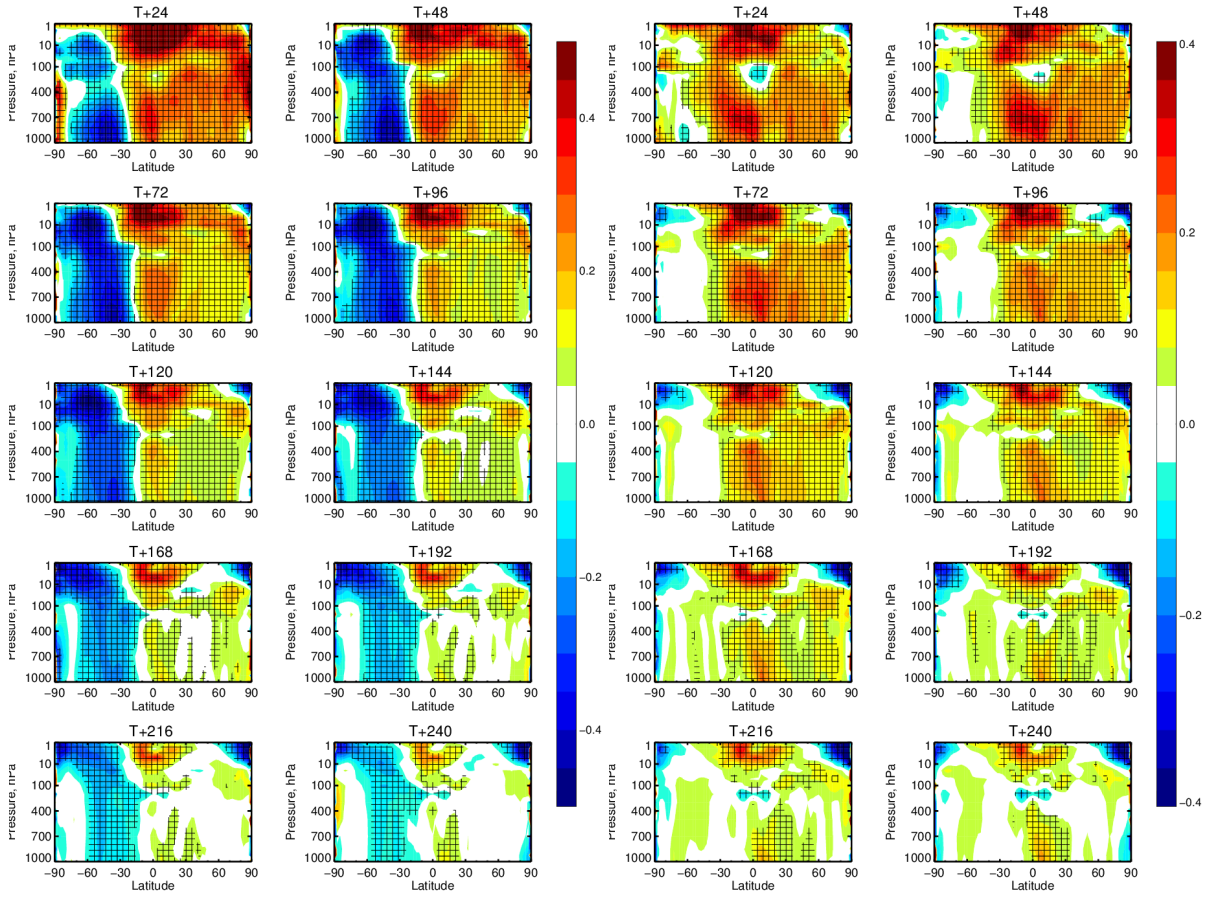

Figure 8: Comparison of the change in anomaly correlation of geopotential forecast for T+24 up to T+240 hours between ERA5 and ERA-Interim, from 1 February to 30 September 1979, with ERA5 analyses performed using respectively the standard 41r2-$\mathbf{B}_{\mathrm{cli}}$ (left panels) and the later developed 1979-$\mathbf{B}_{\mathrm{cli}}$ (right panels). The forecasts are verified against own analysis. Warm colours indicate higher anomaly correlation (better performance) for ERA5, while cold colours are in favour for ERA-Interim. Hatched areas indicate points of statistical significance.

As the **B** matrix is modeled using the wavelet formulation, allowing background error correlations to be scale- and location-dependent, notable differences were indeed found in data sparse regions, such as the Pacific Ocean, where, in the year 1979, the number of conventional observations as well as the satellite data was significantly smaller than in the present time. Figure 9 shows a comparison of background error horizontal correlation lengths for temperature at 10 hPa (left panel) and 500 hPa (right panel). The 1979-$\mathbf{B}_{\text{cli}}$ horizontal correlation lengths scales are longer, particularly in the stratosphere, where, for the selected location over the South Pacific the e-folding distance is around 500 km (blue solid line) whereas in 41r2-$\mathbf{B}_{\text{cli}}$ about 300 km (red solid line). At 500 hPa, over the South Pacific, the correlation length are the same in the 1979-$\mathbf{B}_{\text{cli}}$ and ERA-Interim and smaller in 41r2-$\mathbf{B}_{\text{cli}}$. Over North America, a data rich region, the correlation length are smaller than over South Pacific, as expected. However, in the 1979-$\mathbf{B}_{\text{cli}}$ these are longer. The vertical correlations are broader in the troposphere (not shown) for the 1979-$\mathbf{B}_{\text{cli}}$.

For ozone, the creation of the 1979-$\mathbf{B}_{\text{cli}}$ led to anomalous values that seemed so wrong that it was decided to keep the 41r2-$\mathbf{B}_{\text{cli}}$ part for this quantity. These anomalous results were later connected with problems in the polar night, as detailed in Section 3.4.4.

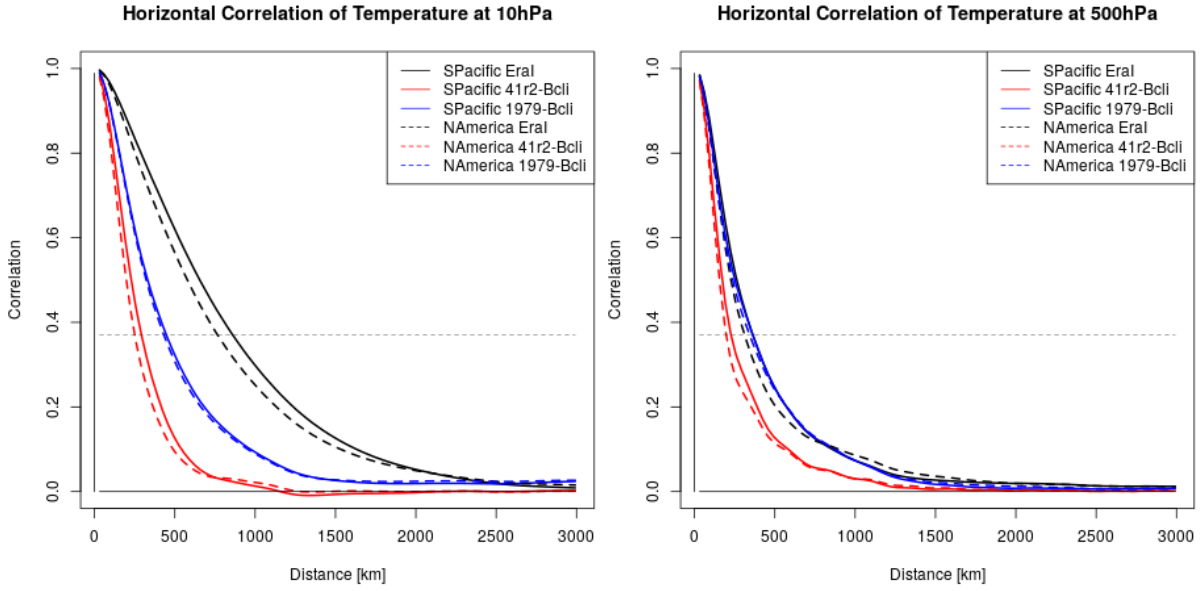

Figure 9: Background error horizontal correlation for temperature at 10 hPa *(left) and 500* hPa *(right) for a location in the South Pacific (solid line) and North America (dashed line), for respectively ERA-Interim (black), 41r2-*$\mathbf{B}_{\text{cli}}$ *(red) and 1979-*$\mathbf{B}_{\text{cli}}$ *(blue) . The dotted horizontal line represents the e-folding value.*

Subsequent scout runs based on the newly determined 1979-$\mathbf{B}_{\text{cli}}$ now showed very promising results and, finally, the degradation over the southern hemisphere had disappeared. This is demonstrated in the right panels of Figure 8. The positive impact of the full ERA5 system (HRES plus EDA using the hybrid formulation) can be seen from Figure 1. For the 1980s results improved as well, while in the stratosphere the 1979-$\mathbf{B}_{\text{cli}}$ provides a much more effective anchoring of model bias by radiosonde data, until increasing amounts of GNSS-RO from the year 2006 largely take over this role (Section 3.9.6).

The 1979-$\mathbf{B}_{\text{cli}}$ is used for the ERA5 final product from 1979 to 1999 inclusive, while the 41r2-$\mathbf{B}_{\text{cli}}$ is used afterwards. For the back extension, a dedicated 1958-$\mathbf{B}_{\text{cli}}$ has been created to better represent the pre-satellite era.

3.4.2 *Quality control for surface pressure*

As was previously identified in the ERA-20C and CERA-20C century-long reanalyses, quality control is very important for conventional data over the southern hemisphere in early decades, where no or few neighbouring (conventional or satellite) data are available for cross-checking. This necessary condition was confirmed in ERA5 when the time series of mean global mass showed significant reductions for March 1985, and forecast skill became considerably degraded. The problem was traced back to the assimilation of one faulty drifting buoy (55513), for which the sensor appeared to be stuck and reported a surface pressure of 916.9 hPa for over one month. As a result ERA5 repeatedly developed very deep (down to around 915hPa) spurious low-pressure systems off Antarctica. Blacklisting this particular sensor did resolve the problem, and since that production stream was still in spin-up mode the affected period did not need a rerun. However it was soon realized that quite a few pressure sensors have such issues, and it was decided to go through the entire ERA-Interim feedback archive (which had basically extracted the same data) to identify all stuck sensors and to blacklist each of them in ERA5. Although typically only a few sensors are affected per analysis cycle, they have the potential to cause very damaging results.

Another issue was frequent failures in the 4D-Var outer loops of the EDA, where typically the usage of poor data pushes the analysis outside reasonable boundaries leading to unphysical values in the model code. Blacklisting suspicious data by hand afterwards usually resolved the issue, but at some point failures were so frequent that the production in the early 1980s did not progress any more. Such behaviour had not occurred in preceding test scout runs, which were using a static background, rather than an evolving one through the EDA. Quality control for ERA5 which, like the current operational NWP system, is based on the Hüber norm (Tavolato and Isaksen, 2015), scales with the first-guess error. For the scout runs those errors are typically well below 1 hPa, but for the EDA, they were found to grow dramatically south of 30S because of large ensemble spread. As a result, poor data (even those with first-guess departures over 100 hPa) were not rejected, leading to even more spread in the ensemble, so even larger first-guess error, accepting even poorer data. A scan through the available feedback archive from ERA-Interim confirmed the presence of other very poor data; pressure tendencies over 50 hPa in one hour are not an exception. Technically, the large ensemble spread correctly indicates large analysis errors, but obviously this is not what is desired. The way to remove this positive feedback loop is to hard-limit the first-guess check, rather than have it proportional to the first-guess error. An upper limit of 15 hPa was imposed south of 30S, since this is the typical limit for a first-guess error of 1 hPa, and this region mostly excludes tropical cyclones. This change worked extremely well; the EDA no longer failed frequently and production speed could be resumed.

3.4.3 *Seams between production streams*

As described in Section 3.3, ERA5 is produced in a number of parallel streams, which are later appended together into one consolidated final product. Details on which streams are joined together can be extracted from Figure 7. The disadvantage of this approach is that there can be discontinuities in the final product at the transition points between the different streams. Here, as an example, we consider the transition at the start of 2010, for the repair run of 2003, and for the end of a one-year overlap period in ERA-Interim at the end of 1989.

The seam at 1 January 2010 represents the transition of the production stream (2504) that had been running over the entire 2000s and a stream (2502) that was initiated from the last day of 1998, to allow for a spin up period of one year. The left panels of Figure 10 show how well these two streams overlap for temperature and zonal wind during the last three months prior to the transition. In general a very smooth

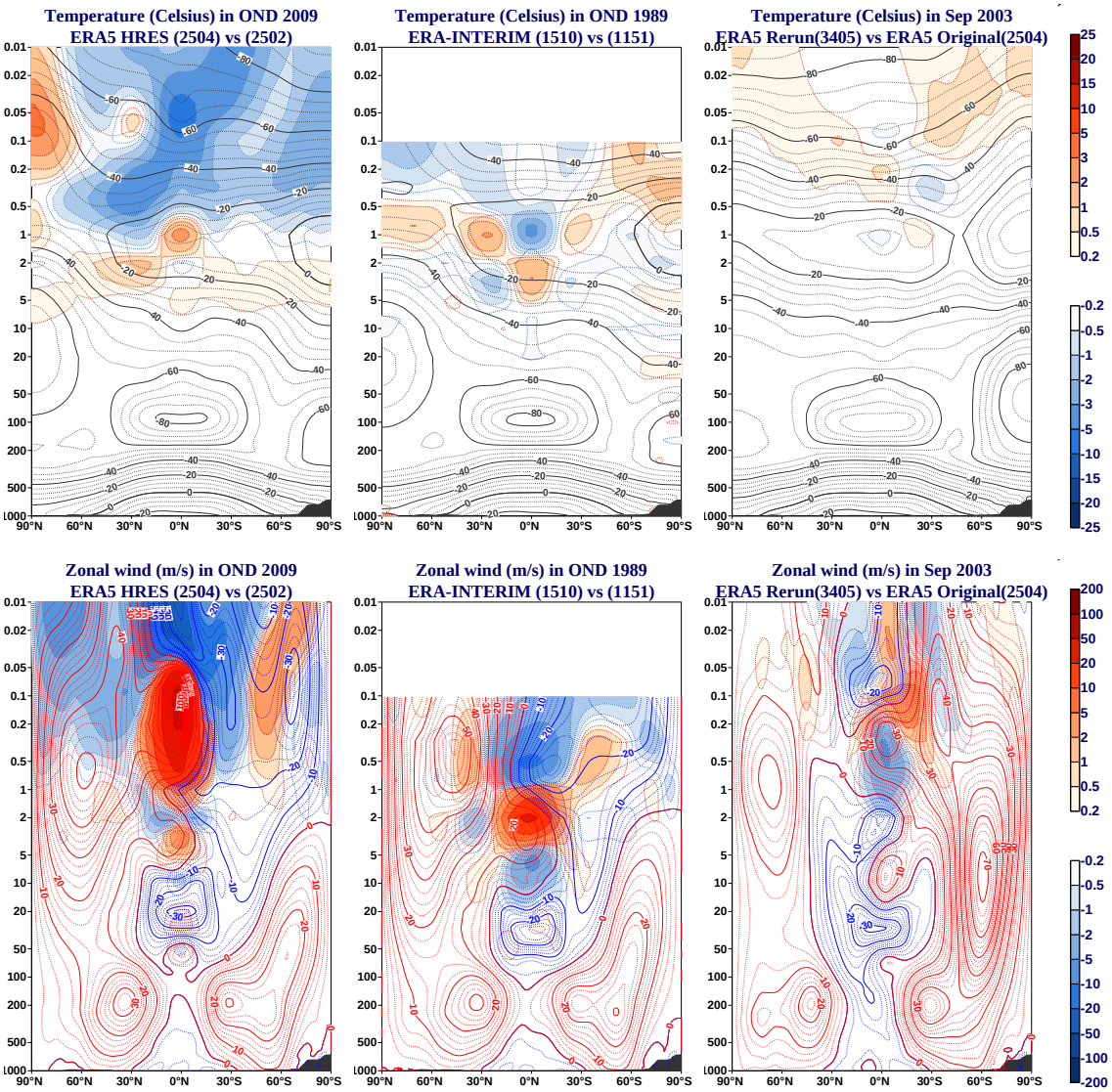

Figure 10: Seams for the HRES production streams (left, October-December 2009 mean), ERA-Interim (middle, October-December 1989 mean) and 2003 repair run (right, September 2003 mean) for temperature (top, Celsius) and zonal wind (lower panels, m/s), throughout the entire vertical (hPa). Contours are values for the final product, while shading is the difference with an overlapping stream.

transition is found over the entire troposphere and lower part of the stratosphere. For temperature there is a difference of about 2K at the tropical stratopause, and larger differences are observed higher up in the mesosphere. For wind, very large systematic differences occur in the tropical mesosphere. Part of these differences may be exaggerated by the occurrence of a spurious mesospheric jet that ERA5 suffers from (IFS cycle 41r2, details in Section 3.9.4), which, not being directly constrained by observations, may be in a different 'state' between the two streams.

A similar, but not identical, comparison of an overlap in 1989 for ERA-Interim (middle panels) reveals that in the troposphere and stratosphere the differences have, if anything, a slightly larger magnitude than those in the ERA5 transition, and ERA-Interim exhibits transition differences lower down in the atmosphere. However, in the lower to mid-mesosphere (from about 1 hPa to 0.1 hPa, with the latter being the top of the ERA-Interim domain), the differences in the ERA-Interim transition are generally smaller than in the ERA5 transition, having magnitudes less than 2 K. The equatorial transition differences in eastward wind in ERA-Interim in the lower stratosphere are slightly smaller than those in ERA5, though above in the mid to upper stratosphere, the differences are somewhat larger than those in ERA5. In the mesosphere, the transition differences in ERA-Interim are much smaller than those in ERA5.

The ERA5 transition differences for specific humidity are generally below 5%, apart from low latitudes in the mesosphere above 0.05 hPa, where differences exceed 10%. The transition differences for ozone are generally below 5% in the troposphere and stratosphere. However, in the mesosphere the ozone differences are large in the polar regions, where magnitudes exceed 20% or even 50% (not shown).

An indication for the seam is that for the streams for 2009 VarBC bias estimates do not converge to the same values. For all three available AMSU-A instruments at the time, for channel 13 VarBC indicates a bias that is about 0.2K higher in 2502, which given the fact that the observations are the same, relates to a warm bias of 2504 with respect to 2502. This is exactly observed in the left top panel of Figure 10 around 5 hPa, where channel 13 peaks. Channel 14, which peaks at around 2 hPa, is anchored, i.e., imposing smaller model differences at that height. This strong constraint together with the slight difference in temperatures below may have steered larger, opposite differences aloft.

The non-convergence of some VarBC bias estimates, even after long spin-up has been known to exist in IFS. This is one of the reasons why all perturbed EDA members use the same bias estimate from the control (see Section 3.2). For ERA5, these members are known to stay relatively close together indeed (Section 3.8), so ensuring that VarBC estimates stay close together may be a key to reduce seams. For the original production streams this is not an option, however, for the repair runs (Figure 7), an original stream is already available. Given the requirement that these runs should only deviate locally (mainly close to the surface due to differences in sea ice), it was decided to enforce the bias corrections from the original stream. This appeared to give very good results. An example is given in the right panels of Figure 10 for the repair run with seam in October 2003. Differences with the original stream are generally small, and they were even smaller for the other repair runs (not shown).

3.4.4 Ozone in the polar night

In recent years, significant effort was directed towards improved treatment of prognostic ozone in the IFS. Compared with ERA-Interim, the ozone representation in ERA5 benefits from (i) an updated version of the stratospheric ozone chemistry parametrization, (ii) assimilation of level-2 ozone observations reprocessed using improved algorithms, and ozone retrievals from new instruments, (iii) flow-dependent ozone error variances, (iv) variational bias correction of ozone observations for selected instruments (e.g. GOME, ozone-sensitive infrared radiances).

The ozone model includes the representation of the stratospheric ozone chemistry based on the Cariolle and Teyssèdre (2007) parametrization scheme in which the time evolution is expressed as a linear expansion with respect to the photochemical equilibrium for the local value of the ozone mass mixing ratio, the local overhead ozone column, the local temperature and an additional term for the rapid depletion associated with the emergence of the ozone hole.

ERA5 assimilates ozone profile and total column retrievals from a suite of instruments (e.g. GOME, MLS, OMI, BUV, SBUV, SCIAMACHY, TOMS), many of them reprocessed (see Table 5), as well as ozone-sensitive infrared radiances from HIRS and the (hyperspectral) spectrometers AIRS, CrIS and IASI (Dragani and McNally, 2013). The combined observational record for ozone spans the full period from 1979 to the present (see panel (j) of Figure 17), and several periods in the 1970s (BUV). The assimilation of ozone observations is implemented in a univariate way, decoupled from other meteorological variables.

Routine monitoring of ERA5 ozone fields during production has shown in general an improvement on ERA-Interim. However, during the 1980s and 1990s in polar night conditions ERA5 produced massive, physically unrealistic, amounts of ozone in the high stratosphere (between 1-5 hPa), increasing the total ozone column (TCO3) to up to 6 times above realistic values. Investigation of this issue has led to the preliminary conclusion that assimilating SBUV observations above 5 hPa induces increments over the (unobserved) winter pole as illustrated in panel (a) of Figure 11 for the Austral winter of 1990. Simultaneously, the ensemble spread and ozone background error variances (Figure 11, panel (e)) are significantly inflated, reducing the weight given to the model background. These conditions facilitate a positive feedback loop, allowing increasingly large ozone increments above the 5 hPa level which are transported downward with the subsiding air masses in the polar vortex and accumulate over time. This is clearly illustrated in panel (c) of Figure 11.

The mechanism through which the assimilation of SBUV data affects the ozone field during polar night is not fully understood at the moment. SBUV is a nadir-sounding instrument that measures ultraviolet sunlight scattered by the Earth's atmosphere and, therefore, is not available in polar night conditions where the problems arise. They are not subject to bias corrections in VarBC (i.e., they serve as anchors). As a pragmatic solution for ERA5, it was decided not to use any SBUV ozone observations in the EDA system and to partially blacklist (< 5 hPa) these observations in the high-resolution system. The resulting ozone increments, fields and background error standard deviation are much improved as is illustrated in panels (b), (d) and (f) respectively. The latter represent the final ERA5 product that will be released to the public.

Research into the root cause and mechanisms behind the large ozone increments over the winter poles and their relation to SBUV observations is ongoing and expected to benefit the IFS and the next generation of ECMWF reanalyses. In a previous study focused on the ERA-40 reanalysis, Dethof and Hólm (2004) discuss the problem of accurately modelling the ozone field during the polar night. They already showed that the model tends to accumulate ozone in the polar night region when no ozone observations are assimilated. Their results indicate that in ERA-40 the transport and not the ozone chemistry parametrization was responsible for the accumulation of ozone at the winter pole. They notice that the chemistry parametrization responds to changes caused by transport almost everywhere, except in the polar-night region, where the chemistry scheme is inactive for lack of incident sunlight. Whether and to what extent their conclusions apply to ERA5 is unclear at the time of writing.

In a recent line of research, J Flemming has undertaken to review the representation of the stratospheric ozone chemistry in the IFS as used in the CAMS system. In that context, he has proposed a modification in which the relaxation to the ozone climatology above 5 hPa is stronger, with imposed relaxation

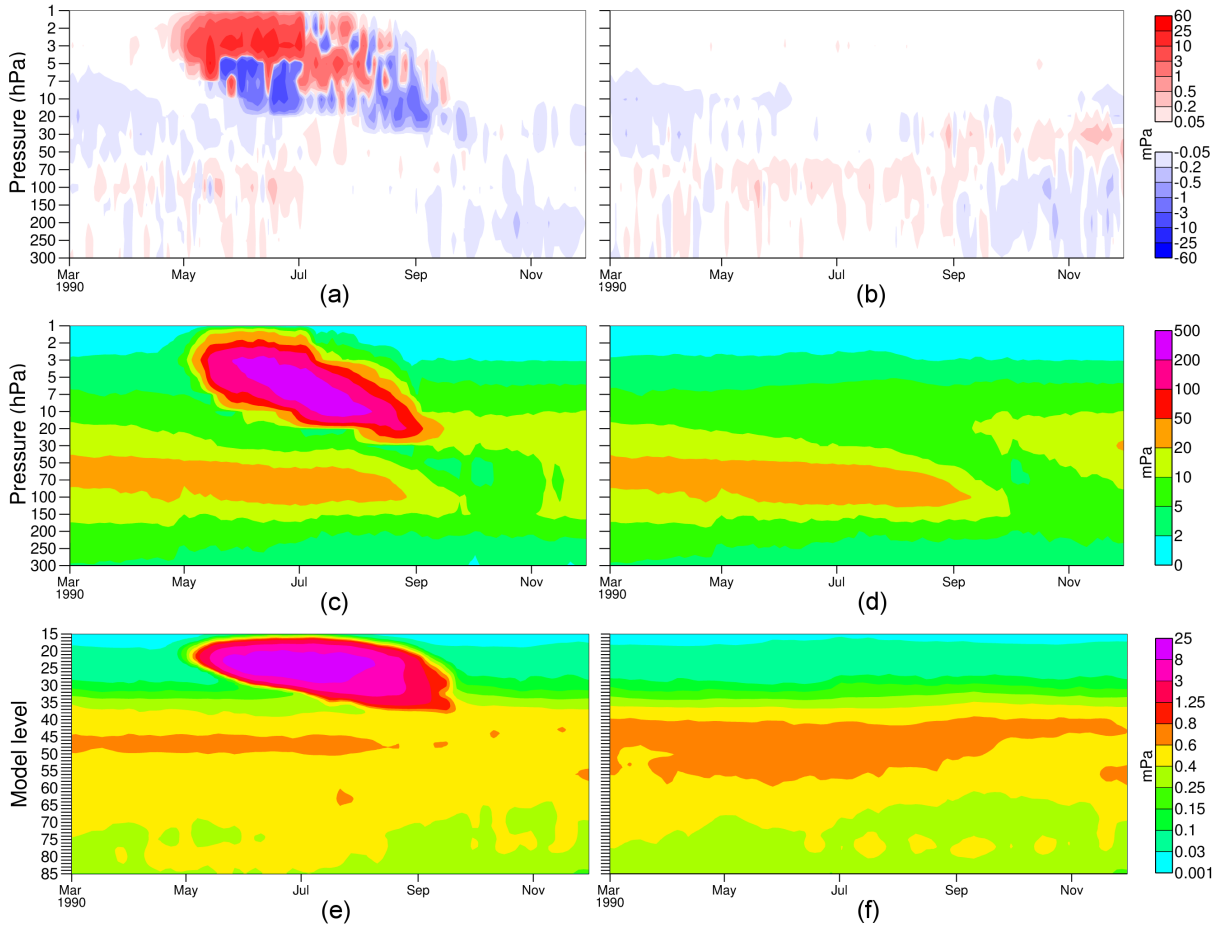

Figure 11: Area-averaged ozone increments (panels (a) and (b)), ozone fields (panels (c) and (d)) over the Antarctic continent and global-average ozone background error standard deviation from the EDA (panels (e) and (f), with comparable vertical range). Left-hand panels illustrate the situation arising in the original ERA5 production assimilating all SBUV ozone profile observation in EDA and high-resolution systems. Right-hand panels show the equivalent for the final ERA5 product assimilating limited SBUV observations in the high-resolution system only. All quantities are partial pressure (mPa).

timescale of one day (instead of un-constrained) during polar night and a corresponding weakening of the relaxation towards temperature and local ozone column. Preliminary results indicate that the stronger relaxation towards climatology is able to suppress the spurious ozone increments in polar night conditions, suggesting that modelling of ozone during the polar night can be improved upon. This modification of the Cariolle ozone scheme has recently been successfully tested for the medium-range forecasting system (E Hólm), and is considered to be part of the next possible IFS cycle upgrade. This should prevent the undesired practical solution of partly blacklisting SBUV data in future reanalysis.

3.5 Benefit from a decade of improvements in the Integrated Forecasting System

In the 10-year period between starting ERA-Interim (Cy312) and starting ERA5 (Cy41r2) many significant improvements have been made to the representation of model processes and data assimilation in the IFS. This section provides a summary of some of the major changes as well as some of the special adaptations that were required for the reanalysis effort.

3.5.1 Atmosphere

The radiation scheme used in ERA5, 'McRad', was described by Morcrette et al. (2008) and is a major upgrade from the scheme used by ERA-Interim. It incorporates the Monte Carlo Independent Column Approximation (Pincus et al., 2003) for representing subgrid cloud structure and overlap, and the shortwave Rapid Radiative Transfer Model for GCMs (RRTMG; Iacono et al., 2008), consistent with the existing use of RRTMG in the longwave. The radiation scheme is called every hour on a grid 2.5 times coarser in each horizontal direction. To mitigate erroneous temperatures at coastlines caused by the coarser grid, approximate updates to the fluxes are performed every time step and gridpoint (Hogan and Bozzo, 2015). Infrequent radiation calls can lead to a warm bias in the stratosphere, but this has been mitigated by the Hogan and Hirahara (2016) scheme for computing effective solar zenith angle.

The large-scale cloud and precipitation scheme, based on Tiedtke (1993), was upgraded with an improved representation of mixed-phase clouds (Forbes and Ahlgrimm, 2014), and prognostic variables for precipitating rain and snow (Forbes and Tompkins (2011); Forbes et al. (2011)). In addition, there were numerous improvements to the parametrization of microphysics, particularly for warm-rain processes (Ahlgrimm and Forbes, 2014) but also ice-phase processes and ice supersaturation.

Changes to the parametrization of convection, originally based on Tiedtke (1989), include a thorough revision of the entrainment and the coupling with the large-scale, leading to a large redistribution of rainfall from the Hadley cell to the Walker cell, a large improvement in the distribution of rainrate versus TRMM and an improved representation of tropical variability (Bechtold et al., 2008; Hirons et al., 2013). Improvements in the diurnal cycle of convection, shifting the rainfall peak over land from noon to late afternoon, have been achieved by use of a modified CAPE closure (Bechtold et al., 2014).

There were changes to the parametrizations of orographic drag, subgrid turbulent mixing and interactions with the surface in unstable and stable conditions (Sandu et al., 2011, 2014).

A non-orographic gravity wave drag parametrization was introduced to represent the effects of upward propagating gravity waves from tropospheric sources such as deep convection, frontal disturbances, and shear zones. The parametrization uses a globally uniform wave spectrum, and propagates it vertically through changing horizontal winds and air density, thereby representing the wave breaking effects and associated drag due to critical level filtering and non-linear dissipation in the stratosphere and mesosphere (Orr et al., 2010).

An improvement in the wind extrapolation scheme SETTLS used for the departure point calculation, described in Diamantakis (2014), reduced numerical noise in the upper stratosphere typically occurring during Sudden Stratospheric Warming (SSW) events. The practical benefits of this modification was a large reduction of both analysis and forecast temperature error and an overall enhanced medium range predictability of SSW events.

Improved de-aliasing of the pressure gradient term (see ECMWF (2016)), reduced numerical noise in the adiabatic tendencies allowing a reduction of the horizontal diffusion used in the forecast.

Regarding the tangent-linear and adjoint physics that is used in the inner loops of the 4D-Var data-assimilation system, improvements include (Janisková and Lopez, 2013) i) inclusion of the freezing of rain in the moist physics, ii) substantial revision of the moist physics to match the nonlinear reference large-scale cloud and convection schemes, iii) replacement of the old longwave radiation parametrization (neural network) by the more elaborate scheme by Morcrette (1991), iv) linearized version of the new non-orographic gravity wave drag, v) added simplified linearized parametrization scheme for surface processes to represent the evolution of the top-soil layer, snow and sea-ice temperatures and vi) revision of the linearized vertical diffusion to match the changes of the exchange coefficients in the non-linear scheme.

3.5.2 Land

In ERA5 the HTESSEL scheme is used. ERA-Interim/Land (Balsamo et al. (2015)) documented the HTESSEL scheme in its revised hydrology with respect to the TESSEL land surface scheme (van den Hurk et al. (2000)) used in ERA-Interim. Some of the most significant changes in the ERA5 land surface model compared to ERA-Interim are related to i) the introduction of the soil texture map Balsamo et al. (2009), and ii) an improved representation of bare soil evaporation Albergel et al. (2012). The new scheme also accounts for seasonally varying monthly vegetation maps specified from a MODIS-based satellite dataset (Boussetta et al. (2013)). In addition, an enhanced snowpack parametrization allows a more realistic timing of runoff and terrestrial water storage variations and a better match of the albedo to satellite products Dutra et al. (2010). Balsamo et al. (2012) introduced the capacity of forecasting of inland-water bodies and evaluated the impact when coupled to the atmosphere, following a previous offline evaluation of lakes sensitivity (Dutra et al. (2009)). The chosen parametrization for lakes (FLake, Mironov et al. (2010)), allows consideration of both sub-grid and resolved water bodies (Manrique-Suñén et al. (2013)). This series of changes all contributes to significantly improving the consistency of soil moisture and land surface fluxes in the ERA5 model compared to ERA-Interim, opening the possibility to assimilate satellite data to analyse soil moisture as described below. Furthermore, the ERA5 HTESSEL has the capacity of simulating natural land carbon simulation (Balsamo et al. (2014); Boussetta et al. (2013)). This enables representation of the CO2 exchanges along with evaporation and heat exchanges for weather and Earth system applications as operated within the Copernicus services (C3S, CAMS).

ERA5 includes an advanced land data assimilation system to analyze land surface prognostic variables: snow water equivalent, snow density, snow temperature, soil temperature and soil moisture as described in de Rosnay et al. (2014). The ERA5 land data assimilation relies on a weakly coupled land-atmosphere data assimilation approach where the land and atmospheric assimilation are running separately whereas the background forecast is fully coupled. So, feedbacks between the land and atmospheric analyses are enabled through the short forecast (see Figure 3). A 2-dimensional optimal interpolation is used to analyze screen level variables and snow variables (de Rosnay et al., 2015), in contrast to ERA-Interim which was using a Cressman interpolation for snow. The soil moisture analysis uses a simplified Extended Kalman Filter which also constitutes a major improvement compared to ERA-Interim which was

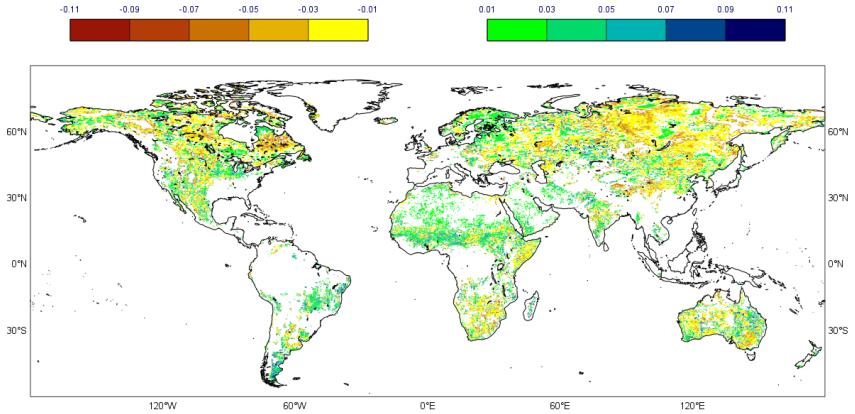

Figure 12: ERS scatterometer soil moisture mean first-guess departure (used observations minus model background, in m^3m^{-3}) for the period from 1 July 1997 to 30 September 1997.

using a 1D-OI (de Rosnay et al., 2013). Over land ERA5 assimilates conventional and satellite observations, including land surface data records of snow cover and scatterometer soil moisture. Figure 12 illustrates the mean innovation (observation minus model background) for reprocessed ERS scatterometer soil moisture as prepared by the Technische Universität Wien, assimilated for the period covering July to September 1997. Land surface observations used in ERA5 are described in more detail in section 3.7.2. At the production level, in ERA5 the analysis of surface fields of the first reanalysis production stream initially showed spurious increments of 2m temperature and 2m relative humidity over oceans. They extended offshore up to a few dozen of km. While the land data assimilation system is designed to assimilate observations and adjust surface variables only over land masses, these spurious increments reflected just the radius of influence of surface observations close to the coastlines. This problem was identified and resolved.

3.5.3 Ocean waves

The model bathymetry was updated to use a more recent version of ETOPO2 (NOAA, 2006). A new wave advection scheme was introduced with a revised unresolved bathymetry scheme to account better for the propagation along coastlines and to model better the impact of unresolved islands (Bidlot, 2012). The slow attenuation of long period swell as well as the impact of shallow water on the wind input was introduced with an overall retuning of the level of dissipation due to white-capping (Bidlot, 2012). Extra output parameters were introduced to better characterise freak waves (Janssen and Bidlot, 2009), swell systems and wave modified fluxes to the oceans.

The ocean wave data assimilation is not part of the 4D-Var cost function but rather it is performed as part of the model integration in the last trajectory based on a sequential optimal interpolation scheme. Originally set-up to assimilate altimeter wave height data in centered 6-hourly windows, it was adapted to be done hourly in order to match the hourly output of ERA5. It was found that because of the sequential nature of the scheme, it yields smoother hourly time series.

The quality of the ERA5 ocean-wave analyses is much improved (as can be seen from a comparison with independent data in Figure 13). This is the result of improvements and increased resolution for the atmosphere (providing better winds that generate better ocean waves), the wave model, and the improved observing system and assimilation system as a whole.

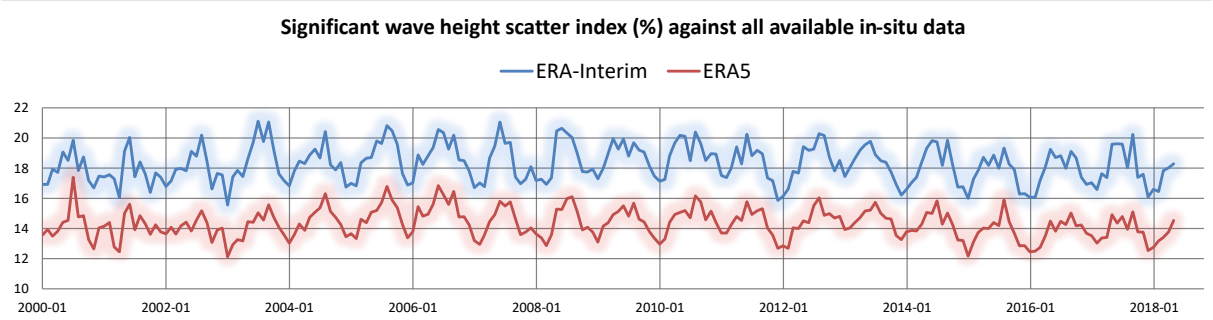

Figure 13: Scatter index (percent, lower is better) with respect to independent buoy wave height observations for ERA-Interim (blue) and ERA5 (red) analyses.

3.5.4 Observation bias correction

Like ERA-Interim, ERA5 uses a variational bias correction scheme (Dee, 2004). This method is able to correct biases and changes in these that occur either gradually or abruptly. It formed one of the important innovative features of ERA-Interim with respect to ERA-40. Although for ERA-Interim VarBC was limited to satellite radiances, ERA5 benefits from the extensions that have been introduced in IFS, since. These include observations for Ground-Based Radar observations, ozone level-2 (with the exception of MLS, BUV, SBUV-2 and MIPAS), ozone level-1B data (channel 9 on HIRS instruments), surface pressure and aircraft temperatures. With regards to aircraft data, only one predictor per group (one constant per aircraft) is used, rather than the three predictors in the operational system (also ascent and descent speed), since during the preparations for ERA5 that implementation was discovered to be flawed. This has since been corrected (Ingleby et al., 2018) in the latest operational model cycle (CY45r1). At cruise level (around 200 hPa) aircraft data are on average found to be biased warm by about 0.2K, which had affected the temperature estimate in ERA-Interim when their numbers significantly increased around 1999 (Dee and Uppala, 2009), and which has been alleviated in ERA5.

Although, in general, VarBC is working extremely well, a number of issues were found during the production of ERA5. One example is the incorrect initialization of bias coefficients for cloud-affected channels on some infrared instruments. In VarBC such initialization is based on the mode (most populated bin) of the departure statistics of first occurrence. In the case of non-optimally calibrated data, this estimate can be so wrong that the cloud-detection scheme, which depends on (in this case poorly) bias-corrected first-guess departures, rejects almost all data. As a result, the very limited amounts of data that are assimilated have insufficient weight to improve on the bias estimate. Such situation can remain for over a year until, by coincidence, a critical threshold is hit and after a quick bias adjustment, the data are finally assimilated normally. This non-optimal situation will not, as such, lead to a clear degradation of reanalysis products and can be seen as a missed opportunity, instead. More serious, though, is when the quality control does not screen out data with poorly initialized bias estimates. This can lead to degradation of model estimates during the bias spin-up (which can last several months). In addition, this can affect bias estimates for other, related parts of the observing system, as well, by aliasing of the temporarily imposed model bias. For ERA5 this was observed several times (an example is MSU channel 4 on AMSU-A in 1986), and where possible was resolved by setting back the production suite and reinitializing VarBC coefficients by hand just prior to the first active use.

For surface pressure, bias estimates are also updated by VarBC as it was developed for the ERA-20C reanalysis (Poli et al., 2016), using one constant predictor per platform with a response time of 60 days. For these observations, VarBC is performed in the screening task, i.e., before the minimization in 4D-Var.

Model	TFK09	ERA5	ERA-Interim	ERA-20CM
Incoming Solar Radiation	341.3	340.4	344.2	340.4
Net Absorbed Solar Radiation (ASR)	239.4	242.7	244.3	240.9
Outgoing Long-wave Radiation (OLR)	238.5	242.2	245.5	240.6
TOA Net in ($\mathbf{R_T}$)	0.9	0.4	-1.2	0.3
Net Absorbed by surface ($\mathbf{F_S}$)	0.9	6.1	6.9	1.9
Atmosphere Net (TEI=$\mathbf{R_T} - \mathbf{F_S}$)	0.0	-5.6	-8.1	-1.6

Table 3: Global mean energy budgets (Wm^{-2}) according to TFK09, ERA-Interim and the ensemble mean of ERA-20CM, averaged from March 2000 to May 2004 for TFK09, and from 1989 to 2008 for ERA5, ERA-Interim (both based on the first 12 hour forecasts) and ERA-20CM.

Reason for this is to avoid an undesired (understood) interaction with the applied Hüber norm (Tavolato and Isaksen, 2015) that would lead to a far too slow response.

Regarding bias corrections for radiosonde temperature, an update of the method of a pre-calculated RAOBCORE (Haimberger et al., 2008) homogenization as in ERA-Interim is used. In this collaboration with the Universität Wien, estimates are now also based on comparison between neighbouring stations, rather than from departure statistics alone (RISE, Haimberger et al. (2012)). From 1 January 2015 onwards such estimates are not available and ERA5 follows the bias-correction scheme in the operational medium-range forecast system, instead.

For altimeter significant wave height bias-corrections were pre-determined such that these observations emerge unbiased with respect to the ERA5 model, rather than unbiased with respect to independent in-situ measurements.

3.6 Dedicated model input data for ERA5

Besides information from synoptic observations, the IFS relies on other external information, such as forcing into the radiation scheme and the prescription of sea-surface temperature and sea ice over the global oceans. For ERA5 a special effort was made to include state-of-the-art datasets that describe well the low-frequency variability of the climate system. A large part of this work was prepared during the ERA-CLIM project. A short overview of the ingested datasets is presented, as well as their effect on the ERA5 reanalysis products.

3.6.1 CMIP5 forcing terms in radiation

Clearly the provision of the total solar irradiance (TSI) is very important, but also the provision of aerosols, greenhouse gases and ozone. In principle such fields (except TSI) should be prognostic in a fully coupled Earth system, however, currently these are still imposed. A reanalysis spanning several decades requires that such fields follow the observed 20th and 21st century evolution. Within the ERA-CLIM project, state-of-the-art and standardized sets of such long-term forcing fields as available from the World Climate Research Programme (WCRP) initiative CMIP5 were implemented as options in the IFS, and were first tested in an ensemble of century-long model integrations (ERA-20CM). Details may be found in (Hersbach et al., 2015). This capability is used in ERA5. It forms an improvement on ERA-Interim, which, e.g., omitted the occurrence of stratospheric sulphate due to major volcanic eruptions.

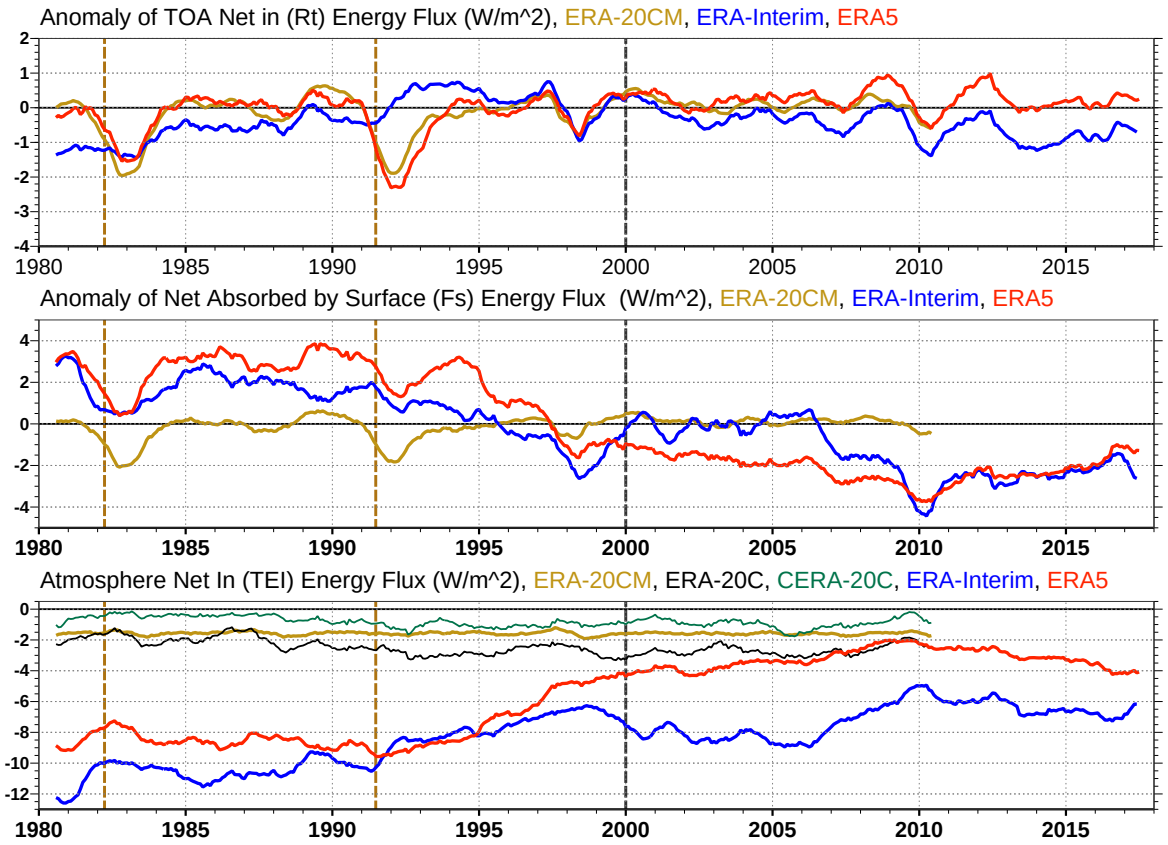

Figure 14: Evolution of one-year moving average of energy budgets in ERA5 (red), ERA-Interim (blue) and ERA-20CM (gold), for the TOA Net-in radiation (top panel, relative to 1989-2008), Net Absorbed Surface radiation (middle panel, relative to 1989-2008) and for the Atmosphere Net flux (lower panel) which latter includes ERA-20C (black) and CERA-20C (green). The vertical ochre dashed lines indicate the eruption dates of El Chichón and Pinatubo, while the solid black line (Jan 2000) marks the date from which ERA5 is publicly available at the time of writing.

The average effect (1989 to 2008) of these forcings on global radiation budgets is displayed in Table 3 where, like Berrisford et al. (2011), values are compared with Trenberth et al. (2009), denoted hereafter by TFK09. From this it directly emerges that the lower value of TSI for ERA5 (based on TIM rescaling (Lean et al., 2005), first used at ECMWF in the Seasonal System 4 implementation, (Molteni et al., 2011)) compares considerably better with the estimates from TFK09 than ERA-Interim does, which by mistake used too high values. The net energy input at the top of the atmosphere (TOA), which results in a net global warming, agrees within known uncertainty (Trenberth et al. (2014), Allan et al. (2014)); this in contrast to ERA-Interim, which has the wrong sign. Like for ERA-Interim the net absorbed energy at the surface, however, is far too large. This would lead to an atmosphere net (TEI) energy loss of about 5.6 Wm^{-2} (8.1 Wm^{-2} for ERA-Interim). Apparently the assimilation system systematically adds energy, which is then dumped into the surface during the connecting short forecasts, which emerges as the diagnosed loss (Mayer and Haimberger, 2012). For ERA-20CM the alleged atmosphere net loss of -1.6 Wm^{-2} results from an unknown error in the book keeping of energy budgets, since for these model-only runs energy is observed to rise by only about 0.01 Wm^{-2} (i.e., according to global warming). Although the magnitude of this deficit varies with model cycle, this would suggest that the actual energy imbalance in ERA5 is in the order of 4 Wm^{-2}.

A more detailed picture is presented in Figure 14, which shows the evolution from 1979. The top panel shows that the response from the El Chichón and Pinatubo eruptions is clearly captured by ERA5 and

Time period	Sea-Surface Temperature	Sea-Ice Cover	grid (deg)
Jan 1949 - Dec 1960	HadISST2.1.0.0 (monthly)	HadISST2.0.0.0	0.25x0.25
Jan 1961 - Dec 1978	HadISST2.1.1.0 (pentad)	HadISST2.0.0.0	0.25x0.25
Jan 1979 - Aug 2007	HadISST2.1.1.0 (pentad)	OSI-SAF (409a)	0.25x0.25
Sep 2007 - onwards	OSTIA	OSI-SAF oper	0.05x0.05

*Table 4: SST and SIC products as used in ERA5. All products are daily, although 'pentad' is based on 5-daily and 'monthly' (and all HadISST2 ice datasets) on one-monthly assimilation windows. HadISST2 sea ice is gridded on a quarter degree; however, the native resolution is one degree. The OIS-SAF (409a) 10*km*polar stereographic grid is regridded in-house to facilitate its usage.*

ERA-20CM, but missed by ERA-Interim. Responses from El Niño events are captured by all. At the TOA there is no real long-term trend. This is in sharp contrast to the surface (middle panel), and the resulting net loss in energy (lower panel) is worse when going further back in time. This could be the result of larger systematic increments. Around 2010 ERA5 briefly almost reaches the 'energy-neutral' state of ERA-20CM. A detailed study is required from where the evolution of sinks (and sources) originate. For ERA-20C and CERA-20C TEI is remarkably good and comparable to that for ERA-20CM.

3.6.2 Sea-surface boundary conditions

As ERA5 does not contain prognostic parts for the ocean or sea ice, conditions for sea-surface temperature (SST) and sea-ice cover (SIC) need to be prescribed. ERA-Interim had followed a configuration as it was partly used in the operational medium-range forecasting system at the time and partly as what was used in ERA-40 (Fiorino, 2004). The configuration may be found in Table 1 of Dee et al. (2011). For ERA5 a careful selection procedure was conducted within the visiting scientist programme with the Japan Meteorological Agency (Hirahara et al., 2016). The goal was to compile a dataset from 1950 onwards that is i) as accurate as possible at each moment in time ii) has climate quality, such as no noticeable breaks at transitions between products, and iii) is able to provide timely data for the ERA5T continuation close to real time. For SST various flavours of the Met Office Hadley Centre HadISST2 product (Kennedy et al., 2016) were considered (as developed within the ERA-CLIM project and used in the ERA-20CM, ERA-20C and CERA-20C centennial products), as well as the Climate Change Initiative (ESA CCI) SST v1.1 (Merchant et al., 2014), to be combined with the Met Office OSTIA product (Donlon et al., 2012) which latter is used in the ECMWF medium-range forecasting system since 2007. For SIC the EUMETSAT OSI-SAF reanalysis product (version 409a, Eastwood et al. (2014)) and various flavours of the HadISST2 sea-ice product (Titchner and Rayner, 2014) were regarded, to be combined with the operational OSI-SAF product which latter is also part of the OSTIA product.

As a result of this study, the choices for ERA5 are displayed in Table 4. The OSTIA product as used in the ECMWF operational forecasting system is valid for the previous day, since that is the latest product available at analysis cut-off time. ERA5T is conducted two days later, and this extra time allows the usage of OSTIA for the valid date. The long-term evolution of SST and SIC is displayed Figure 15. The global-mean SST shows the impact of global warming from the mid 1970s, as well as the influence from El Niño events and major volcanic eruptions. Arctic sea ice shows a general decline over time, especially during summer time (minimum extent usually in September).

Quite late into the production (Dec 2017) it was realized that there is an issue with the quality control on spurious coastal sea ice as it was applied in ERA5 to OSI-SAF (409a) data. It is based on a land-spillover correction from Markus and Cavalieri (2009), rather than relying on quality flags in the product. Unfortunately, that method did not remove erroneous sea ice around the Gulf of Finland, which appeared

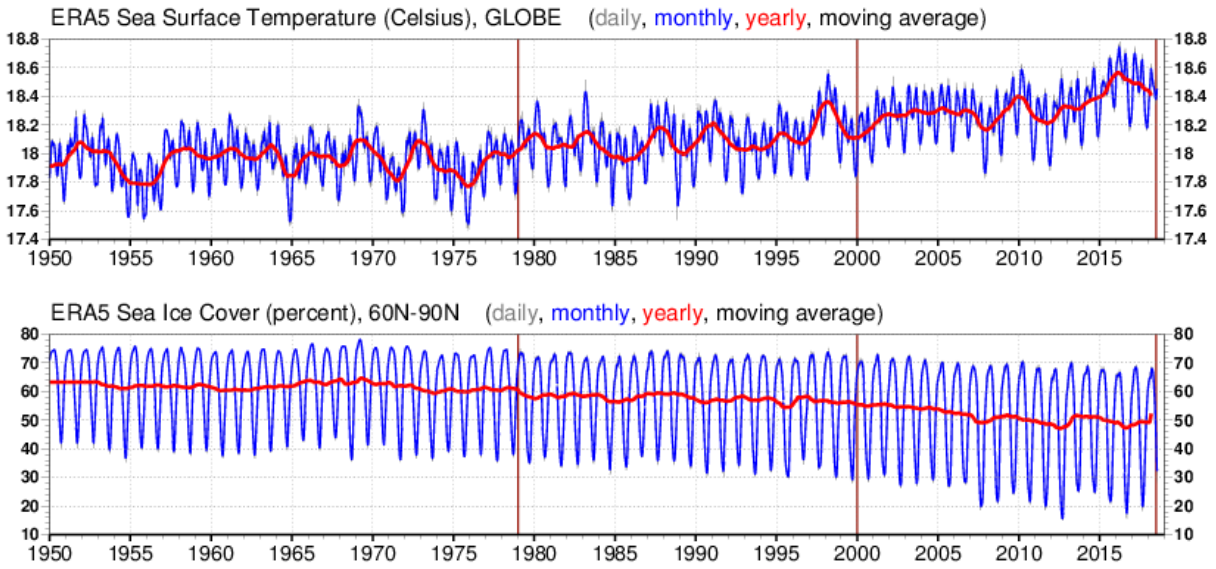

Figure 15: Time series of global sea-surface temperature (Celsius, top panel) and Arctic sea-ice cover (percent, lower panel) as used in ERA5 for data that has been released (from 2000), is produced but not yet released (1979-1999), and still to be produced (1950-1978), for daily (grey), monthly (blue) and yearly (red) running mean averages.

to occur during most of June and July for every single year between 1979 to 2007. An example is provided in the left panel of Figure 16 for 27 July 2006. The incorrect sea ice has a big adverse impact on the local surface temperature (being about 10 degrees too cold) and weather. Since this problem emerged in a prime area of Europe, close to Helsinki, it was realized that this is an unacceptable flaw. A workable solution was found by re-imposing a consistency check on SST that had been disabled in the operational forecasting system a few IFS cycles before to resolve the incorrect clearing of ice below melt water in the Arctic. A set of fast-running experiments was conducted for the entire affected period (1979-2007) where only the SST and SIC analysis is activated. Based on this it was reassured that by reactivating the check, and by raising the limit from 1 Celsius to 3 Celsius, not only the sea-ice issue in the Baltic was resolved, but also that is was not overactive. This latter issue occasionally occurs over the Hudson Bay for ERA-Interim, which does use the clearing flag for 1 Celsius. In addition it was checked that other regions of spurious ice such as south of Novaya Zemlya in the left panel of Figure 16 are also successfully cleared (middle panel). It should be noted that ERA5 resolves the incorrect 100% ice concentration north of 82.5N as it was applied to ERA-Interim prior to February 2009 (right panel), which was particularly poor in September 2007 when see ice retreated beyond that perimeter.

In general, land contamination does not affect Antarctic ice and the re-instated check on SST appears neutral in this region. For this continent, however, spuriously low concentrations were identified during the Austral winters of 1979, 1986 and 2004, which can be attributed to periods where the available passive microwave radiometer data, on which the product relies, was limited. Ice edge looked nominal during such periods. The HadiSST2.0.0.0 product (as to be used prior to 1979) did not show such behaviour, and a method was found to merge both products during affected periods such that ice concentration is improved, but ice edge is maintained (overwrite with HadiSST2.0.0.0 where both products are above 15%).

In addition it was also realized that OSI-SAF(409-a) did not provide ice over the Caspian Sea in winter, and that the choice of the FLake model Mironov et al. (2010) over the Great Lakes for the period where no information was available from OSTIA gave rise to a far too large annual cycle for its lake temperature.

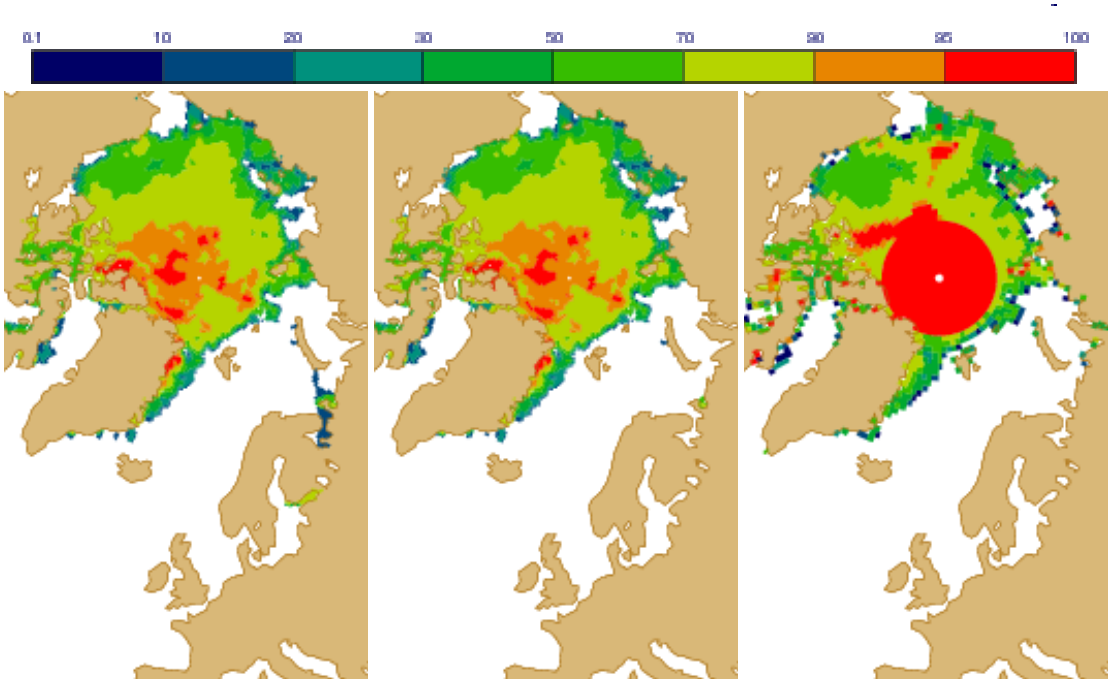

Figure 16: Sea-ice fraction (percent) for 27 July 2006 for the original ERA5 HRES production (left), the final product (middle) and ERA-Interim (right panel).

For these, practical solutions were found as well.

As said, the problem was discovered quite late, and it was impossible to re-run or locally repair ERA5. It was decided to only rerun the ERA5 HRES, and not the EDA (the ensemble spread, i.e., the ERA5 uncertainty estimate, was found to be much less affected). This was achieved in 8 one-year parallel repair streams from 2000 to 2008 (to allow for a fast recreation of this time-critical period that was to be released in 2018 Q1), and three less time-critical repair runs in earlier decades (see lower part of Figure 7). Total impact on production schedule and cost could in this way be limited. In order to prevent these runs to deviate too much from the original production (particularly in the stratosphere, see Section 3.4.3 for details), it was decided to impose the VarBC coefficients of the original production, as this method had proven to avoid a too large deviation of ensemble members in the EDA (see Section 3.1). As was discussed in Section 3.4.3, this was found to work extremely well.

3.7 The improved observing system

3.7.1 General overview

The number of observations assimilated in ERA5 has increased from approximately 0.75 million per day on average in 1979 to around 21 million per day by July 2018. Figure 17 shows, on a logarithmic scale, the daily counts for all observations used in the atmospheric analysis for each of the observables assimilated. The radiance data are the dominant and growing type of data throughout the period. Major developments for this class of observations have included the transition from the TOVS to ATOVS suite of sounding instruments, the introduction of hyperspectral infrared radiances from AIRS, IASI and CrIS and the increasing availability of data from a growing constellation of microwave imagers (SSMI, SSMI/S, TMI, GMI and AMSR-E/-2). There has been a marked increase in the number of other satellite

observations assimilated, notably GNSS-Radio Occultation bending angles, scatterometer wind data and Level-2 ozone products. The volume of conventional data has increased steadily throughout the period. An analysis of the observation impact, based on the Degrees of Freedom for Signal diagnostic (DFS, Cardinali et al. (2004)) shows that, as expected, satellite observations play a progressively more important role through the period, with radiosonde observations providing the dominant impact in the earliest streams and the radiance observations dominating in the current era, with a cross-over around the late 1980s when the impact of HIRS (in terms of DFS) matched that of the radiosondes (Horányi, 2017).

Figure 17 also shows the data volumes assimilated in ERA-Interim. Generally, more observations are assimilated in ERA5. Several discrepancies are apparent. The divergence in the volume of radiance data assimilated post-2007 (panel **a** of Figure 17) is due to the assimilation of many new observations in ERA5, such as the hyperspectral data from IASI and CrIS, which are not assimilated in ERA-Interim, together with the gradual decline in the numbers assimilated in ERA-Interim, as instruments and channels gradually fail. ERA5 uses a revised cloud detection scheme for HIRS (Krzeminski et al., 2009) which appears to remove more data and this is why, initially, fewer radiance data are used in ERA5. The initially smaller gain in forecast skill for ERA5 (lower panel of Figure 1) seems to be unrelated to this scheme, though, since ERA-Interim type experiments with the revised scheme performed comparably to ERA-Interim itself. ERA-Interim also shows a sharp decline in the number of surface pressure and upper air winds and temperatures following the transition to BUFR format from 2013 onwards that it cannot handle. Finally, as discussed in more detail in Section 3.7.2 below, ERA5 makes use of several new and improved reprocessed datasets.

ERA5 benefits from many improvements in the observation operators and in the handling of observations implemented in the IFS since the start of ERA-Interim (based on IFS cycle 31r2, with RTTOV-7 as the radiative transfer model). ERA5 uses RTTOV-11 as the observation operator for radiance data (Lupu and Geer, 2015), which incorporates improvements in the underlying spectroscopy in both the microwave and infrared as well as improvements in the optical depth predictor model relative to RTTOV-7.

ERA5 also benefits from the ongoing development of all-sky assimilation at ECMWF. Initially implemented for the microwave imagers the scheme was successfully extended to microwave humidity sounding data at Cycle 40r1. The approach exploits the capability of RTTOV to model radiative transfer in cloudy and precipitating atmospheres, as well as the linearised moist physics scheme, to assimilate microwave observations in all-sky conditions. All-sky assimilation improves analyses both through the improved analysis of moist variables, as well as through improved dynamical fields resulting from the ability of 4D-Var to extract wind information from the advection of tracers, in this case humidity, cloud and rain. The scheme rectified a problem with the earlier 1D+4D-Var assimilation of rain affected radiances which, in ERA-Interim, resulted in an underestimation of global rainfall (Dee et al., 2011). More details can be found on the subject in Geer et al. (2017).

Several other developments have enhanced the exploitation of observations since ERA-Interim. The diagnosis and modelling of several types of observation errors has advanced significantly since 2007 (*e.g.* Bormann et al. (2009)). For example, for AMSU-A improvements were made at Cycles 37r2 and 41r2 resulting in increased weights and more optimal handling of observation errors in cloudy scenes and over orography. Situation dependent observation errors for AMVs were introduced at Cycle 40r1, and the observation errors for GNSS-RO bending angle data were re-tuned at Cycle 41r2. Advances have also been made in extending the use of microwave data over land and sea-ice surfaces (Bormann et al., 2017). For GNSS-RO data, allowance for tangent point drift was introduced at Cycle 37r2 (Poli et al., 2009) and a 2D observation operator implemented at Cycle 41r1 (Healy et al., 2007).

Regarding the early satellite era, several aspects of the observation operator for key satellite datasets have

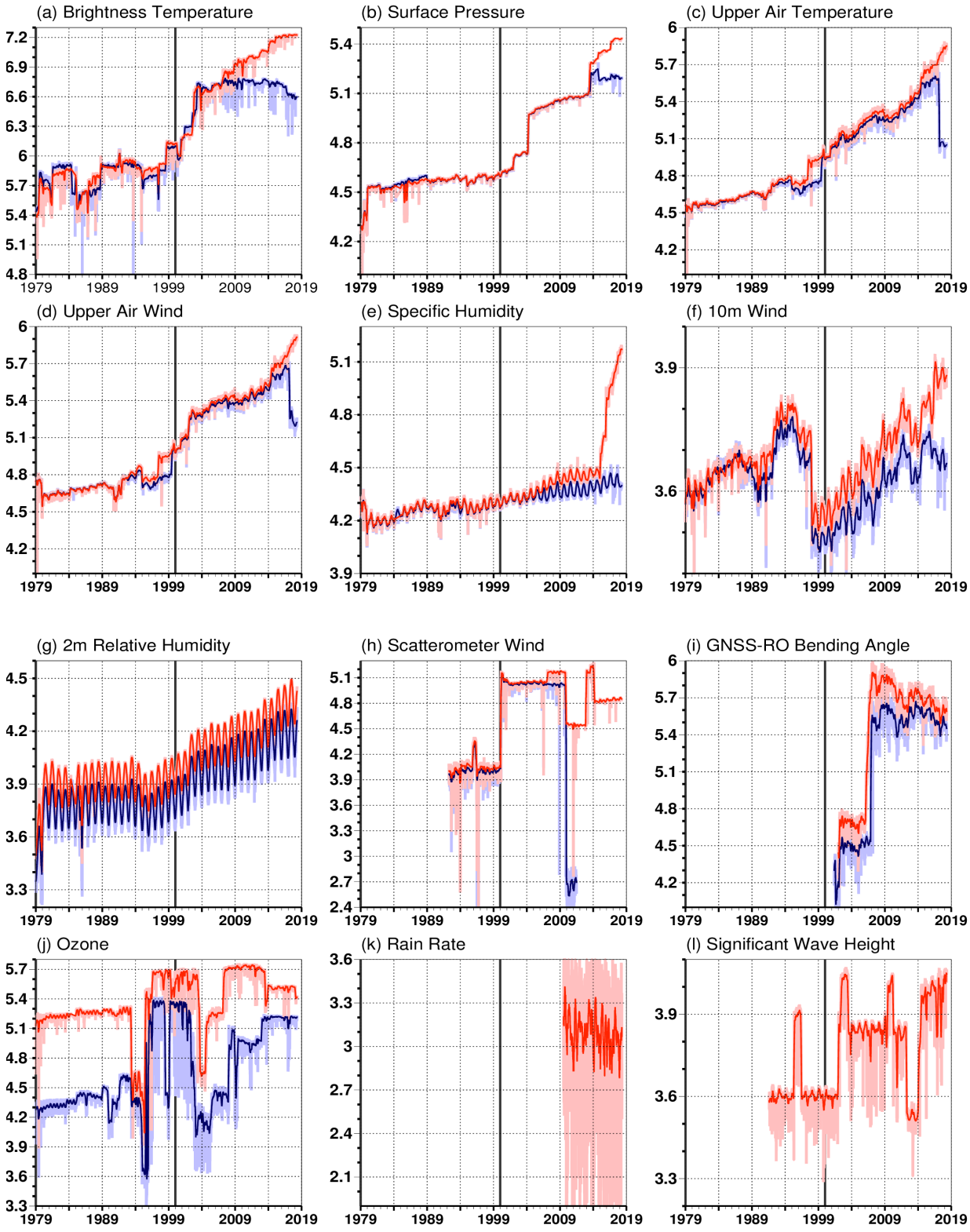

Figure 17: Number of daily used observations (weak colours) and 30-day means (strong colours), both in log10 scale for ERA-Interim (blue) and ERA5 (red) for the observables that are assimilated in the 4D-Var system. No statistics are available for ERA-Interim significant wave height, while rain is only assimilated in ERA5. Numbers for upper-air wind exclude data for assimilated atmospheric motion vector wind. Each tick (0.3) corresponds to a factor of 2 and minor ticks (0.1) to a difference of 26%.

been improved. Observations from IR sounding instruments provide important information on upper-air temperatures. This information is mainly extracted from channels at wavelengths around the 15 μm CO_2 band. For these channels the form of their weighting functions, and in particular the heights of the peaks in the weighting functions, is determined by the form of the CO_2 concentration profile which exhibits seasonal variability as well as long term trends. Shine et al. (2008) have shown that the long term trend in CO_2, if unaccounted for, gives rise to spurious atmospheric temperature trends from SSU observations which range from -0.4 K.decade^{-1} to +0.4 K.decade^{-1}, depending on altitude. In ERA5 the variability in CO_2 is taken into account for the IR sensors assimilated during the early period in the reanalysis: HIRS; SSU and VTPR. CO_2 profiles used in RTTOV-11 are estimated from zonal fields as used in the ERA5 radiation scheme (Section 3.6.1). In pre-production testing the effect of this has been positive, successfully correcting for spurious trends and improving the standard deviation of first guess departures.

In a separate development an improved observation operator for the assimilation of SSU observations has been incorporated in ERA5. The SSU instruments, forming part of the TOVS suite of instruments and operational from late-1978 until mid-2006, provide valuable information on mid-upper stratospheric temperatures in the *pre*-ATOVS era (*i.e.* pre-1998). The SSU instrument is an infrared radiometer employing a detection technique based on pressure modulation. Leaks in the pressure modulator cells have led to complex time-dependent biases in the observations (Nash and Saunders, 2015). A parametrized correction scheme has been developed and tested, based on measured cell pressures, which improves the simulation of brightness temperatures for NOAA-7 and NOAA-11.

3.7.2 Reprocessed and new datasets

Improvements in the characterisation, inter-calibration and processing of conventional and satellite data enable data providers to progressively refine the quality of historic observations, in terms of coverage and accuracy. ERA5 has made use of several reprocessed satellite datasets, which were acquired from a number of space agencies and institutes, as listed in Table 5 below. Also shown in Table 5 are some new datasets not used in earlier reanalyses. As confidence in the observations grows, the results from the assimilation of the reprocessed data can yield valuable insights into both NWP model biases and the bias characteristics of independent observational data. Such an understanding, on the one hand, leads to improved NWP models and, on the other, enables agencies to improve the specification, characterisation and on-orbit performance of satellite instruments.

ERA5 assimilates a number of reprocessed Atmospheric Motion Vector (AMV) datasets from the three major providers and some new datasets (*i.e.* datasets which did not exist previously, *e.g.* recently generated polar winds from NOAA LEO satellites operating in the early 1980s). In pre-production testing significant benefit was obtained by assimilating reprocessed GOES data (-8 to -13, covering the period 1995-2013). For example, the model background fits to low level winds (below 400 hPa) were improved by 10-30% relative to those obtained in experiments assimilating near-real-time operational datasets.

Reprocessed all-sky radiances (ASRs) from Meteosat Second Generation (MSG) have replaced earlier clear sky radiance (CSR) products.

EUMETSATs Climate Monitoring-Satellite Application Facility (CM-SAF) is engaged in the development of long term Fundamental Climate Data Records (FCDRs) from a series of microwave imagers (SMMR, SSMI and SSMIS) spanning the period 1978-present (Fennig et al., 2017). These low frequency (19 - 89 GHz) microwave radiance observations constrain the analysis of lower tropospheric humidity, cloud liquid water and ocean surface wind speed. ERA5 assimilates CM-SAF SSMI FCDRs

Table 5: Reprocessed and new satellite data assimilated in ERA5*

Instrument / Satellite	Period covered	Agency
Atmospheric motion vectors		
Meteosat 1st Gen.(M-2 to -7)	1982-2000	EUMETSAT
Meteosat 2nd Gen.(M-8,-9)	2004-2012	EUMETSAT
GMS (-1,-3,-4,-5)	1979, 1987-2003	JMA
MTSAT-1R	2005-2009	JMA
GOES-9	2003-2009	JMA
GOES GVAR (-8-13,-15)	1995-2013	CIMMS
AVHRR (NOAA-7 to -18)	1981-2014	CIMSS
AVHRR (MetOp-A)	2007-2012	EUMETSAT
Radiances		
DMSP SSMI (F-08 to -15)	1987-2008	CM-SAF
Meteosat Second Gen. ASRs	2003-2012	EUMETAT
IASI* (Metop-A,-B)	2006-present	EUMETSAT
CrIS* (S-NPP/ NOAA-20)	2012-present	NOAA
MWHS*/MWHS-2* (FY-3B,-3C)	2012/14-present	CMA
TMI*/SSMIS*/AMSR-2*/GMI*	2006/10/13/15-2015/(3)present	NASA/DMSP/JAXA/NASA
Ozone channels *(HIRS, AIRS, IASI and CrIS)	1979-present	NOAA, NASA, EUMETSAT and NOAA
Radio Occulation		
Blackjack (GRACE-A,-B, CHAMP, SAC-C)	2001-2008	UCAR
IGOR (TerraSAR-X, COSMIC-1 to -6)	2006-2014	UCAR
Scatterometer		
ASCAT* (MetOp-A,-B)	2007-2014	EUMETSAT
Oceansat*	2012-2014	ISRO
Ozone retrievals		
GOME-2 (Metop-A,-B)	2007-2013	ESA/EUMETSAT
GOME (ERS-2)	1996-2002	ESA
MIPAS (ENVISAT)	2005-2012	ESA
MLS (EOS-AURA)	2004-2014	NASA
OMI (EOS-AURA)	2004-2015	NASA
BUV (Nimbus-4)*	1970-1977	NASA
SBUV and SBUV-2 (Nimbus-7, NOAA-9,-11,-14,-16,-17,-18,-19)	1978-2013	NOAA
SCHIAMACHY (ENVISAT)	2002-2012	ESA
TOMS (NIMBUS-7, ADEOS-1, Earth Probe)	1978-2006	NASA
Soil Moisture		
AMI on ERS-1,-2	1991-2006	TU Wien
MetOp-A,-B ASCAT	2007-2014	EUMETSAT

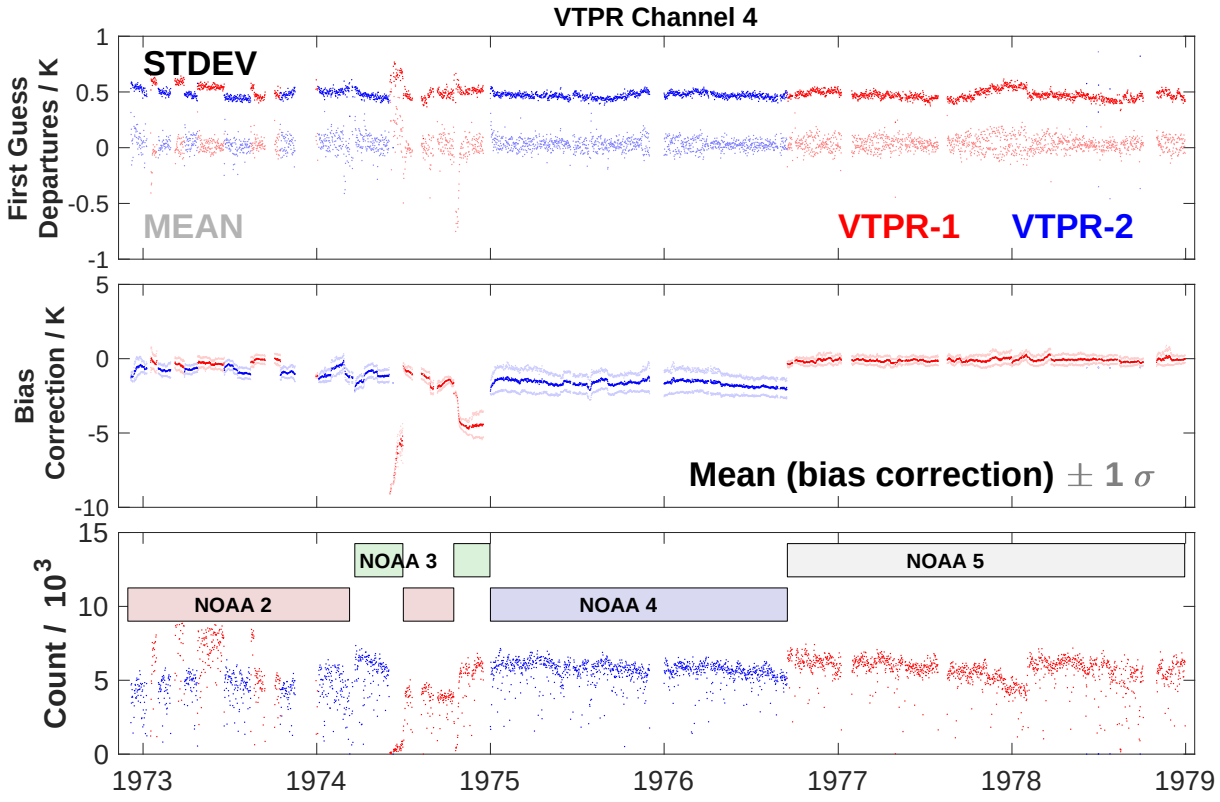

Figure 18: The evolution of (top to bottom) first guess departures (mean and standard deviation), bias corrections and observation counts for VTPR data assimilated in ERA5 scout runs covering late 1972 until the end of 1978 for VTPR channel 4, a tropospheric temperature sounding channel.

covering the period August 1987 - December 2008.

The reprocessed COSMIC GNSS-RO dataset, provided by UCAR, incorporates improved filtering of the measured phase delays. The improvement was implemented in the near real-time operational COSMIC RO dataset in November 2009 and resulted in departure statistics in much closer agreement with those of MetOp-A GRAS.

Reprocessed scatterometer (ASCAT) data from Metop-A corrects inconsistencies in the bias resulting from biases in the level-0 (backscatter) data and brings the 2007-2014 data into agreement with the operational data stream from 2014 onwards.

Several Level-2 ozone products assimilated in ERA5 have been improved through recent re-processing efforts. For example, GOME, GOME-2 and MIPAS observations were reprocessed as part of the European Space Agency-Climate Change Initiative (ESA-CCI) which improved inter-satellite consistency and uncertainty characterisation. Reprocessed SBUV/SBUV-2 datasets (version 8.6, (McPeters et al., 2013)), from NOAA/NASA, offer an increased number of levels in the vertical relative to earlier releases of the data, as well as improved consistency over the entire 40-year period covered by the data. Additional information on ozone in ERA5 is provided by ozone sensitive channels of the nadir-viewing infrared sounders (HIRS, AIRS, IASI and CrIS). ERA5 uses the initial near real-time operational NWP datasets for these sensors, but future reanalyses will make use of ongoing re-processing efforts for at least some of these datasets.

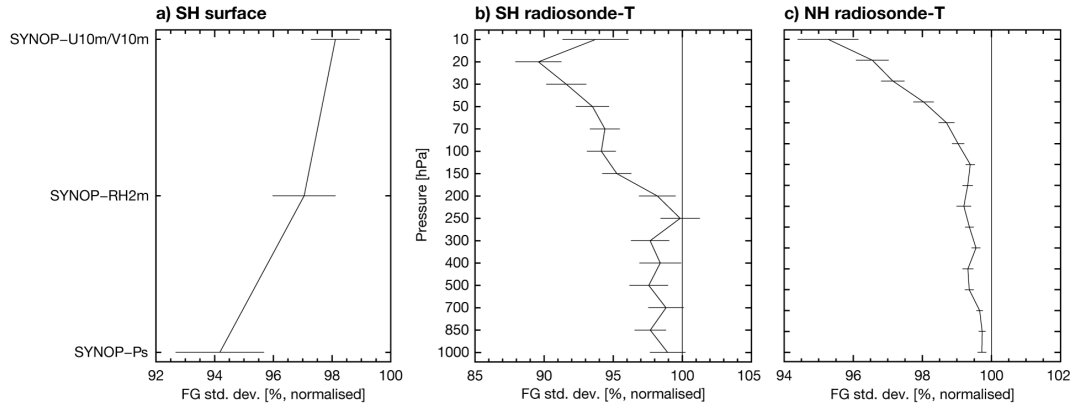

Figure 19: Change in first guess departure standard deviations for: (a) surface observations in the southern hemisphere; radiosonde temperatures in (b) the southern hemisphere and (c) the northern hemisphere, for a scout experiment in which VTPR is assimilated, compared to (i.e. normalised by) a control without VTPR, covering the period 15 January - 15 November 1975.

The re-processing of soil moisture estimates from ERS-1 and -2 brings the entire time series from 1991-2006 into consistency with the soil moisture products from MetOp-A/-B ASCAT (2007-present). ERA5 is the first reanalysis to include an analysis of soil moisture (see Section 4 for further details).

Data assimilated in ERA5 includes that from the Vertical Temperature Profiling Radiometer (VTPR), a precursor to the HIRS instrument. VTPR was flown on a series of satellites (NOAA-2, -3, -4 and -5) during the period November 1972 - February 1979. VTPR was assimilated in ERA-40 (Uppala et al., 2005) and in JRA-55 (Ebita et al., 2011). The assimilation of VTPR data in ERA5 constitutes a 6-year extension to the 40-year (1979-present) satellite-era, and benefits from a number of developments since ERA-40, most notably: variational bias correction, improved cloud detection and more optimal observation error tuning. In pre-production testing the data appear to be of good quality (see Figure 18). Initial experiments indicate VTPR has a strong positive effect on analysis and forecast quality, especially throughout the southern hemisphere and in the northern hemisphere stratosphere (Figure 19).

ERA5 will also benefit from the assimilation of improved reprocessed conventional datasets, including the ISPD, ICOADS and data collections from the National Centers for Environmental Prediction (NCEP) holdings for the pre-1979 period (Hersbach et al., 2017).

3.8 ERA5 uncertainty information

The EDA system was designed and tuned to provide flow-dependent background error covariances for the data assimilation system (Section 3.2). In the ERA5 context, it is additionally used for uncertainty estimation. This approach is different from operational probabilistic medium-range forecasts, where the ECMWF Ensemble (ENS) is the vehicle. It should also be kept in mind that the ERA5 EDA system has a lower spatial and temporal resolution than the main ERA5 products, which sometimes makes it difficult to make the right match between the two systems. In addition the low number of 10 members (versus 25 in the operational EDA) increases sample noise.

The statistical consistency of the ensemble system can be measured by reliability diagrams. Such diagrams (or spread-skill relationships) provide a graphical view of how the skill of the system is modeled by the ensemble spread. Ideally the spread-skill curve is along the diagonal indicating a perfect match between the spread and the skill. The match is varying over space and time and also depends on the

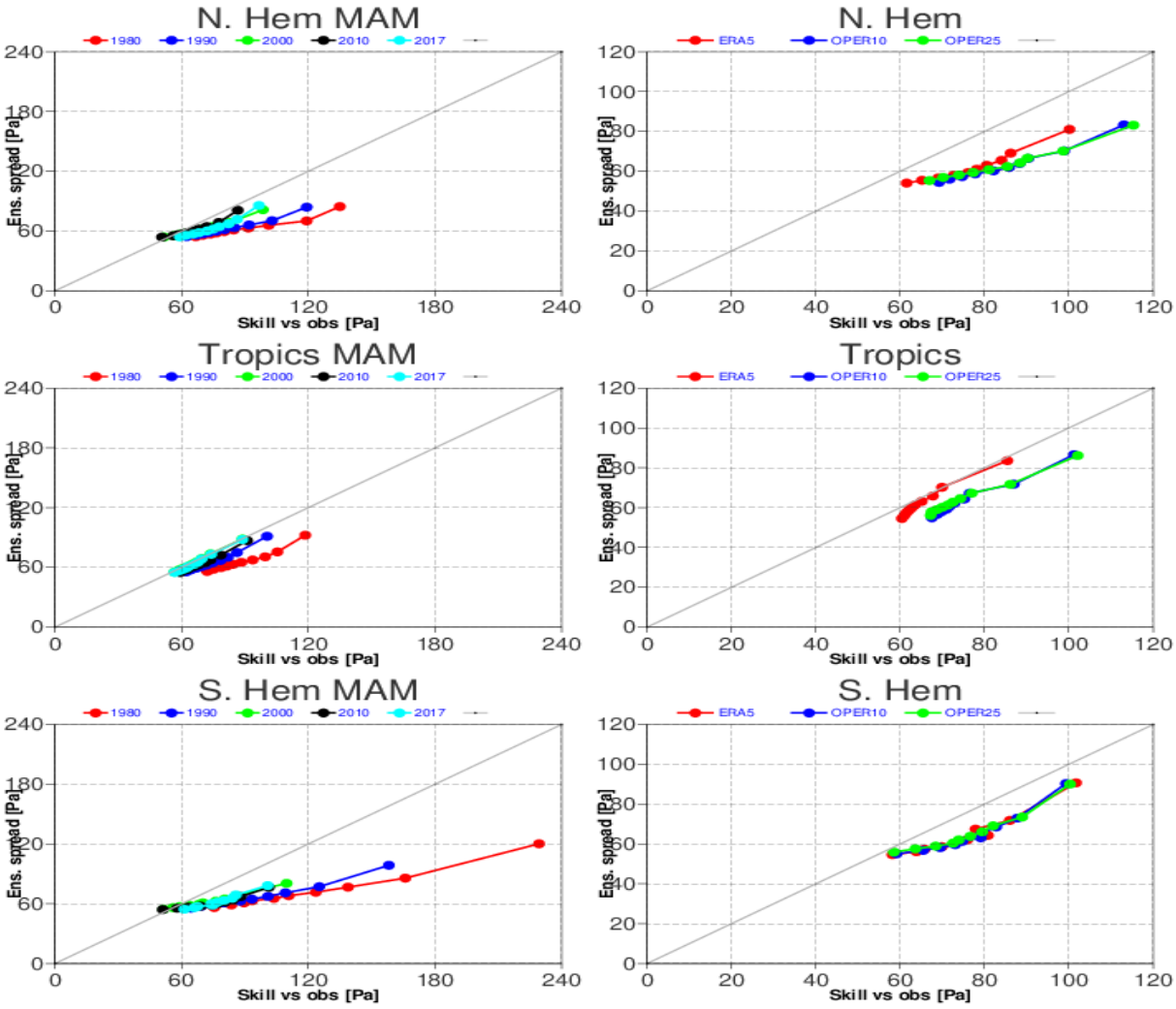

Figure 20: Surface pressure (Pa) spread-skill relationship for ERA5 and the operational (OPER) EDA system. Left: ERA5 for different reanalysis periods for spring (MAM) season (red: 1980, dark blue: 1990, green: 2000, black: 2010 and light blue: 2017). Right: comparison of ERA5 and operational EDA system for DJF2017 (red: ERA5, blue: EDA OPER based on 10 members, green: EDA OPER based on 25 members). The indicated skill is related the root-mean-square error with respect to SYNOP observations.

variables. Figure 20 shows the reliability for surface pressure for various ERA5 streams and a comparison with the operational EDA system. The ERA5 diagnostics (left panels) show that generally ERA5 is slightly under-dispersive, which is improving with time providing rather reliable spread-skill curves for the latest years. Comparison to the operational EDA system shows (right panels) that the reliability of ERA5 is slightly better (particularly in the tropics). The reliability curve is very similar if 10 members or 25 members are taken into account for the OPER spread computations. This would suggest that the ensemble size might not play a big role in the reliability of the ERA5 ensemble. The evaluation and diagnostics of the CERA-20C system can be seen in Dahlgren (2018b).

Some case studies were examined and as an example the situation of hurricanes Irma and Jose in September 2017 is shown in Figure 21. ERA5 is able to indicate the uncertain regions of the hurricane development though to a smaller extent than the OPER EDA (which has higher resolution). The use of 25 members in OPER EDA is improving (increasing) the spread values in the dynamically active regions

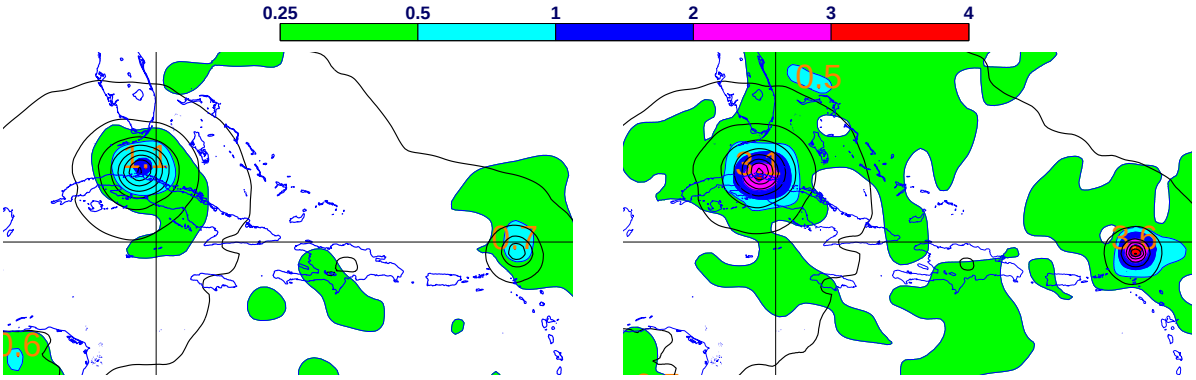

Figure 21: MSLP (contours) and ensemble spread (colours) in hPa for hurricanes IRMA (west) and Jose (east) for 10 September, 2017. Left: ERA5, right: the operational EDA (limited to 10 members).

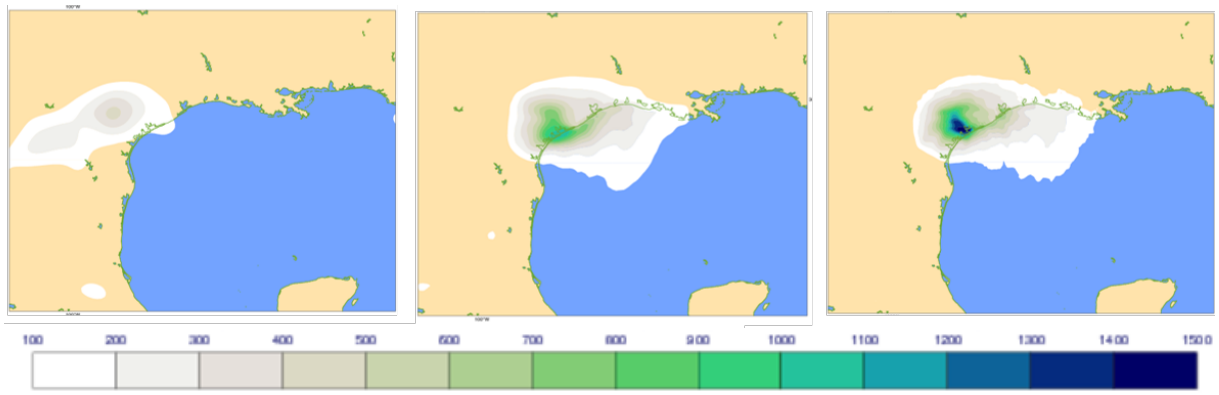

Figure 22: Accumulated 5-day total precipitation (mm) for Harvey from 26 August 2017 00UTC from ERA-Interim (left), ERA5 (middle) and the operational HRES medium-range forecast (right panel).

(not shown).

3.9 ERA5 Performance and Characteristics

3.9.1 Benefit of improved resolution

The considerable increase in resolution of ERA5 allows much more detail to be represented both in space and in time (hourly output). Many examples can be provided. In general, ERA5 improves the representation of tropical cyclones. Central pressure is much lower, and closer to that of the operational HRES analysis than it is to ERA-Interim. For Harvey, which produced locally over 1 metre of precipitation in the Houston area in August 2017, ERA5 locally provides estimates of about 80-90 cm, as is displayed in the middle panel of Figure 22. Although the level of detail of the intense maximum in the operational HRES medium-range forecast (right panel) is missed, the representation is much better than in ERA-Interim (left). Another example is presented in Figure 23, which shows the monthly-mean precipitation in the North-Atlantic for September 2017, when rainfall is dominated by the contribution from tropical cyclones. Again ERA5 (middle panel) shows much more detail than ERA-Interim (left panel) and is much closer to the precipitation in the first 12 hours of the operational HRES medium-range forecast

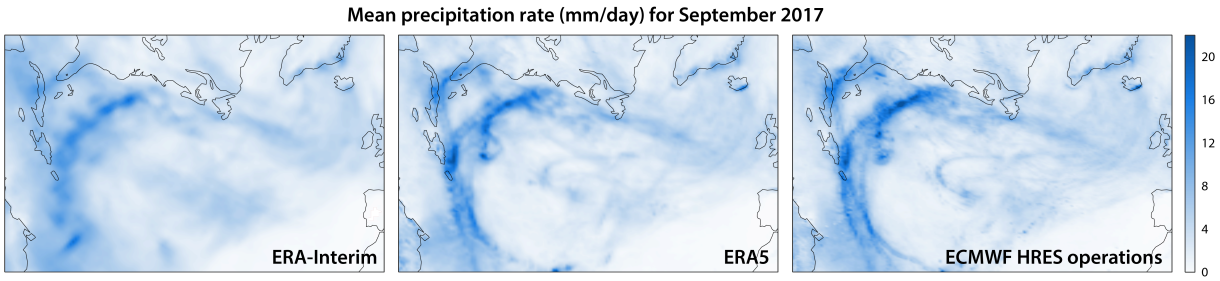

Figure 23: Mean precipitation rate for September 2017 over the North Atlantic from ERA-Interim (left), ERA5 (middle) and ECMWF HRES (right panel).

(right panel).

3.9.2 Improved forecast skill

One way to assess the improved quality of the ERA5 reanalysis is to look at the performance of ten-day forecasts, with the notion that better (re)analyses produce better forecasts. Such forecasts have been run twice daily from ERA5 analyses for 00 and 12 UTC, as they were for ERA-Interim. Scores based on 500 hPa height anomaly correlations for the extratropical northern and southern hemispheres from 1979 onwards are presented in Figure 1. It must be kept in mind that ERA5 has the advantage of using a shifted 12-hour assimilation window that extends six hours further into the future than the window used in ERA-Interim (Table 2) and ECMWF operations. This enables an additional six hours of satellite data and frequently reported conventional data to be used to determine the 00 and 12 UTC analyses. Very few additional radiosonde data are used, however, so ERA5's net advantage is likely a little under six hours. Overall, the skill of ERA5 forecasts is substantially higher than that of ERA-Interim forecasts for both hemispheres over the last fifteen or so years, when the difference amounts to an improvement of around a day or more in the forecast range at which a particular level of performance is on average reached.

Variations in the accuracy of forecasts on timescales of up to a few years, such as associated with the peaking of scores in 2010-2011, are clearly similar for the two reanalyses (and operations, not shown). The skill scores from ERA5 forecasts increase more over time than those from ERA-Interim. This was to some extent expected, as the frozen 2006 version of the forecasting system used by ERA-Interim was unable to use some recent types of satellite data and the newly introduced BUFR-encoded conventional data, in contrast to ERA5. The increase is, however, larger than can be explained by this alone. It can be seen most clearly for the southern hemisphere at shorter forecast ranges. Here ERA5 improves only a little over ERA-Interim in 1979 and 1980 according to 500 hPa height anomaly correlations, and corresponding 850 hPa root-mean-square vector-wind errors (not shown) are in fact larger for ERA5 than ERA-Interim. This is despite the use of the 1979-$\mathbf{B}_{\mathrm{cli}}$. Moreover, the two quite sharp improvements in ERA5's southern-hemisphere scores from 1998 to 1999 and from 2000 to 2001 are likely indicative of a greater impact in ERA5 of the introduction of data from the AMSU instruments on NOAA-15 and NOAA-16.

It is understandable that improvement of the ECMWF forecasting system over the ten years since ERA-Interim began has focused on the better exploitation of the observing system as it existed and developed over these ten years. But attention also needs to be paid for the purpose of reanalysis in improving the exploitation of the observing system as it was in earlier years. ERA5's use of a revised set of $\mathbf{B}_{\mathrm{cli}}$ statistics before the year 2000 is just one step in this direction.

3.9.3 Variability and trends of surface air temperature

ERA-Interim analyses of 2m temperature have been used for more than three years as input to monthly summaries published by the C3S. These analyses, and earlier ones from ERA-40, have been shown to be of reasonable quality and complementary to the products of conventional analyses of climatological station data (Simmons et al. (2017), and references). They are the result of applying a secondary univariate optimal interpolation scheme that uses synoptic observations of surface air temperature to adjust the 2m temperature fields provided by the background forecasts of the primary upper-air data assimilation, 4D-Var in the case of ERA-Interim and ERA5. The scheme used in ERA5 is the same as in ERA-Interim, but is applied hourly rather than six-hourly. ERA5 is also expected to improve on the earlier reanalyses due to the better representation of surface conditions that its higher resolution provides, due to other improvements made in recent years in the modelling of these conditions, and due to use of SST and sea-ice analyses that are more consistent over time.

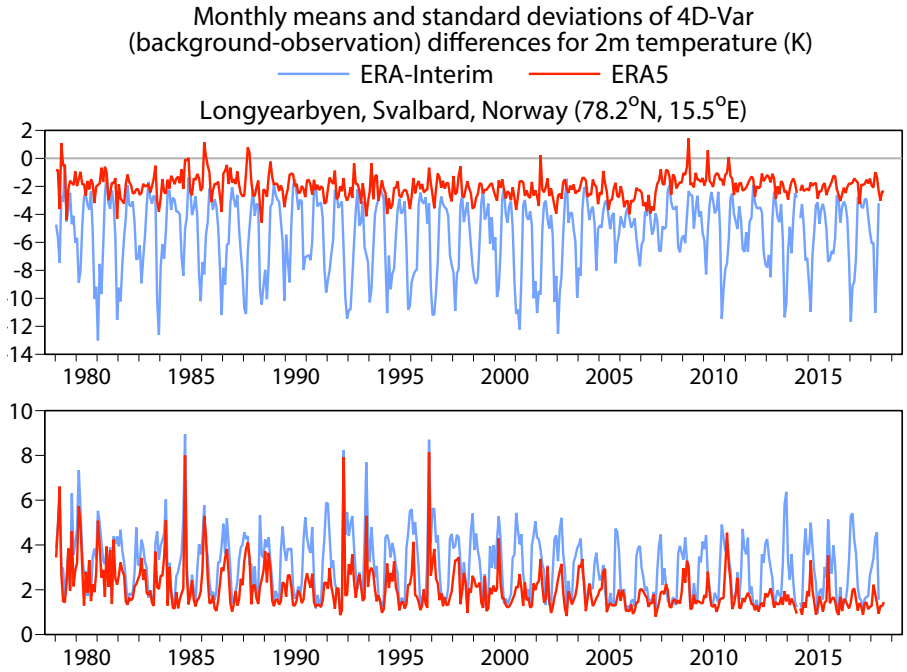

Figure 24: Monthly means (top) and standard deviations (lower panel) of 4D-Var (background-observation) departures of 2m temperature (K) at Longyearbyen, Svalbard, Norway (78.2N, 15.5E) for ERA-Interim (blue) and ERA5 (red).

A number of regional and local improvements are found in ERA5. An example is displayed in Figure 24 which shows a considerably improved fit to observations for a location in the Arctic. Annual-mean analysis increments are smaller in most regions. This is largely due to smaller mean background errors, although some differences have been traced to differences in data quality control: ERA5 rejects fewer data as it has fewer instances of large differences from background values.

ERA5 also provides more feedback on the use of observations by the surface analysis, and an indication of uncertainty from its ensemble data assimilation.

The agreement found previously among various datasets including ERA-Interim led to the expectation that time-series of global-mean temperature from ERA5 would not be substantially different to those from ERA-Interim. This is confirmed by Figure 25. The largest differences between ERA5 and ERA-Interim occur in 2005 and 2006, a period when the differences among various datasets are relatively large.

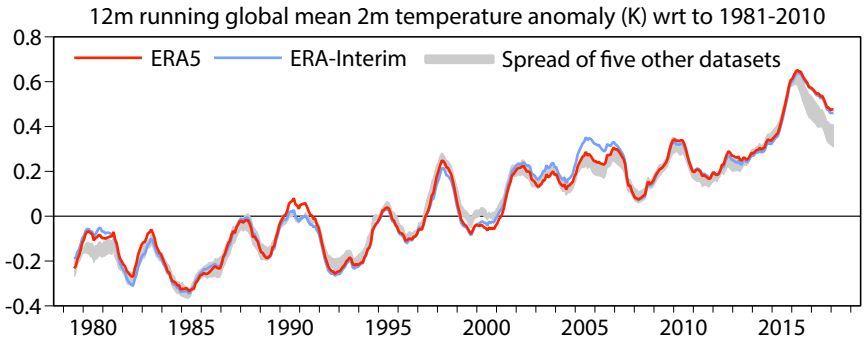

Figure 25: Twelve-month running averages from 1979 onwards of global-mean surface air temperature anomalies (K) relative to 1981-2010 for ERA5 (red) and ERA-Interim (blue). Grey shading denotes the spread of values from five datasets: JRA-55, GISTEMP, HadCRUT4, NOAAGlobalTemp and an infilled version of HadCRUT4 from Cowtan and Way.

This is also a period in which differences in SST analysis are quite large and in which the reanalyses have large anomalies in polar regions that are not sampled well by the conventional analyses. Differences in the relationship between SST and marine air temperature also play a part. Relatively large differences among datasets have happened again recently, but in this case ERA5 and ERA-Interim (which at this time use common SST and sea-ice analyses) give very similar results.

The global fit of the analysis to observations shows little drift over time (not shown). The background forecasts have a global cold bias that is largely removed by the optimal interpolation scheme: the monthly-mean analysis fit varies between zero and -0.16 K, and its annual range decreases over time. These variations are small compared with the rise in mean temperature over land, which for the past four decades has been rather larger than the rise in global-mean temperature shown in Figure 25.

3.9.4 Tropical upper-air wind

The representation of the Quasi-Biennial Oscillation (QBO) and Semi-Annual Oscillation (SAO) in the IFS depends on the model formulation in the tropical region, particularly the parametrization of the effects of gravity waves. Therefore, the representation of the QBO and SAO varies with model cycle and resolution. Observations do provide constraints for the analyses, but poorly observed regions, such as the upper stratosphere and the mesosphere, will exhibit similar characteristics to those of the forecast model.

The depiction of the QBO in the lower to mid stratosphere (from about 50 to 5 hPa) in ERA5 is very similar to that in ERA-Interim (Figure 26a and b), at least for the period considered here, 2008 to 2017. The similarity is present in both the strength of the descending easterlies and westerlies and in their phase and periodicity. The disruption of the westerlies just above 50 hPa in early 2016 is clearly visible in both reanalyses.

Although the broad representation of the SAO between 5 and 0.5 hPa is reasonably similar in the two reanalyses, with descending easterlies and westerlies at similar times of the year, the magnitude of the winds and the exact pattern of descent are not the same (Figure 26c and d). However, between 0.5 and 0.1 hPa the agreement between the reanalyses is poor, with the two representations of the SAO being very different. In this region, ERA5 has westerlies that are much larger than those in ERA-Interim and ERA5 also has a complete absence of descending easterlies. This predominance of westerlies in ERA5 is related to a spurious equatorial mesospheric jet that occurs in cycle 41r2 of the IFS and which peaks

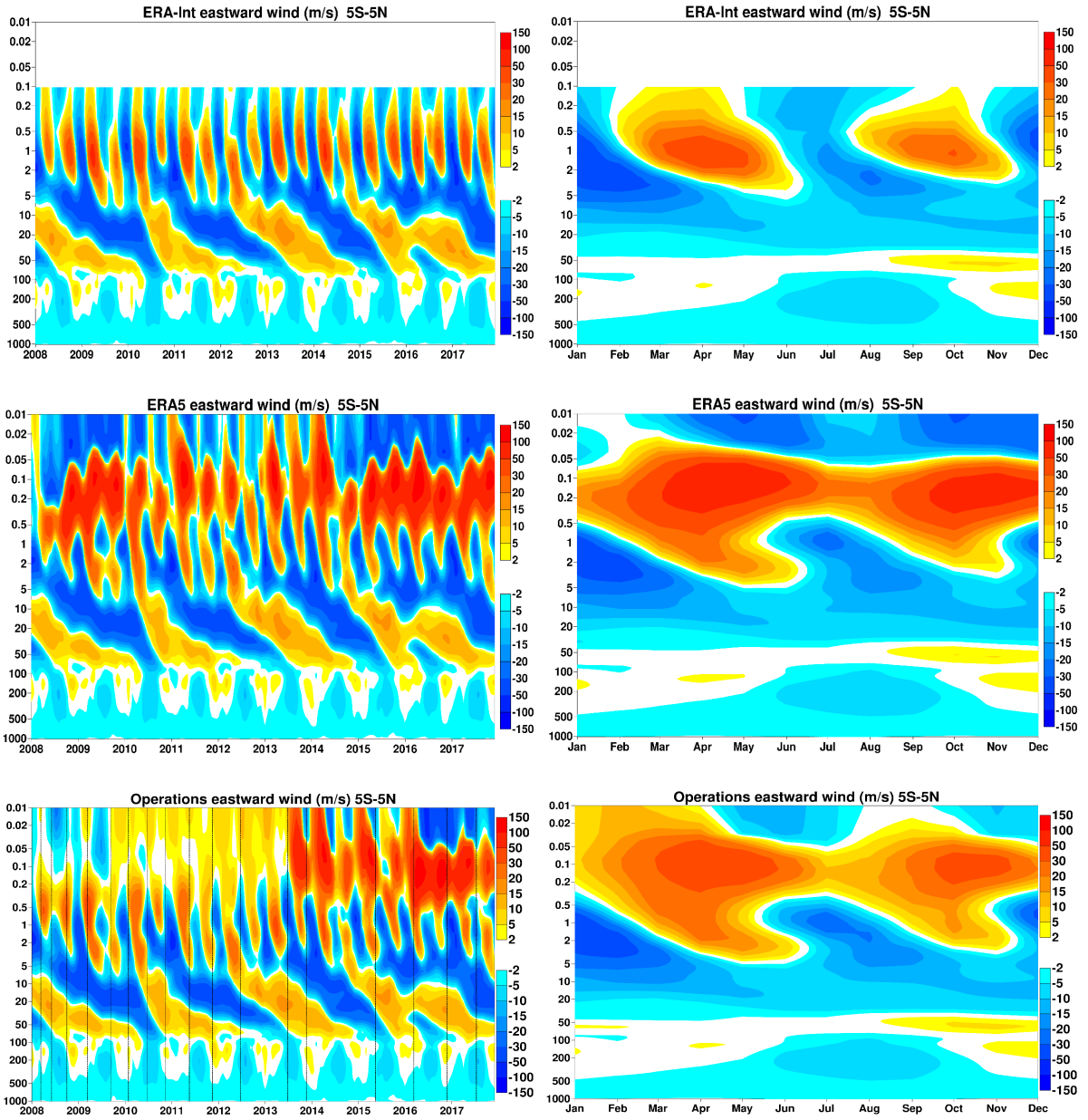

Figure 26: The zonal mean, eastward (i.e. westerly) wind for 2008-2017, averaged over 5S-5N, for the monthly mean (left) and for the mean annual cycle (right) in ERA-Interim (top), ERA5 (middle) and ECMWF operations (lower panel). Vertical coordinate is the reference pressure of the model levels. Vertical lines in the lower left panel indicate the implementation dates of operational IFS cycles.

in the transition seasons (for realistic values of such winds, see Smith et al. (2017)).

From the lower left panel it is seen that the spurious jet emerged after the introduction of IFS cycle 38r2 (25 June 2013) when the number of levels in the vertical was increased from 91 to 137. Its presence, which does not emerge in 'free' extended IFS forecasts, has recently been traced down to severe tapering of vorticity errors in the mesosphere that had been introduced to remove soliton-like behaviour near the model top. This has been resolved from the introduction of IFS cycle 43r3 (11 July 2017), and the mesospheric equatorial winds are much closer to reality since.

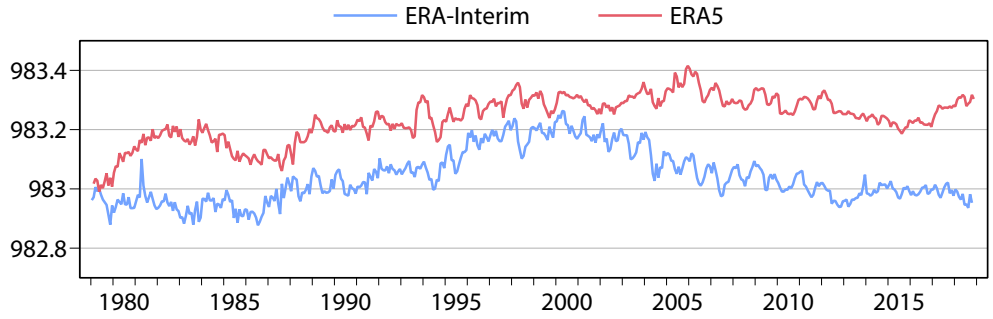

Figure 27: Monthly estimates from 1979 onwards of the contribution of dry air to the global-mean surface pressure (hPa) from ERA5 (red) and ERA-Interim (blue), computed by subtracting the contribution from the total water content of the atmosphere from the global-mean surface pressure.

3.9.5 Global balance

The extent to which the sequence of ERA analyses achieves global balance of quantities such as mass and water provides measures of the consistency of these analyses, and of general progress made in data assimilation and in observational quality and coverage. The approach adopted for ERA5 and its predecessors contrasts with that adopted by the producers of the MERRA-2 reanalysis (Gelaro et al., 2017), for which the assimilation scheme was adapted to impose global balance of mass and water.

Berrisford et al. (2011) examined the global atmospheric budgets from ERA-Interim and made comparisons with ERA-40. Although most measures indicated improvement of ERA-Interim over ERA-40, this was not the case for the global budget of dry mass for the years compared (1989-2002), though as shown earlier by Trenberth and Smith (2005), ERA-40 performed much more poorly prior to the early 1970s. This was found by Uppala et al. (2005) to be associated with higher analysed surface pressure, particularly over the data-sparse oceans of the southern hemisphere, and with lower analysed water vapour prior to assimilation of IR soundings, which began in 1973.

The dry mass of the atmosphere is estimated from the global-mean surface pressure by subtracting the contribution from the water content of the atmosphere. Figure 27 shows the dry mass for ERA5 and ERA-Interim. Neither reanalysis conserves the contribution of dry air to surface pressure to within 0.3 hPa over the whole period. They differ in behaviour, however. ERA-Interim has similar values at the beginning and end of the period, but a spurious rise and fall in dry mass centred around the year 2000. In contrast, dry mass increases quite sharply in the early years of ERA5, but is reasonably uniform after 1990. The range of values is a little larger in ERA5 than ERA-Interim. ERA5's rise in dry mass in the early and late 1980s is due to rises in the global mean of the analysed surface pressure that are not accompanied by rise in analysed moisture content (not shown). The variations in dry mass in ERA-Interim are likewise due mainly to variations in global-mean surface pressure that are not matched by variations in the contribution from moisture. Reasons for the different variations in surface-pressure analyses have yet to be identified. However, given that the spurious variations occur in different periods in the two reanalyses, these problems may well be due to a separate cause in each reanalysis.

Aspects of the global hydrological budget are presented in Figure 28. Variations over time and imbalance are generally larger in ERA-Interim than in ERA5.

In the period when ERA5 is in good balance, both precipitation and evaporation increase over sea but not over land. An increase over sea has been inferred from salinity observations (Durack and Wijffels, 2010),

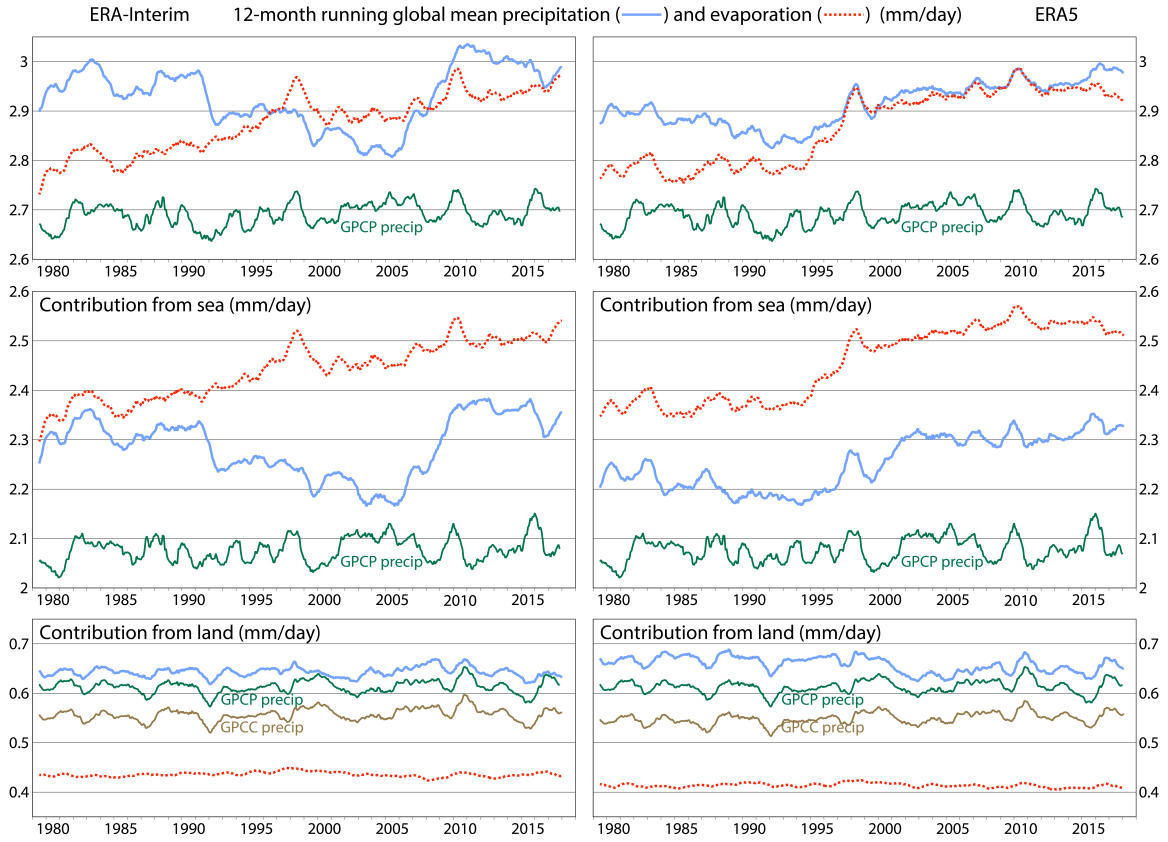

Figure 28: Upper: Twelve-month running averages from 1979 onwards of global mean precipitation (blue) and evaporation (red) rates (mm/day) from ERA-Interim (left) and ERA5 (right). The precipitation estimates from version 2.3 of GPCP are also shown (green). The corresponding contributions to these global averages from sea and land are shown in the middle and bottom panels. Precipitation rates over land are also shown for estimates from GPCC (brown). The latter are based on GPCC's v.2018 monthly full-data product until the end of 2016, version 6 of its monitoring product for most of the following period, and its first-guess monthly product for the latest two months.

but Figure 28 shows a very much smaller increase in marine precipitation from the Global Precipitation Climatology Project (GPCP) than from ERA5. Interannual variations in net precipitation over land from ERA5 agree quite well with values from GPCP and the underlying data of the Global Precipitation Climatology Centre (GPCC[1]). Although an improvement over ERA-Interim in this respect, ERA5 exhibits a larger decline in precipitation over land from the 1980s and 1990s to the 2000s than is the case for ERA-Interim (discussed by Simmons et al. (2014)). Such a decline is not seen in the GPCC and GPCP data, and was not expected in ERA5 as it addressed issues believed to be responsible for this behaviour in ERA-Interim. Further effort is needed to understand these findings.

3.9.6 Stratospheric temperature biases

The choice of static background covariance matrix (specifically the 41r2 and 1979 formulations discussed in Section 3.4.1) is one factor influencing differences in lower stratospheric temperatures between ERA5 and ERA-Interim. The other main factors are a larger lower stratospheric cold bias of the ERA5 version of the model, a change from ERA-Interim to ERA5 in the bias adjustment of radiosonde data prior to the 1990s and the assimilation of plentiful amounts of GNSS-Radio Occultation bending angles (GNSS-

[1]Data downloaded from https://www.dwd.de/EN/ourservices/gpcc/gpcc.html

RO) from mid-2006 onwards. These factors also influence the bias adjustment of satellite radiance data. ERA5 is poorer than ERA-Interim in the consistency of its representation of global-mean stratospheric temperature over the past twenty years.

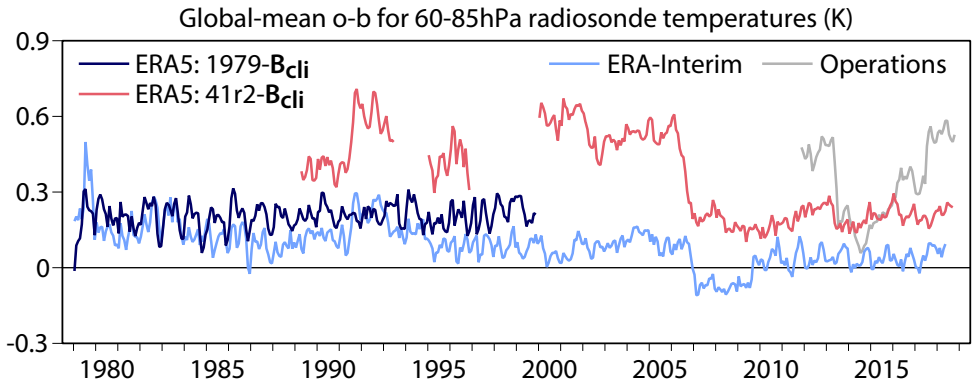

Figure 29: Monthly average observation-background differences from 1979 to 2018 for all assimilated bias-adjusted radiosonde temperature data (K) between 60 and 85 hPa*, for ERA-Interim and for ERA5 using two sets of* $\mathbf{B}_{\text{cli}}$ *statistics: consolidated data prior to 2000 will be based on 1979-*$\mathbf{B}_{\text{cli}}$*, while it is based on 41r2-*$\mathbf{B}_{\text{cli}}$ *afterwards.*

Figure 29 shows the fit to bias-adjusted radiosonde data of the ERA5 and ERA-Interim background forecasts, averaged over all assimilated radiosonde data from 60 to 85 hPa. The ERA5 results are shown both for the latest production streams that use the 1979-$\mathbf{B}_{\text{cli}}$ prior to the year 2000 and for two segments of earlier production streams that used the 41r2-$\mathbf{B}_{\text{cli}}$. The ERA5 data from 2000 onwards, which have already been released for public use, are all based on use of the 41r2-$\mathbf{B}_{\text{cli}}$.

The narrower structure functions of the 41r2-$\mathbf{B}_{\text{cli}}$, together with the larger observation errors specified in cycle 41r2 compared with the ERA-Interim version of the IFS, cause the analysis to make a smaller adjustment of larger scales when presented with radiosonde data that differ from the cold-biased background. Figure 29 shows that the ERA5 background is biased substantially colder relative to bias-adjusted lower stratospheric radiosonde data than the ERA-Interim background is from 2000 to 2006, and the same is seen in the earlier ERA5 runs with the 41r2-$\mathbf{B}_{\text{cli}}$, especially for a period of about two years following the eruption of Mt. Pinatubo in June 1991. The ERA5 fit to the radiosonde data using the 41r2-$\mathbf{B}_{\text{cli}}$ is better once plentiful GNSS-RO data are assimilated, but still poorer than the corresponding ERA-Interim fit. The ERA5 fit using the 41r2-$\mathbf{B}_{\text{cli}}$ and plentiful GNSS-RO data is similar to the ERA5 fit using the 1979-$\mathbf{B}_{\text{cli}}$ before GNSS-RO data are available. Similar results are found for analysis fits (not shown).

The operational fit to lower stratospheric radiosonde temperature data is even poorer than that of ERA5 for recent years. Although the root cause is the cold lower stratospheric bias of the model, which is a little larger in operations than ERA5, operational ECMWF performance may benefit from making better use of the information on large-scale background biases provided by radiosondes.

The upward spike in the ERA-Interim radiosonde fit in mid-1979 is due to a slow adaptation to a change in calibration of the MSU radiances from TIROS-N; the radiance bias correction was adjusted for ERA5 to account for this special case.

The situation in the upper stratosphere is more complicated, as there are also differences between ERA5 and ERA-Interim due to ERA5's use of revised fast radiative transfer calculations for data from the SSU instruments, and differences due to ERA5's use of unadjusted SSU-3 as well as AMSUA-14 data as an anchor for the bias adjustment of other radiance data during the period both SSU and AMSUA data are

available. Time series of global-mean temperature analyses for the upper stratosphere nevertheless show shifts associated with the changes in $\mathbf{B}_{\text{cli}}$, particularly at 5 hPa.

4 ERA5-Land: an ensemble approach of down-scaled land surface model simulations

The ERA5 land surface component is also part of the ERA5 portfolio. However, with the objective of serving, primarily, the climate community, some inconsistencies in the surface fields of ERA5 reanalysis can arise in the temporal-spatial description of land surface components. For example, a well-defined spin-up strategy to avoid jumps in the seam between different production streams for long memory variables is needed. In order to support communities focused on land applications and requiring higher resolution consistent datasets, C3S has taken the initiative to develop ERA5-Land. It will provide a global scale, consistent description of the most important land variables from 1950 and is planned to be continued close to real time through the C3S operational service. ERA5-Land will make available surface fields at hourly resolution through a single simulation driven by near-surface atmospheric fields from ERA5, with thermodynamical orographic adjustment of temperature. The latter is achieved by the daily computation of lapse-rates accounting for the synoptic meteorological situation of the day. The synchronization with the ERA5T mode will also make it possible to provide the timely updates. One of the added values of ERA5-Land with respect to the land component of the ERA5 reanalysis (Section 3.5.2) is a global horizontal resolution of approximately 9 km (around 4 times finer resolution than ERA5), matching the current operational ECMWF TCo1279 operational grid, and therefore providing consistent input for NWP and climate studies involving land water resources, but also for accurate hydrological and agricultural modelling. It will also include, for the first time, an estimation of key land-variables error based on meteorological forcing and model parameters uncertainties supplied by a 10-member ensemble parallel run, thus providing vital information to land-surface data assimilation systems. Finally, the offline nature of ERA5-Land allows to incorporate forefront ECMWF model developments before the production phase. For example, ERA5-Land will benefit from a revision of the soil thermal conductivity, making the heat transfer through the vertical dimension more accurate.

Figure 30 shows an example of a result obtained from the recent integration of demonstrative scout-runs. In this figure, the difference in discharge time-series correlation with in-situ observations (at observation location) initializing from ERA5-Land or ERA5 soil moisture initial conditions is presented. Blue circles indicate enhanced discharge when soil moisture is initialized from ERA5-Land fields. This preliminary result is encouraging and shows added value of specialized land reanalysis.

5 Ocean reanalysis

The current Ocean ReAnalysis System 5 (ORAS5) is a key component of the seasonal forecasting system 5 (Stockdale et al., 2018). It was run from 1979 onwards and includes a new global eddy-permitting 5-member ocean ensemble (Zuo et al., 2018). ORAS5 is based on the IFS cycle 42r1, which was operational in 2016. ORAS5 is an update of ORAP5 (Zuo et al., 2017), a prototype system which was developed within the EU funded research projects MyOcean and MyOcean2. Continuing development of ORAS5 has then been funded by the Global Reanalysis project under the Copernicus Marine Environment Monitoring Service (CMEMS). The HPC requirements have been funded by C3S. ORAS5 is one of the four members of the CMEMS Global Reanalysis Ensemble Product (GREP) that are distributed

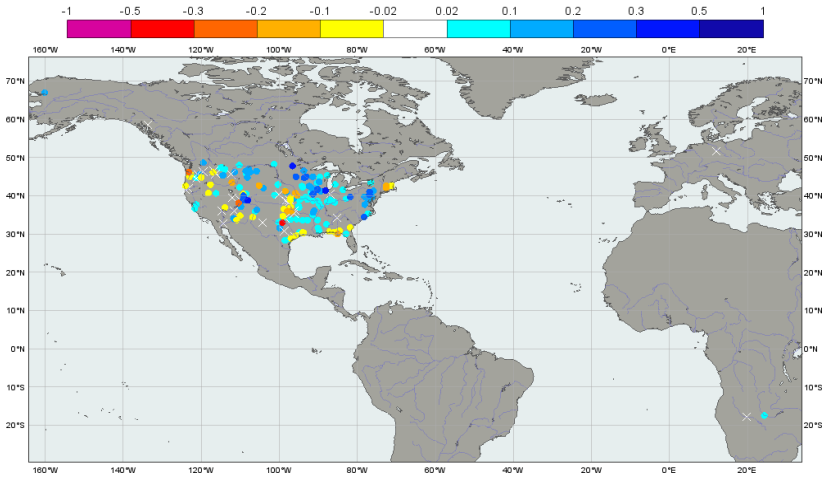

Figure 30: Difference in discharge time-series correlation with in-situ observations (at observation location) between ERA5-Land or ERA5 soil moisture initial conditions. Blue dots represent an improvement of ERA5-Land over ERA5 at the location of in-situ stations.

through the CMEMS data portal.

As a successor to the much used ORAS4 reanalysis (Balmaseda et al., 2013b), ORAS5 benefits from many upgrades in both model physics and data assimilation method, as well as in source/use of observation datasets. The ocean model resolution has been increased to 0.25 degrees in the horizontal and 75 levels in the vertical, compared to 1 degree and 42 layers in ORAS4. ORAS5 also includes a prognostic thermodynamic-dynamic sea-ice model (LIM2, see Fichefet and Maqueda (1997)) with assimilation of sea-ice concentration data. Another important novelty in ORAS5 is to account for the impact of surface waves in the exchange of momentum and turbulent kinetic energy (Breivik et al., 2015). The NEMOVAR data assimilation scheme has been updated with a new Rossby-radius dependent spatial correlation length-scales (Zuo et al., 2015) and a new generic ensemble generation scheme which accounts for both representativeness errors in observation and structure/analysis errors in surface forcing (Zuo et al., 2017). ORAS5 is consistent with ERA5 in the sense that it also uses the HadISST2 SST and the OSTIA sea-ice concentration products. Other innovative features include an ensemble based a-priori bias correction scheme and the spin-up strategy, as well as revised observation QC procedures. Atmospheric fluxes from ERA-interim were used to drive ORAS5 reanalysis until 2015; then it was replaced by the ECMWF operational NWP.

The ORAS5 system has been expanded to include a Real-Time analysis stream which accounts for all upgrades developed for ocean reanalysis. This forms the Real-Time (RT) component of the operational OCEAN5 system, which has been providing initial conditions for the ocean and sea-ice components of ECMWF coupled forecasting systems in the medium-range/monthly ensemble forecast (ENS) since November 2016 with the implementation of IFS cycle 43r1 (Buizza et al., 2016). Since November 2017, ORAS5 started to provide initial conditions for the ECMWF new long-range forecasting system SEAS5 (Stockdale et al., 2017). A consistency between ocean reanalysis and Real-Time analysis, by keeping model and data assimilation method frozen, is considered to be critical for climate application and for a posteriori calibration of the seasonal forecast outputs.

6 Centennial reanalysis for the atmosphere and ocean

Centennial reanalysis and coupled reanalysis development and production were conducted within the ERA-CLIM and ERA-CLIM2 FP7 European projects. This section shows the major contribution of reanalysis research to support coupled data assimilation developments at ECMWF and it illustrates how future requirements for NWP can be shaped and tested for reanalysis. Centennial coupled reanalysis activities initiated coupled atmosphere-ocean data assimilation system research and helped pave the way for ECMWF Earth system coupled assimilation 2016-2015 strategy.

6.1 History of centennial reanalysis developments

The production of a model-based reanalysis that extends back to the beginning of the instrumental record was first pursued in the 20th Century Reanalysis Project (Compo et al. (2006)) at NOAA's Earth Systems Research Laboratory, where a reanalysis spanning the period 1871-2010 was conducted (20CR, Compo et al. (2011)). The project was based on the idea that a reanalysis assimilating only surface pressure observations is feasible and avoids many of the problems associated with significant changes in the observing system. Surface weather observations are available in large numbers throughout the twentieth century, initially concentrated in the northern hemisphere but with global coverage increasing with time. Remarkably, modern data assimilation systems are able to reconstruct realistic large-scale tropospheric circulation patterns from surface pressure observations alone (Whitaker et al., 2009). An improved version of the 20th Century Reanalysis, 20CRv2c, was completed in 2016, while a version 3 is under way.

From 2011-2017 the European Commission funded two consecutive research and development projects, ERA-CLIM and ERA-CLIM2, aimed at developing global climate reanalyses extending back to the beginning of the twentieth century. Both projects were led by ECMWF, and involved participants from a number of EU member states as well as from Russia and Chile. ERA-CLIM focused on data rescue of early in situ upper-air observations, preparation and preprocessing of satellite datasets for reanalysis, and the production of a number of pilot reanalyses.

Within ERA-CLIM, the first ECMWF global centennial reanalysis was produced for the period 1900-2010. This reanalysis, ERA-20C (Poli et al., 2016), included a 10-member ensemble at 125 km resolution using historical surface pressure and marine wind observations (Hersbach et al., 2015). Atmospheric forcing related to model radiation and land-surface processes (Hersbach et al., 2015) was based on CMIP5 recommended datasets. Ocean boundary conditions (HadISST2) were provided by the Met Office Hadley Centre, also as part of ERA-CLIM. Part of these developments were later used in ERA5 (Section 3.6). The second global centennial reanalysis, CERA-20C, incorporates coupling between the ocean and atmosphere (Section 6.2).

Centennial climate reanalysis is based on a restricted set of observations. In contrast, for a multi-decadal comprehensive reanalysis like ERA-Interim and ERA5, all possible observations are ingested with the aim to produce the best possible estimate of its components (atmosphere, land, ocean waves) at any given time. Both types of reanalyses have a role in climate studies and climate change monitoring. Centennial reanalysis provides the longest possible record of low-frequency variability, which helps to put more recent large-scale anomalies in perspective. In contrast, a shorter reanalysis of the full observing system provides a more accurate view of recent changes and can be continued close to real time to allow for climate monitoring.

6.2 Century-long ECMWF coupled atmosphere-ocean reanalysis (CERA-20C)

As part of ERA-CLIM2 (Buizza et al., 2018, see also the ERA-CLIM2 website: http://www.era-clim2.eu), a new assimilation system (CERA) has been developed to simultaneously ingest atmospheric and ocean observations in the coupled Earth system model used for ECMWF's ensemble forecasts (Laloyaux et al., 2016). This approach accounts for interactions between the atmosphere and the ocean during the assimilation process and has the potential to generate a more balanced and consistent Earth system climate reconstruction (Laloyaux et al., 2016).

As part of the ERA-CLIM2 project, the CERA system has been used to generate CERA-20C (Laloyaux et al., 2018), the first European coupled reanalysis of the 20th century which includes a ten-member ensemble to estimate the reanalysis uncertainty. CERA-20C assimilates only surface pressure and marine wind observations as well as ocean temperature and salinity profiles. The air-sea interface is relaxed towards the SST from the HadISST2 monthly product to avoid model drift while enabling the simulation of coupled processes. No data assimilation is performed in the land, wave and sea-ice components, but the use of the coupled model ensures a dynamically consistent Earth system estimate at any time.

Results of the ensemble indicated that the sample distributions of the reanalysis products give a realistic representation of the true uncertainty, as can be seen by comparing the CERA-20C ensemble of reanalyses with other reanalysis products or independent observations. An example is given in Figure 31, which shows the heat content of the upper 300m of the ocean from the CERA20C ensemble, compared with pure ocean reanalyses. Results indicate an overall good agreement. The large uncertainty before 1950 is consistent with the sparse observation coverage during this time. Short-term variations are caused by internal variability; volcanic eruptions of e.g. Agung 1963, El Chichon 1982 and Pinatubo 1991 lead to temporary cooling. The increase since 1970 is well represented by observations and is the manifestation of global warming in the ocean state.

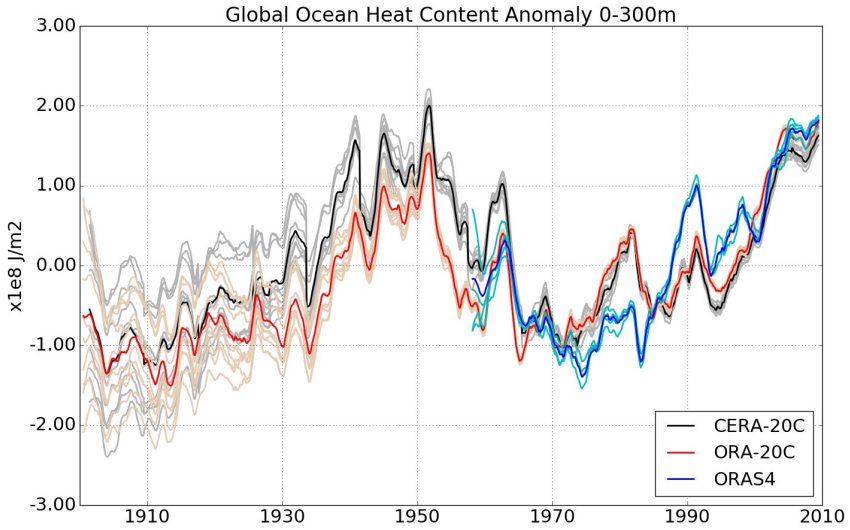

Figure 31: Global 0-300m ocean heat content (OHC) anomalies with respect to 1958-2010. ORA-20C ensemble (10 members) is in light red, with the ensemble mean in red. CERA-20C ensemble (10 members) in grey, with the mean in black, ORAS4 ensemble (5 members) in light blue with the ensemble mean in blue. An OHC increase of $1.0\,10^8\,\mathrm{Jm}^{-2}$ *corresponds to a temperature increase of 0.08K averaged over the top 300m.*

It is important for a product such as CERA-20C to capture seasonal and sub-seasonal coupled pro-

cesses as they will have a crucial impact for climate monitoring and predictability studies. Among such processes, Tropical Instability Waves (TIW) are known to influence ENSO inter-annual variability and impact ENSO predictability. TIWs are westward-propagating features of SST mostly visible in the eastern equatorial Pacific and are characterized by a tight coupling between SST and wind stress. Figure 32 shows the filtered SST and wind stress at 1°N in the Pacific for the La Niña event of 1973-1974. The atmosphere-ocean coupling in CERA-20C allows the system to capture the westward propagation of the TIWs in both atmospheric and ocean components. Filtered SST (contours) and wind stress (shading) are in phase. Positive SST values (plain contours) trigger stronger wind stress while negative SST values (dashed contours) coincide with weaker wind stress. By contrast, ERA-20C being forced by a monthly SST analysis cannot represent the atmospheric response to a signal that is not present in its lower boundary conditions. In this context, CERA-20C is showcasing the benefits of a coupled approach for the representation of processes that are not captured in uncoupled mode.

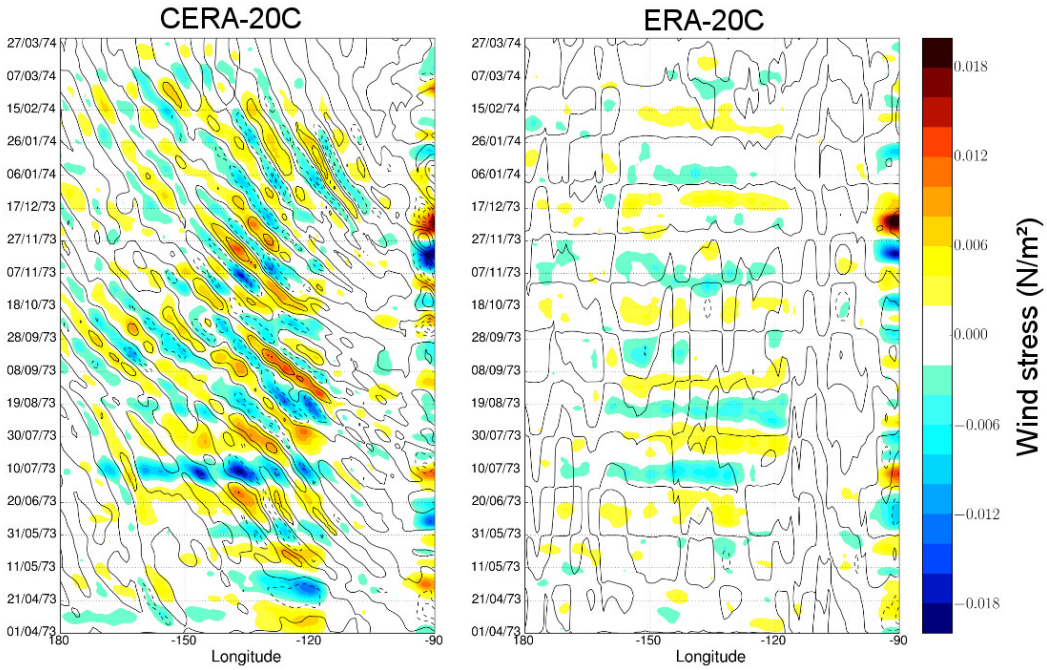

Figure 32: Hovmöller diagram of spatially high-pass filtered SST (in degrees Celsius, contours) and wind stress (in $\mathrm{N/m^2}$*, shading) at 1°N in the eastern Pacific from April 1973 to April 1974. SST contours range from* $-1°C$ *to* $1°C$ *every* $0.25°C$*. Positive (negative) contours are plain (dashed). CERA-20C represents the Tropical Instability Waves (TIWs) due to the ocean dynamics and the atmosphere is responding accordingly with the surface wind stress sensitive to the ocean TIWs.*

CERA-20C provided a proof of concept of the outer-loop coupling method. It was evaluated over a century long period showing good stability of the coupled system when running TL159 (125 km resolution) and using conventional surface observations only in the atmospheric and ocean assimilation systems. To further evaluate the outer-loop approach, CERA was extended to generate a second coupled reanalysis, produced within ERA-CLIM2, at a higher resolution and assimilating all available data, CERA-SAT (see Section 6.3).

6.3 Coupled atmosphere-ocean reanalysis for the current-day observing system (CERA-SAT)

Within the ERA-CLIM2 project, satellite-era reanalysis capabilities at the Centre have been extended to include coupling with ocean, sea-ice and land-surface. In 2017, CERA-SAT (Schepers et al., 2018), a nine-year proof of concept coupled reanalysis dataset was produced and made publicly available.

The 10-member ensemble of data assimilations comprising the CERA-SAT dataset was produced using IFS cycle 42r1 with an atmospheric resolution that matches that of the ERA5 EDA (TL319 on 137 levels). The ocean component, NEMO v3.4, is specified on the tripolar ORCA025 grid with an approximate horizontal resolution of 0.25 degrees on 75 levels. Sea ice is represented using the LIM2 model. The land surface model H-TESSEL comprises four soil layers, including three in the top metre of soil. A dedicated land surface analysis is weakly coupled through a shared background forecast.

Preliminary assessment by comparison to an uncoupled (atmosphere only) control experiment shows reductions in forecast error standard deviation of up to about 10% in tropical areas (for surface pressure and geopotential at forecast day 5), while in the extratropics standard deviations are increased. In terms of background departures, CERA-SAT generally shows improved fits in the tropics while fits are degraded in the extratropics. The degradation in the extratropics is likely a symptom of known shortcomings in the coupled model related to the representation of boundary currents, most evident in the North Atlantic.

The CERA-SAT reanalysis provides the first coupled satellite era reanalysis. The outer-loop coupling used in CERA-SAT served as a basis for coupled assimilation developments in the operational code as described in the next section.

7 Shaping future reanalysis along the requirements for NWP

7.1 Coupled Earth system approach

A range of coupling methods including outer-loop coupling (a form of Quasi-Strong Coupled Data Assimilation), weak coupling and a combination of weak and outer-loop coupling are being evaluated for seamless NWP and reanalysis purposes (the difference between weak and outer-loop coupling is illustrated in Figure 3).

The ECMWF land and atmosphere data assimilation systems are currently weakly coupled both in ERA5 and in the operational NWP system. In 2019 the Ensemble Data Assimilation (EDA) will be used to compute the Jacobians needed for the extended Kalman filter (EKF) soil moisture analysis (in IFS cycle 46r1). This approach will reduce the cost of the SEKF to the cost of a single model trajectory, making it affordable to run a stand-alone land reanalysis. It will be used to produce high-resolution land products from future generations of reanalyses (ERA6 onwards). The EDA-SEKF will enable a more dynamic link to the meteorological conditions, providing a new component to land-atmosphere coupling. In addition, enhanced land-atmosphere coupling will also be investigated by extending and evaluating the CERA outer-loop coupling method to land (Figure 3).

The CERA sea-ice/ocean/atmosphere outer-loop coupling facility is now available for testing as part of the most recent IFS cycles (45r1 onwards). It has been used for an extensive evaluation of the CERA system in the NWP framework, including in the early-delivery system. As shown from the CERA-SAT results, ocean-atmosphere model and assimilation coupling is highly beneficial in the tropical areas and in particular for tropical cyclone representation. However ocean-atmosphere model and assimilation

coupling remains challenging in the extratropics where issues in the western boundary current representation in the ocean model, that affect in particular the Gulf Stream and the Kuroshio positions, lead to erroneous sea-surface temperature patterns. These propagate into the atmosphere leading to degradation of the NWP performance in the extratropics. This issue has been accounted for in the coupled ocean-atmosphere model operational implementation in IFS cycle 45r1 in June 2018, with coupled ocean-atmosphere model initialized by OCEAN5 used in the inter-tropical area and partial coupling initialized by OSTIA SST in the extratropics. Efforts to address the ocean model issues in the extratropics are underway.

With the introduction of the coupled model in the HRES operational NWP forecasts in June 2018 (IFS 45r1), experiments were conducted to disentangle the relative impacts of coupled assimilation and coupled forecasts on NWP performance. These experiments showed that improvements arising from the forecast model coupling in the tropics are comparable to those from the outer-loop coupling, in the CERA system. Although the outer-loop coupling brings improvements to the forecasts in the tropics, due to the ocean bias issues, it leads to degradations in the extratropics. A weakly-coupled ocean-atmosphere assimilation approach was developed and tested, that can improve the forecast performance in the tropics, albeit less than the outer-loop coupling, but without inheriting the problems in the extratropics. In the weakly coupled system, the OCEAN5 analysis which uses the atmospheric analysis as forcing, is also used in the atmospheric analysis, so that there is a two-way coupling between the ocean and atmospheric analyses. A weakly-coupled sea-ice atmosphere assimilation was implemented in operations in June 2018 with IFS cycle 45r1 and weakly coupled ocean-atmosphere assimilation in the tropics is expected in IFS cycle 46r1 in 2019.

Near-future developments will include partial outer-loop coupling, for the inter-tropical area, consistent with the partial model coupling used in operations. New coupling methods combining weak and outer-loop coupling will also be explored. In addition, developments towards SST data assimilation are expected to be highly beneficial and to contribute to enhanced coupled assimilation developments beyond the weakly coupled approach.

These developments will be progressively implemented in the ECMWF system in the next few years. Close synergies between NWP and reanalysis are essential and continue to be an area of active development.

7.2 Developments needed for reanalysis

As mentioned earlier, for reanalysis the latest operational IFS cycle is an excellent starting point, since it incorporates the most advanced operational system available. In this way the latest developments in data assimilation, such as the coupling described in Section 7.1, can be incorporated. The IFS has been optimized to maximize forecast skill in the medium range for the current-day observing system. Reanalysis should not only be able to provide optimal results for today but also for several decades in the past where the observing system was much less dense. This requires that a standard IFS cycle needs a number of adaptations before it is suitable for reanalysis. Some extensions are of a technical nature. Other modifications are related to the special challenges that are encountered when running IFS for a historical period. Broadly, the special needs and challenges for reanalysis can be divided into these categories:

i) The challenge to ensure optimal results back in time where the observing system was much less dense.

- **Evolving background error estimates**. Although ERA5 makes use of the hybrid-**B** formulation

to account for flow-dependent correlation structures in the background error covariance matrix, it was found that the static part of **B** needs updating over time to cope with the substantial evolution of the observing system. For ERA5, this is incorporated in a rather ad hoc way, using a dedicated $\mathbf{B}_{\text{cli}}$ from 1950-1972 (pre-satellite era), 1973-1999 (early-to-mid-satellite era) and 2000 onwards (modern-satellite era). For future reanalysis, a more dynamic system needs to be put in place that allows for a more appropriate response to the major changes in the observing system. For the ocean (and land as well) a similar system would be required, such as to account for the enormous change since the advent of Argo floats in the early 2000s. Only after an optimal evolution of background covariances, reanalysis can fully exploit the information from the ingested observations.

- **Reprocessed datasets**. Clearly better and more observations produce more accurate reanalysis products. Selection, assessment and ingestion of the latest available reprocessed datasets and data that has not been used before is important.

- **Treatment of model and observation biases**. Interaction between model bias and an evolving observing system (that may be biased too) is a major concern in climate reanalysis, since it can introduce spurious climate signals. For ERA5 a prime example is a temporary shift in stratospheric temperature in the early 2000s. Research is needed to tailor the latest available formulation of weak-constraint 4D-Var for reanalysis as well as the optimization of the use of anchor data in VarBC. Both these developments should help to limit the aliasing between systematic model error and observation bias.

- **Improved quality control, bias correction and observation error estimation**. Optimal usage of available observations is challenging. The past observing system is very complex. It consists of a large number of satellite sensors each with a number of channels and each with their own lifespan, and a very diverse set of conventional data distributed over many stations. In addition, each has its own history of anomalies. A dedicated extraction mechanism and blacklist needs to be maintained, which is non-trivial as the way in which this information is organized in IFS has evolved over time. In addition, VarBC sometimes provides an incorrect initialization of bias estimates which can result in either unnecessary rejections (like for a few HIRS channels), or damaging results (like for some MSU channels). Besides quality control and bias estimates, there is scope to optimize observation errors and also how these should evolve over time to reflect improvements in instrumentation.

- **Improved model-space diagnostics**. The non-closure of energy budgets and particularly its evolution over time need to be better understood, as well as the lack of conservation of the global dry mass and hydrological balance.

- **Impacts of data assimilation in data sparse areas**. Non-local effects in the data assimilation system over sparsely observed areas need to be better handled. In ERA5, the initially very poor response of ozone in the polar night from remote good-quality SBUV data is an example.

ii) The need for forcing and boundary input datasets that accurately describe the low-frequency evolution over time whilst ensuring continuity in near-real time.

- There is a constant need to update the selection of the best available datasets, such as the replacement of CMIP5 recommended datasets by CMIP6.

- Account for changes in vegetation and land use in future reanalysis.

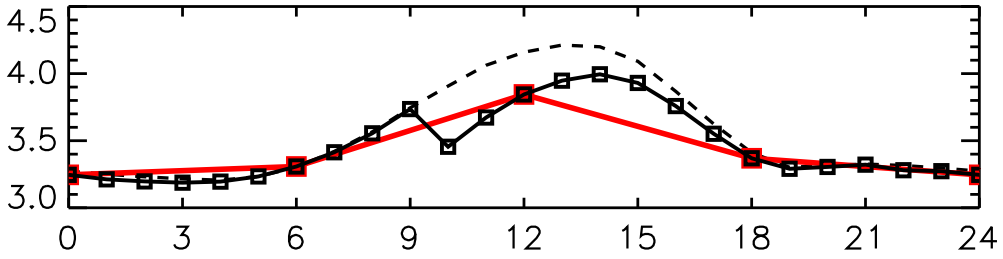

Figure 33: Paris 10-metre wind speed (m/s) at UTC averaged over 2010-2017 from ERA5 hourly analysis output (solid black), 6-hourly analysis output (red) and 1-12 hour short forecasts starting from 06 and 18 UTC (dashed black).

iii) The challenge to ensure optimal results for all parts of the atmosphere, land and ocean. In particular parts that do not critically contribute to NWP forecast skill and therefore may receive less attention in ECMWF R&D planning. Some examples are :

- **The representation of the stratosphere and mesosphere**. Although ERA5 provides many improvements over ERA-Interim, ERA5 has larger stratospheric temperature biases. This is partly due to a larger model bias, which had worsened in IFS since version 31r2. In addition, an anomalously strong jet in the equatorial mesosphere had emerged. These and other issues in the stratosphere and mesosphere were addressed with the formation of a Stratospheric Task Force in collaboration with the University of Reading in November 2016 (Hogan and Polichtchouk (2018), Shepherd et al. (2018), Polichtchouk et al. (2017)), as a result of which a number of improvements have been implemented in the most recent operational IFS cycle 45r1. Although for ERA5 these improvements arrived too late, future reanalysis will benefit.

- **Features of hourly analysis output**. The ERA5 hourly output shows more details of the assimilation system than the previous 6-hourly output. Consequently, non-ideal features that were previously hidden may surface. One example is wind fields in the boundary layer. It was noticed by one of the major European energy suppliers that although the climatology for ERA5 shows a diurnal cycle for Paris, it also displays a jump (about 0.25 m/s at 10-metre height, see Figure 33) between 9 and 10 UTC. This is exactly between two 12-hourly analysis windows, and investigation at other locations around the globe confirmed this behaviour between analysis cycles (no jumps were observed for the short forecasts connecting the analyses). The cause of this clearly undesirable behaviour needs further investigation.

iv) The need to provide adequate uncertainty estimates.

- **Random and systematic components**. Currently, ERA5 uncertainty estimates are based on the spread in the EDA which mainly samples random error (although the perturbed HadISST2 realizations do introduce long-term correlations near the surface). Information on systematic errors that, e.g., capture and explain large-scale and long-term systematic differences with respect to reanalyses produced elsewhere (see www.reanalysis.org for an overview) is required. This, in addition to indications that the ERA5 spread is probably too low and, consequently, confidence estimates are too high, requires further work.

v) The need for an enhanced monitoring system that allows for adequate quality assurance of the products while they are produced at high speed in various parallel streams.

- **Challenges of high throughput**. The reanalysis system is as complex as the operational analysis system, yet during production many days per day are generated, rather than one for the operational medium-range forecast. This also implies special performance requirements for the HPC and data handling system.

A large part of the special (future) requirements for reanalysis are being addressed at ECMWF, while part of the work can be outsourced via external C3S contracts with other European organisations. This includes the considerable effort by EUMETSAT on reprocessing of a large number of satellite datasets for usage in ERA6. Support for climate reanalysis regarding satellite data rescue has been initiated, as is the development and maintenance of quality-controlled global databases containing all known digitised in-situ upper-air weather observations. These will contain metadata and information needed for data assimilation such as bias adjustments and uncertainty estimates. In addition a set of services to improve access to available in situ instrumental data records and data streams from observing networks is in place, as needed for monitoring climate change and to support climate science. A contract on support for handling model and observation bias as pointed out in the third bullet point of category i) mentioned above has just started. An invitation to tender (ITT) to enhance ocean ensemble data assimilation for initialization of seasonal forecasts and ERA6 had just closed at the time of writing. In addition to activities on global reanalysis at ECMWF, C3S has outsourced two contracts on regional reanalysis, one for Europe and one focused on the Arctic. These regional reanalysis activities are based on mature science as was developed in the 3-year European-Commission funded UERRA project. Boundary conditions will be provided by ERA5. These regional reanalyses will be produced at the ECMWF high-performance computing facility, and the expertise of the partners allows for synergy with reanalysis at ECMWF.

7.3 Reanalysis future plans

As discussed throughout this paper, ECMWF has produced both centennial reanalyses (like CERA-20C) using a selected baseline of observations which provides the longest possible record of low-frequency variability, and full-observing-system reanalysis (like ERA5), spanning a shorter period. These latter offer a more accurate view of recent changes and which can be continued close to real time to allow for climate monitoring. Within the framework of C3S post-2020 it is envisaged to produce both types of reanalyses. The proposed strategy is to produce the centennial reanalysis prior to the next full-observing-system reanalysis ERA6. The projected framework of post-2020 also intends to support production (via third parties) of a centennial regional reanalysis for Europe using the global centennial reanalysis for boundary conditions. In addition, given the improved affordability as described in Section 7.1, a follow-up of ERA5-Land will allow for a proper land surface reanalysis that actually assimilates observations, which will be a big step forward. On the longer term a joint CAMS/C3S reanalysis with coupled chemistry, extending back to 1979, is envisaged.

Regarding centennial reanalysis, production should start in 2021 after the move of the data centre to Bologna. It needs to improve on the known problems in ERA-20C (Poli et al., 2016) and CERA-20C (Laloyaux et al., 2018). Some examples are listed below. Ideally this reanalysis should extend back to 1850. However, given the very reduced observation coverage prior to 1900 it is currently unclear until how far back into the 19th century a reliable reanalysis product can be obtained. Resolution of the ensemble will probably not be significantly higher than CERA-20C (TL159). The value of a higher-resolution control needs to be investigated. This reanalysis is likely to be coupled with the ocean. The issues in the NWP context, as discussed above regarding western boundary currents, may be less problematic given the reduced resolution at which this reanalysis will be conducted. Strong advantages of coupling are physically consistent fluxes, and a better representation of the variability not represented in the ingested

SST fields (such as tropical instability waves). The risks are a more complicated control of model bias, and considerable discontinuities in the ocean component between production streams. These could be tempered by using CERA-20C to constrain biases in the ocean as well as reanalysis states.

The centennial reanalysis should use the latest available archives for surface pressure observations (like ISPD, ICOADS and archives managed by C3S tendered activities), while the usage of marine surface winds needs to be improved (bias-corrected) since these may have contributed to a spurious trend for wind in (C)ERA-20C. Available upper-air data should be used. The encouraging results from the ERA-CLIM Pre-SAT pilot reanalysis (Hersbach et al., 2017) together with the experience being accrued in the ERA5 pre-satellite back extension, data from recent upper-air rescue activities and newly available temperature bias corrections, all contribute to a solid base system for the successful ingestion of such observations. Although 2m temperature is one of the most widely used products of centennial reanalysis, neither (C)ERA-20C nor 20CR (Compo et al. (2011)) assimilate sub-daily observations of this quantity. Reanalysis temperature trends are largely controlled by similar trends in the ingested SST products that are either imposed as boundary condition (ERA-20C) or nudged into the ocean model (CERA-20C). Although centennial reanalysis is able to represent the synoptic situation, it is not straightforward to improve on low-frequency variability of 2m temperature from free model integrations (Hersbach et al., 2015), when compared to gridded monthly station-based climate products such as CRUTEM4 (Osborn and Jones, 2014). Further investigations into the assimilation of 2m temperature and humidity observations are required.

Regarding the improvement on CERA-20C, the lack of summer-ice melting, which led to the accumulation of Arctic sea ice over the years in CERA-20C, will be corrected. The solution to this issue is known and it was already used in CERA-SAT. As mentioned above, the spurious trend in the wind needs to be understood and resolved. The representation of tropical cyclones also needs to be improved.

Production of ERA6 should start in 2023, which should ideally be based on outer-loop coupling between all its components (atmosphere, ocean waves, ocean, sea ice and land surface), and follow a structure as depicted in the right-hand panel of Figure 3. This scenario leans on the assumption that by then, the challenges in the extratropics (Section 7.1) have been resolved. Otherwise, a mix of weak and outer-loop coupling is to be followed along the then state-of-the-art NWP configuration. All points that were depicted in Section 7.2 should be addressed or incorporated. As described, part of these preparations will be carried out by tendered C3S activities. It is uncertain to what extent the resolution can be increased. The resolution of ERA5 already represents a major step forward with respect to previous reanalyses. Assimilation of surface temperature in ERA5 and operational NWP at ECMWF is currently based on optimal interpolation as part of the land assimilation scheme and does not properly account for the exact timing of the observations. The envisaged outer-loop coupling in the land-surface component should provide an opportunity to improve on the current situation.

8 Concluding remarks

Reanalysis has become a fundamental resource for ECMWF and the scientific community in general. Reanalysis is used in verifying, initialising and calibrating many ECMWF products. ECMWF has a long history with global reanalyses that has gradually encompassed all components of the climate system. Research on coupled data assimilation for Earth system models was initiated primarily for reanalysis applications and carried out in the European-Commission ERA-CLIM and ERA-CLIM2 projects. Such coupling is now a key priority for NWP in the ECMWF road map for 2016-2025.

The first phase of the ERA5 reanalysis is nearing completion. Data from 2000 onwards is publicly

available via the C3S Climate Data Store, and all data from 1979 should be available by the end of 2018. Timely updates with an availability within 2-5 days will serve a large community of users. Production of the second phase, which will extend the record back to 1950 has just started and should be completed by autumn 2019. Compared to its predecessor, ERA-Interim, ERA5 has a number of innovative features. The increased resolution, as well as the benefits from ten years of intensive development of the IFS, and improvements in the ingested observations collectively provide a large step forward. However, there are some weak elements that need to be addressed in future reanalysis. Examples are inconsistencies in stratospheric temperature as well as deficiencies in the mass, energy and hydrological budgets.

The ongoing production of the ERA5 global reanalysis is entirely undertaken within the Copernicus C3S framework, which fully supports both development and production manpower as well as the intensive high-performance computing usage. Compared to previous ECMWF reanalyses, C3S dedicated resources for the development, implementation, production and consolidation of reanalysis as an operational service has dramatically reduced the ERA5 production life cycle while ensuring high-quality products and data services for ECMWF and international users. Copernicus has enabled a world leading position for reanalysis at ECMWF, by supporting the development of a truly operational framework. Reciprocally, the Copernicus programme as well as the C3S reanalysis developments and ERA5 production have benefitted considerably from the heritage and unique expertise at ECMWF in NWP and reanalysis.

In addition to the ERA5 global reanalysis, many reanalysis-related tasks are being carried out by C3S using third-parties. Two high-resolution regional reanalyses, for Europe and the Arctic, are underway and will deliver results by 2019-20. ECMWF has also awarded several contracts for the preparation of input observations for climate reanalysis. These address satellite data reprocessing, data rescue (both satellite and conventional), and the collection of in-situ surface observations and upper-air observations into well-maintained archives.

All these datasets will feed into and improve the next generation of global (ERA6) and regional reanalyses. It is worth pointing out that these reprocessed datasets hold their own merits as climate data records that will be made available to the research community in Europe.

ECMWFs vision for C3S post-2020 continues to allocate a very high priority to reanalysis. A centennial global reanalysis back to 1900 or earlier is proposed and is to start in 2021. The next full-observing-system reanalysis, ERA6, will be based on a coupled Earth system modelling and data assimilation approach and will assimilate the new datasets mentioned above. It will be started by 2023. The production of a centennial reanalysis first provides more time for the development of a mature coupled data assimilation system for ERA6. Future regional reanalyses will also possibly be extended to centennial too, with a full pan-Arctic component. On the longer term a joint CAMS/C3S reanalysis with coupled chemistry is envisaged as well.

Acknowledgments

Reanalysis touches on a large number of activities at ECMWF and its success relies on the efforts from many, many people across the Centre and from many collaborations. The research leading to results on centennial reanalysis and CERA-SAT has received funding from the European Union's Seventh Framework Programme (FP7/2007-2013) under grant agreement numbers 265229 (ERA-CLIM Project) and 607029 (ERA-CLIM2 Project). We thank Peter Bauer, Andy Brown, Stephen English, Juan Garces de Marcilla and Florence Rabier for their detailed feedback which improved this document.

References

Ahlgrimm, M. and R. Forbes (2014). Improving the representation of low clouds and drizzle in the ECMWF model based on ARM observations from the Azores. *Monthly Weather Review 142*(2), 668–685.

Albergel, C., G. Balsamo, P. de Rosnay, J. Muñoz Sabater, and S. Boussetta (2012). A bare ground evaporation revision in the ECMWF land-surface scheme: evaluation of its impact using ground soil moisture and satellite microwave data. *Hydrology and Earth System Sciences 16*, 3607–3620. 10.5194/hess-16-3607-2012.

Allan, R. P., C. Liu, N. G. Loeb, M. D. Palmer, M. Roberts, D. Smith, and P.-L. Vidale (2014). Changes in global net radiative imbalance 1985-2012. *Geophys. Res. Lett.*.

Balmaseda, M., K. Mogensen, and A. Weaver (2013a). Evaluation of the ECMWF ocean reanalysis system ORAS4. *Quarterly Journal of the Royal Meteorological Society 139*, 1132–1161.

Balmaseda, M., A. Vidard, and D. Anderson (2008). The ECMWF Ocean Analysis System: ORA-S3. *Mon. Wea. Rev. 136*, 3018–3034.

Balmaseda, M. A., K. Mogensen, and A. T. Weaver (2013b). Evaluation of the ECMWF ocean reanalysis system ORAS4. *Quarterly Journal of the Royal Meteorological Society 139*(674), 1132–1161.

Balsamo, G., A. Agusti-Panareda, C. Albergel, A. Beljaars, S. Boussetta, E. Dutra, T. Komori, S. Lang, J. Munoz-Sabater, F. Pappenberger, P. de Rosnay, I. Sandu, N. Wedi, A. Weisheimer, F. Wetterhall, and E. Zsótér (2014). Representing the Earth surfaces in the Integrated Forecasting System: Recent advances and future challenges. ECMWF Technical Memorandum 729, ECMWF, Shinfield Park, Reading.

Balsamo, G., C. Albergel, A. Beljaars, S. Boussetta, E. Brun, H. Cloke, D. Dee, E. Dutra, J. Muñoz Sabater, F. Pappenberger, P. de Rosnay, T. Stockdale, and F. Vitart (2015). ERA-Interim/land: a global land surface reanalysis data set. *Hydrology and Earth System Sciences 19*(1), 389–407.

Balsamo, G., R. Salgado, E. Dutra, S. Boussetta, T. Stockdale, and M. Potes (2012). On the contribution of lakes in predicting near-surface temperature in a global weather forecasting model. *TDMO 64*(1), 15829.

Balsamo, G., P. Viterbo, A. Beljaars, B. van den Hurk, M. Hirschi, A. Betts, and K. Scipal (2009). A revised hydrology for the ECMWF model: Verification from field site to terrestrial water storage and impact in the integrated forecast system. *J. Hydrometeor. 10*, 623–643. doi: 10.1175/2008JHM1068.1.

Bechtold, P., M. Köhler, T. Jung, F. Doblas-Reyes, M. Leutbecher, M. J. Rodwell, F. Vitart, and G. Balsamo (2008). Advances in simulating atmospheric variability with the ECMWF model: From synoptic to decadal time-scales. *Quarterly Journal of the Royal Meteorological Society 134*(634), 1337–1351.

Bechtold, P., N. Semane, P. Lopez, J.-P. Chaboureau, A. Beljaars, and N. Bormann (2014). Representing equilibrium and nonequilibrium convection in large-scale models. *Journal of the Atmospheric Sciences 71*(2), 734–753.

Berrisford, P., P. Kållberg, S. Kobayashi, D. Dee, S. Uppala, A. Simmons, P. Poli, and H. Sato (2011). Atmospheric conservation properties in ERA-Interim. *Quarterly Journal of the Royal Meteorological Society 137*(659), 1381–1399.

Bidlot, J.-R. (2012). Present status of wave forecasting at ECMWF. In *Workshop on ocean waves*, pp. 25–27.

Bonavita, M., E. Hólm, L. Isaksen, and M. Fisher (2016). The evolution of the ecmwf hybrid data assimilation system. *Quarterly Journal of the Royal Meteorological Society 142*(694), 287–303.

Bormann, N., A. Collard, and P. Bauer (2009). Estimates of spatial and inter-channel observation error characteristics for current sounder radiances for NWP. ECMWF Technical Memorandum 600, ECMWF, Shinfield Park, Reading.

Bormann, N., C. Lupu, A. J. Geer, H. Lawrence, P. Weston, and S. English (2017). Assessment of the forecast impact of suface-sensitive microwave radiances over land and sea-ice. ECMWF Technical Memorandum 804, ECMWF, Shinfield Park, Reading.

Boussetta, S., G. Balsamo, A. Beljaars, T. Kral, and L. Jarlan (2013). Impact of a satellite-derived leaf area index monthly climatology in a global numerical weather prediction model. *International Journal of Remote Sensing 34*(9-10), 3520–3542.

Boussetta, S., G. Balsamo, A. Beljaars, and other authors (2013). Natural land carbon dioxide exchanges in the ECMWF Integrated Forecasting System: implementation and offline validation. *J. Geophys. Res. 118*, 5923–5946.

Breivik, ., K. Mogensen, J. R. Bidlot, M. A. Balmaseda, and P. A. E. M. Janssen (2015). Surface wave effects in the NEMO ocean model: Forced and coupled experiments. *Journal of Geophysical Research C: Oceans 120*(4), 2973–2992.

Buizza, R., J. R. Bidlot, M. Janousek, S. Keeley, K. Mogensen, and D. Richardson (2016). New IFS cycle brings sea-ice coupling and higher ocean resolution. *ECMWF Newsletter 150*, 14–17.

Buizza, R., S. Bronnimann, L. Haimberger, P. Laloyaux, M. J. Martin, M. Fuentes, M. Alonso-Balmaseda, A. Becker, M. Blaschek, P. Dahlgren, E. de Boisseson, D. Dee, M. Doutriaux-Boucher, X. Feng, V. John, K. Haines, S. Jourdain, Y. Kosaka, D. Lea, F. Lemarie, M. Mayer, P. Messina, C. Perruche, P. Peylin, J. Pullainen, N. Rayner, E. Rustemeier, D. Schepers, R. Saunders, J. Schulz, A. Sterin, S. Stichelberger, A. Storto, C.-E. Testut, M.-A. Valente, A. Vidard, N. Vuichard, A. Weaver, J. While, and M. Ziese (2018). The EU-FP7 ERA-CLIM2 project contribution to advancing science and production of earth-system climate reanalyses. *Bulletin of the American Meteorological Society*.

Cardinali, C., S. Pezzulli, and E. Anderson (2004). Influence-matrix diagnostic of a data assimilation system. *Quart. J. Roy. Meteor. Soc. 130*, 2767–2786.

Cariolle, D. and H. Teyssèdre (2007). A revised linear ozone photochemistry parameterization for use in transport and general circulation models: multi-annual simulations. *Atmos. Chem. and Phys. Disc. 7*, 1655–1697.

Compo, G. P., J. S. Whitaker, and P. D. Sardeshmukh (2006). Feasibility of a 100-year reanalysis using only surface pressure data. *Bulletin of the American Meteorological Society 87*(2), 175–190.

Compo, G. P., J. S. Whitaker, P. D. Sardeshmukh, N. Matsui, R. J. Allan, X. Yin, B. E. Gleason, R. S. Vose, G. Rutledge, P. Bessemoulin, S. Brönnimann, M. Brunet, R. I. Crouthamel, A. N. Grant, P. Y. Groisman, P. D. Jones, M. C. Kruk, A. C. Kruger, G. J. Marshall, M. Maugeri, H. Y. Mok, ø Nordli, T. F. Ross, R. M. Trigo, X. L. Wang, S. D. Woodruff, and S. J. Worley (2011). The twentieth century reanalysis project. *Quart. J. Roy. Meteor. Soc. 137*, 1–28.

Dahlgren, P. (2018a). ERA5 updates for back extension to 1950-1979. Research Department Memorandum, available upon request, RD18-077, ECMWF, Shinfield Park, Reading.

Dahlgren, P. (2018b). Evaluation and diagnostics of the CERA-20C climate reanalysis ensemble. ECMWF Technical Memorandum 820, ECMWF, Shinfield Park, Reading.

de Rosnay, L. Isaksen, and L. Dahoui (2015). Snow data assimilation at ECMWF. *ECMWF Newsletter no 143*, 26–31.

de Rosnay, P., G. Balsamo, C. Albergel, J. Muñoz Sabater, and L. Isaksen (2014). Initialisation of land surface variables for Numerical Weather Prediction. *Surveys of Geophys. 35(3)*, 607–621. doi:10.1007/s10712-012-9207-x.

de Rosnay, P., M. Drusch, D. Vasiljevic, G. Balsamo, C. Albergel, and L. Isaksen (2013). A simplified Extended Kalman Filter for the global operational soil moisture analysis at ECMWF. *Quart. J. Roy. Meteor. Soc. 139*, 1199–1213. doi: 10.1002/qj.2023.

Dee, D. (2004). Variational bias correction of radiance data in the ECMWF system. In *ECMWF Workshop on Assimilation of high spectral resolution sounders in NWP*, Number SP-247, ECMWF, United Kingdom. ECMWF.

Dee, D. (2005). Bias and data assimilation. *Quart. J. Roy. Meteor. Soc. 131*, 3323–3343.

Dee, D. and S. Uppala (2009). Variational bias correction of satellite radiance data in the ERA-Interim reanalysis. *Quart. J. Roy. Meteor. Soc. 135*, 1830–1841.

Dee, D. P., S. M. Uppala, A. J. Simmons, P. Berrisford, P. Poli, S. Kobayashi, U. Andrae, M. A. Balmaseda, G. Balsamo, P. Bauer, P. Bechtold, A. C. M. Beljaars, L. van de Berg, J. Bidlot, N. Bormann, C. Delsol, R. Dragani, M. Fuentes, A. J. Geer, L. Haimberger, S. B. Healy, H. Hersbach, E. V. Hólm, L. Isaksen, P. Kållberg, M. Köhler, M. Matricardi, A. P. McNally, B. M. Monge-Sanz, J.-J. Morcrette, B.-K. Park, C. Peubey, P. de Rosnay, C. Tavolato, J.-N. Thépaut, and F. Vitart (2011). The ERA-Interim reanalysis: configuration and performance of the data assimilation system. *Quart. J. Roy. Meteor. Soc. 137*, 553–597.

Dethof, A. and E. Hólm (2004). Ozone assimilation in the ERA-40 reanalysis project. *Quart. J. Roy. Meteor. Soc. 130*, 2851–2872.

Diamantakis, M. (2014). Improving ECMWF forecasts of sudden stratospheric warmings. *ECMWF Newsletter No. 141-Autumn 2014*, 30–36.

Donlon, C. J., M. Martin, J. Stark, J. Roberts-Jones, E. Fiedler, and W. Wimmer (2012). The operational sea surface temperature and sea ice analysis (OSTIA) system. *Remote Sensing of Environment 116*, 140–158.

Dragani, R. and A. P. McNally (2013). Operational assimilation of ozone-sensitive infrared radiances at ECMWF. *Quart. J. Roy. Meteor. Soc. 139*, 2068–2080.

Durack, P. J. and S. E. Wijffels (2010). Fifty-year trends in global ocean salinities and their relationship to broad-scale warming. *Journal of Climate 23*(16), 4342–4362.

Dutra, E., G. Balsamo, P. Viterbo, P. M. A. Miranda, A. Beljaars, C. Schär, and K. Elder (2010). An Improved Snow Scheme for the ECMWF Land Surface Model: Description and Offline Validation. *JHM 11*(4), 899–916.

Dutra, E., V. Stepanenko, G. Balsamo, P. Viterbo, P. Miranda, D. Mironov, and C. Schär (2009). Impact of lakes on the ECMWF surface scheme. ECMWF Technical Memorandum 608, ECMWF, Shinfield Park, Reading.

Eastwood, S., T. Lavergne, and R. Tonboe (2014). Algorithm Theoretical Basis Document for the OSI SAF global reprocessed sea ice concentration product. *EUMETSAT Satellite Application Facilities*.

Ebita, A., S. Kobayashi, Y. Ota, M. Moriya, R. Kumabe, K. Onogi, Y. Harada, S. Yasui, K. Miyaoka, K. Takahashi, H. Kamahori, C. Kobayashi, H. Endo, M. Soma, Y. Oikawa, and T. Ishimizu (2011). The Japanese 55-year reanalysis "JRA-55": An interim report. Technical report, SOLA. 7.

ECMWF, R.-D. (2016). IFS documentation. https://www.ecmwf.int/sites/default/files/elibrary/2016/16647-part-iii-dynamics-and-numerical-procedures.pdf.

Fennig, K., M. Schroeder, and R. Hollmann (2017). Fundamental Climate Data Record of Microwave Imager Radiances, edition 3. Technical report.

Fichefet, T. and M. A. Maqueda (1997). Sensitivity of a global sea ice model to the treatment of ice thermodynamics and dynamics. *Journal of Geophysical Research: Oceans (1978–2012) 102*(C6), 12609–12646.

Fiorino, M. (2004). A multi-decadal daily sea surface temperature and sea ice concentration data set for the ERA-40 reanalysis. ECMWF ERA-40 Project Report Series 12, European Centre for Medium-Range Weather Forecasts, Shinfield Park. *Reading, United Kingdom*.

Fisher, M. (2003). Background error covariance modelling. In *Seminar on Recent Developments in Data Assimilation for Atmosphere and Ocean*, ECMWF, United Kingdom, pp. 45–63. ECMWF.

Forbes, R. and A. Tompkins (2011). An improved representation of cloud and precipitation. *ECMWF Newsletter 129*(13.18).

Forbes, R. M. and M. Ahlgrimm (2014). On the representation of high-latitude boundary layer mixed-phase cloud in the ECMWF global model. *Monthly Weather Review 142*(9), 3425–3445.

Forbes, R. M., A. M. Tompkins, and A. Untch (2011). A new prognostic bulk microphysics scheme for the IFS. ECMWF Technical Memorandum 649, ECMWF, Shinfield Park, Reading.

Geer, A., M. Ahlgrimm, P. Bechtold, M. Bonavita, N. Bormann, S. English, M. Fielding, R. Forbes, R. Hogan, E. Hólm, M. Janisková, K. Lonitz, P. Lopez, M. Matricardi, I. Sandu, and P. Weston (2017). Assimilating observations sensitive to cloud and precipitation. ECMWF Technical Memorandum 815, ECMWF, Shinfield Park, Reading.

Gelaro, R., W. McCarty, M. J. Suárez, R. Todling, A. Molod, L. Takacs, C. A. Randles, A. Darmenov, M. G. Bosilovich, R. Reichle, et al. (2017). The modern-era retrospective analysis for research and applications, version 2 (merra-2). *Journal of Climate 30*(14), 5419–5454.

Gibson, J., P. Kållberg, S. Uppala, A. Hernandez, A. Nomura, and E. Serrano (1999). ECMWF re-analysis project report series, 1, ERA-15 description (version 2). *UK: Reading*.

Haiden, T., M. Janousek, and H. Hersbach (2017). ERA5 aids in forecast performance monitoring. *ECMWF Newsletter 150*, 8.

Haimberger, L., C. Tavolato, and S. Sperka (2008). Toward elimination of the warm bias in historic radiosonde temperature records: Some new results from a comprehensive intercomparison of upper-air data. *J. Climate 21*, 4587–4606.

Haimberger, L., C. Tavolato, and S. Sperka (2012). Homogenization of the global radiosonde temperature dataset through combined comparison with reanalysis background series and neighboring stations. *J. Climate 25*, 8108–8131.

Healy, S., J. Eyre, M. Hamrud, and J. Thépaut (2007). Assimilating GPS radio occultation measurements with two-dimensional bending angle observation operators. *Quarterly Journal of the Royal Meteorological Society 133*(626), 1213–1227.

Hennermann, K., A. Guillory, and X. Yang (2017). Copernicus users rate services highly. *ECMWF Newsletter 153*, 16–17.

Hersbach, H., S. Brönnimann, L. Haimberger, M. Mayer, L. Villiger, J. Comeaux, A. Simmons, D. Dee, S. Jourdain, C. Peubey, et al. (2017). The potential value of early (1939–1967) upper-air data in atmospheric climate reanalysis. *Quarterly Journal of the Royal Meteorological Society 143*(704), 1197–1210.

Hersbach, H. and D. Dee (2016). ERA5 reanalysis is in production, ECMWF Newsletter 147, ECMWF.

Hersbach, H., C. Peubey, A. Simmons, P. Berrisford, P. Poli, and D. Dee (2015). ERA-20CM: A twentieth-century atmospheric model ensemble. *Quarterly Journal of the Royal Meteorological Society 141*(691), 2350–2375.

Hersbach, H., P. Poli, and D. Dee (2015). The observation feedback archive for the ICOADS and ISPD data sets.

Hirahara, S., M. A. Balmaseda, E. de Boisseson, and H. Hersbach (2016). Sea Surface Temperature and Sea Ice Concentration for ERA5.

Hirons, L., P. Inness, F. Vitart, and P. Bechtold (2013). Understanding advances in the simulation of intraseasonal variability in the ECMWF model. Part II: The application of process-based diagnostics. *Quarterly Journal of the Royal Meteorological Society 139*(675), 1427–1444.

Hogan, R. J. and A. Bozzo (2015). Mitigating errors in surface temperature forecasts using approximate radiation updates. *J. Adv. Model. Earth. Syst. 7*, 836–853.

Hogan, R. J. and S. Hirahara (2016). Effect of solar zenith angle specification in models on mean shortwave fluxes and stratospheric temperatures. *Geophys. Res. Lett. 43*, 482–488.

Hogan, R. J. and I. Polichtchouk (2018). The Stratosphere Task Force one year on. *ECMWF Newsletter*.

Horányi, A. (2017). Some aspects on the use and impact of observations in the ERA5 Copernicus Climate Change Service reanalysis. *IDOJARAS 121*(4), 329–344.

Iacono, M. J., J. S. Delamere, E. J. Mlawer, M. W. Shephard, S. A. Clough, and W. D. Collins (2008). Radiative forcing by long-lived greenhouse gases: Calculations with the AER radiative transfer models. *Journal of Geophysical Research: Atmospheres 113*(D13).

Ingleby, B., L. Isaksen, T. Kral, T. Haiden, and M. Dahoui (2018). Improved use of atmospheric in situ data. *ECMWF Newsletter 155*, 20–25.

Inness, A., F. Baier, A. Benedetti, I. Bouarar, S. Chabrillat, H. Clark, C. Clerbaux, P. Coheur, R. Engelen, Q. Errera, et al. (2013). The MACC reanalysis: an 8 yr data set of atmospheric composition. *Atmospheric chemistry and physics 13*, 4073–4109.

Isaksen, L., M. Bonavita, R. Buizza, M. Fisher, J. Haseler, M. Leutbecher, and L. Raynaud (2010). Ensemble of data assimilations at ECMWF. ECMWF Technical Memorandum No. 636, ECMWF, Shinfield Park, Reading.

Janisková, M. and P. Lopez (2013). Linearized physics for data assimilation at ECMWF. In *Data Assimilation for Atmospheric, Oceanic and Hydrologic Applications (Vol. II)*, pp. 251–286. Springer.

Janssen, P. and J. Bidlot (2009). *On the extension of the freak wave warning system and its verification*. European Centre for Medium-Range Weather Forecasts.

Kennedy, J., N. Rayner, S. C. Millington, and M. Saunby (2016). The Met Office Hadley Centre Sea Ice and Sea-Surface Temperature data set, version 2, part 1: Sea-Surface Temperature Analysis. In preparation.

Krzeminski, B., N. Bormann, G. Kelly, T. McNally, and P. Bauer (2009). Revision of the HIRS cloud detection at ECMWF. EUMETSAT/ECMWF Fellowship Programme, Research Report No. 19, ECMWF, Shinfield Park, Reading.

Laloyaux, P., M. Balmaseda, D. Dee, K. Mogensen, and P. Janssen (2016). A coupled data assimilation system for climate reanalysis. *Quarterly Journal of the Royal Meteorological Society 142*(694), 65–78.

Laloyaux, P., E. de Boisseson, M. Balmaseda, J.-R. Bidlot, S. Broennimann, R. Buizza, P. Dalhgren, D. Dee, L. Haimberger, H. Hersbach, et al. (2018). Cera-20c: A coupled reanalysis of the twentieth century. *Journal of Advances in Modeling Earth Systems*.

Laloyaux, P., J.-N. Thépaut, and D. Dee (2016). Impact of scatterometer surface wind data in the ECMWF coupled assimilation system. *Monthly Weather Review 144*(3), 1203–1217.

Lean, J., G. Rottman, J. Harder, and G. Kopp (2005). Sorce contributions to new understanding of global change and solar variability. *Solar Phys. 230*, 27–53.

Lupu, C. and A. Geer (2015). Operational Implementation of RTTOV-11 in the IFS. ECMWF Technical Memorandum No. 636, ECMWF, Shinfield Park, Reading.

Manrique-Suñén, A., A. Nordbo, G. Balsamo, A. Beljaars, and I. Mammarella (2013). Representing land surface heterogeneity: Offline analysis of the tiling method. *Journal of Hydrometeorology 14*(3), 850–867.

Markus, T. and D. J. Cavalieri (2009). The AMSR-E NT2 sea ice concentration algorithm: Its basis and implementation. *Journal of The Remote Sensing Society of Japan 29*(1), 216–225.

Mayer, M. and L. Haimberger (2012). Poleward atmospheric energy transports and their variability as evaluated from ECMWF reanalysis data. *Journal of Climate 25*(2), 734–752.

McPeters, R. D., P. Bhartia, D. Haffner, G. Labow, and L. Flynn (2013). The version 8.6 SBUV ozone data record: An overview. *Journal of Geophysical Research: Atmospheres 118*(14), 8032–8039.

Merchant, C. J., O. Embury, J. Roberts-Jones, E. Fiedler, C. E. Bulgin, G. K. Corlett, S. Good, A. McLaren, N. Rayner, S. Morak-Bozzo, et al. (2014). Sea surface temperature datasets for climate applications from Phase 1 of the European Space Agency Climate Change Initiative (SST CCI). *Geoscience Data Journal 1*(2), 179–191.

Mironov, D., E. Heise, E. Kourzeneva, B. Ritter, N. Schneider, and A. Terzhevik (2010). Implementation of the lake parameterisation scheme FLake into the numerical weather prediction model COSMO. *Boreal Environment Research 15*(2).

Molteni, F., T. Stockdale, M. Balmaseda, G. Balsamo, R. Buizza, L. Ferranti, L. Magnusson, K. Mogensen, T. Palmer, and F. Vitart (2011). *The new ECMWF seasonal forecast system (System 4)*. European Centre for Medium-Range Weather Forecasts Reading, U. K.

Morcrette, J.-J. (1991). Radiation and cloud radiative properties in the European Centre for Medium Range Weather Forecasts forecasting system. *Journal of Geophysical Research: Atmospheres 96*(D5), 9121–9132.

Morcrette, J.-J., H. W. Barker, J. N. S. Cole, M. J. Iacono, and R. Pincus (2008). Impact of a new radiation package, McRad, in the ECMWF Integrated Forecasting System. *Mon. Weath. Rev. 136*, 4773–4798.

Nash, J. and R. Saunders (2015). A review of stratospheric sounding unit radiance observations for climate trends and reanalyses. *QJRMS 141*, 2103–2113.

NOAA, N. (2006). 2-minute Gridded Global Relief Data (ETOPO2) v2.

Orr, A., P. Bechtold, J. Scinocca, M. Ern, and M. Janisková (2010). Improved middle atmosphere climate and forecasts in the ECMWF model through a nonorographic gravity wave drag parameterization. *Journal of Climate 23*(22), 5905–5926.

Osborn, T. and P. Jones (2014). The crutem4 land-surface air temperature data set: construction, previous versions and dissemination via google earth. *Earth System Science Data 6*(1), 61–68.

Pincus, R., H. W. Barker, and J.-J. Morcrette (2003). A fast, flexible, approximate technique for computing radiative transfer in inhomogeneous clouds. *J. Geophys. Res. Atmos. 103*(4376).

Poli, P., H. Hersbach, D. P. Dee, P. Berrisford, A. J. Simmons, F. Vitart, P. Laloyaux, D. G. Tan, C. Peubey, J.-N. Thépaut, et al. (2016). ERA-20C: An atmospheric reanalysis of the twentieth century. *Journal of Climate 29*(11), 4083–4097.

Poli, P., P. Moll, D. Puech, F. Rabier, and S. B. Healy (2009). Quality control, error analysis, and impact assessment of FORMOSAT-3/COSMIC in numerical weather prediction. *Terr. Atmos. Ocean. Sci. 20*, 101–113.

Polichtchouk, I., R. J. Hogan, T. G. Shepherd, P. Bechtold, T. Stockdale, S. Malardel, S.-J. Lock, and L. Magnusson (2017). *What Influences the Middle Atmosphere Circulation in the IFS?* European Centre for Medium-Range Weather Forecasts.

Raoult, B., C. Bergeron, A. L. Alós, J. Thepaut, and D. Dee (2017). Climate Service Develops User-friendly Data Store. *ECMWF Newsletter 151*, 22–27.

Sandu, I., A. Beljaars, G. Balsamo, and A. Ghelli (2011). Revision of the surface roughness length table. *ECMWF Newsletter 130*, 8–10.

Sandu, I., A. Beljaars, P. Bechtold, T. Mauritsen, and G. Balsamo (2014). Why is it so difficult to represent stably stratified conditions in numerical weather prediction (NWP) models? *Journal of Advances in Modeling Earth Systems 5*(2), 117–133.

Schepers, D., E. D. Boisséson, R. Eresmaa, C. Lupu, and P. D. Rosnay (2018). CERA-SAT: A coupled satellite-era reanalysis, ECMWF Newsletter 155, ECMWF.

Shepherd, T. G., I. Polichtchouk, R. J. Hogan, and A. J. Simmons (2018). Report on stratosphere task force.

Shine, K. P., J. J. Barnett, and W. J. Randel (2008). Temperature trends derived from Stratospheric Sounding Unit radiances: The effect of increasing CO_2 on the weighting function. *Geophys. Res. Lett. 35*, L02710.

Simmons, A., P. Berrisford, D. Dee, H. Hersbach, S. Hirahara, and J.-N. Thépaut (2017). A reassessment of temperature variations and trends from global reanalyses and monthly surface climatological datasets. *Quarterly Journal of the Royal Meteorological Society 143*(702), 101–119.

Simmons, A. J., P. Poli, D. P. Dee, P. Berrisford, H. Hersbach, H. Kobayashi, and C. Peubey (2014). Estimating low-frequency variability and trends in atmospheric temperature from the ERA-Interim reanalysis. *Quart. J. Roy. Meteor. Soc. 140*, 329–353.

Smith, A. K., R. R. Garcia, A. C. Moss, and N. J. Mitchell (2017). The semiannual oscillation of the tropical zonal wind in the middle atmosphere derived from satellite geopotential height retrievals. *Journal of the Atmospheric Sciences 74*(8), 2413–2425.

Stockdale, T., M. Alonso-Balmaseda, S. Johnson, L. Ferranti, F. Molteni, L. Magnusson, S. Tietsche, F. Vitart, D. Decremer, A. Weisheimer, C. D. Roberts, G. Balsamo, S. Keeley, K. Mogensen, H. Zuo, M. Mayer, and B. Monge-Sanz (2018, November). SEAS5 and the future evolution of the long-range forecast system. Technical Memorandum 835, ECMWF, Shinfield Park, Reading.

Stockdale, T., S. Johnson, L. Ferranti, M. A. Balmaseda, and S. Briceag (2017). ECMWF's new long-range forecasting system SEAS5. *ECMWF Newsletter 154*, 15–20.

Tavolato, C. and L. Isaksen (2015). On the use of a Huber norm for observation quality control in the ECMWF 4D-Var. *Quarterly Journal of the Royal Meteorological Society 141*(690), 1514–1527.

Tiedtke, M. (1989). A comprehensive mass flux scheme for cumulus parameterization in large-scale models. *Monthly Weather Review 117*(8), 1779–1800.

Tiedtke, M. (1993). Representation of clouds in large-scale models. *Monthly Weather Review 121*(11), 3040–3061.

Titchner, H. A. and N. A. Rayner (2014). The Met Office Hadley Centre sea ice and sea surface temperature data set, version 2: 1. Sea ice concentrations. *Journal of Geophysical Research: Atmospheres 119*(6), 2864–2889.

Trenberth, K. E., J. T. Fasullo, and M. A. Balmaseda (2014). Earth's global energy imbalance. *J. Climate*.

Trenberth, K. E., J. T. Fasullo, and J. Kiehl (2009). Earth's global energy budget. *Bull. Amer. Meteor. Soc. 90*, 311–323.

Trenberth, K. E. and L. Smith (2005). The mass of the atmosphere: A constraint on global analyses. *Journal of Climate 18*(6), 864–875.

Uppala, S. M., P. W. Kållberg, A. J. Simmons, U. Andrae, V. da Costa Bechtold, M. Fiorino, J. K. Gibson, J. Haseler, A. Hernandez, G. A. Kelly, X. Li, K. Onogi, S. Saarinen, N. Sokka, R. P. Allan, E. Andersson, K. Arpe, A. M. Balmaseda, A. C. M. Beljaars, L. van de Berg, J. Bidlot, N. Bormann, S. Caires, F. Chevallier, A. Dethof, M. Dragosavac, M. Fisher, M. Fuentes, S. Hagemann, E. Hólm, B. J. Hoskins, L. Isaksen, P. A. E. M. Janssen, R. Jenne, A. P. McNally, J.-F. Mahfouf, J.-J. Morcrette, N. A. Rayner, R. W. Saunders, P. Simon, A. Sterl, K. E. Trenberth, A. Untch, D. Vasiljevic, P. Viterbo, and J. Woollen (2005). The ERA-40 re-analysis. *Quart. J. Roy. Meteor. Soc. 131*, 2961–3012.

van den Hurk, B., P. Viterbo, A. Beljaars, and A. Betts (2000, January). Offline validation of the ERA40 surface scheme. *Technical Memorandum* (295).

Whitaker, J. S., G. P. Compo, and J.-N. Thépaut (2009). A comparison of variational and ensemble-based data assimilation systems for reanalysis of sparse observations. *Monthly Weather Review 137*(6), 1991–1999.

Zuo, H., M. A. Balmaseda, E. D. Boisseson, S. Hirahara, M. Chrust, and P. D. Rosnay (2017). A generic ensemble generation scheme for data assimilation and ocean analysis. Technical Report 795, European Centre for Medium-Range Weather Forecasts.

Zuo, H., M. A. Balmaseda, and K. Mogensen (2015). The ECMWF-MyOcean2 eddy-permitting ocean and sea-ice reanalysis ORAP5. Part 1: Implementation. Technical Report 736, European Centre for Medium-Range Weather Forecasts.

Zuo, H., M. A. Balmaseda, and K. Mogensen (2017, aug). The new eddy-permitting ORAP5 ocean reanalysis: description, evaluation and uncertainties in climate signals. *Climate Dynamics 49*(3), 791–811.

Zuo, H., M. A. Balmaseda, K. Mogensen, and S. Tietsche (2018). OCEAN5: the ECMWF Ocean Reanalysis System and its Real-Time analysis component. Technical Report 823, European Centre for Medium-Range Weather Forecasts.